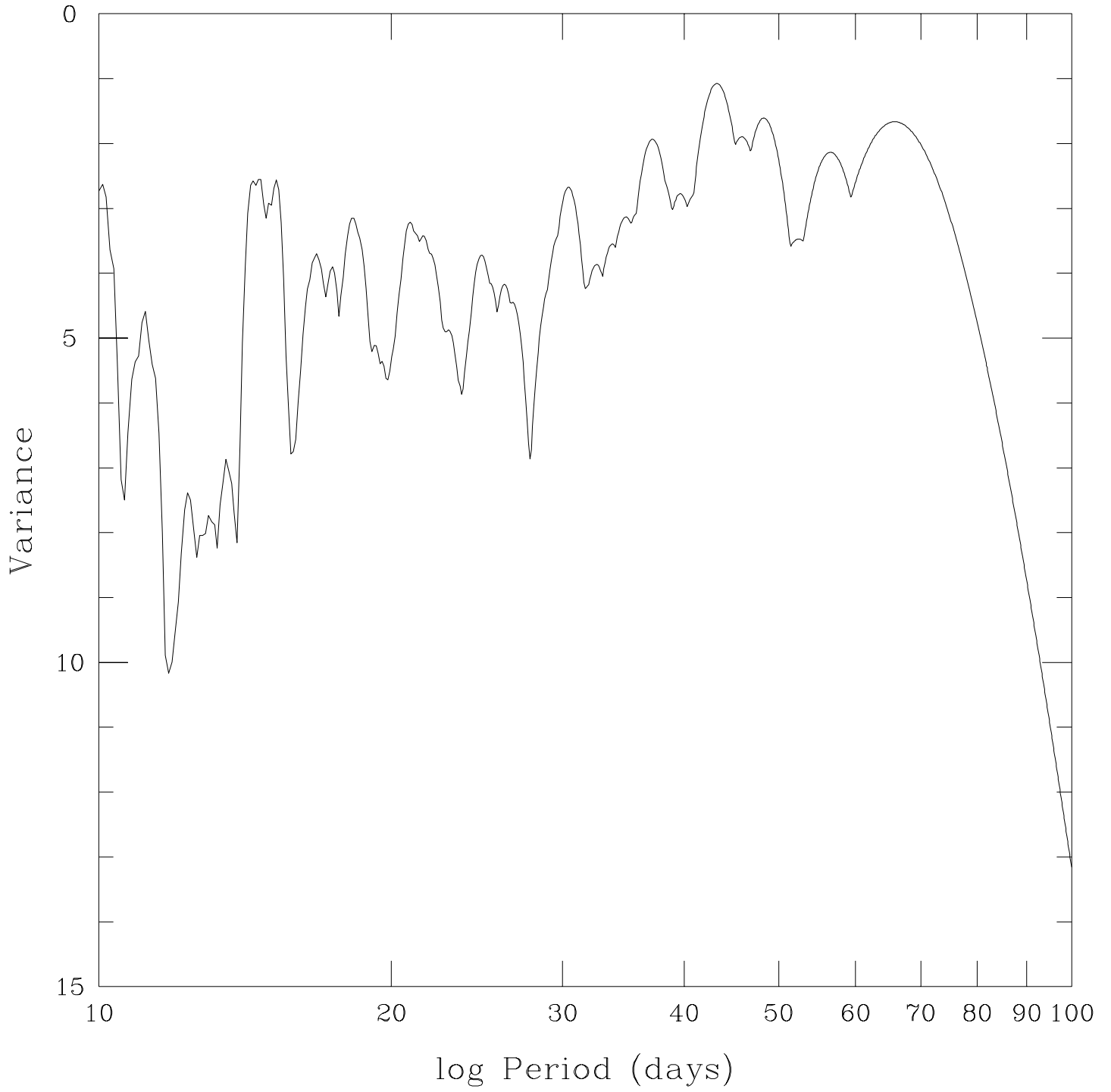


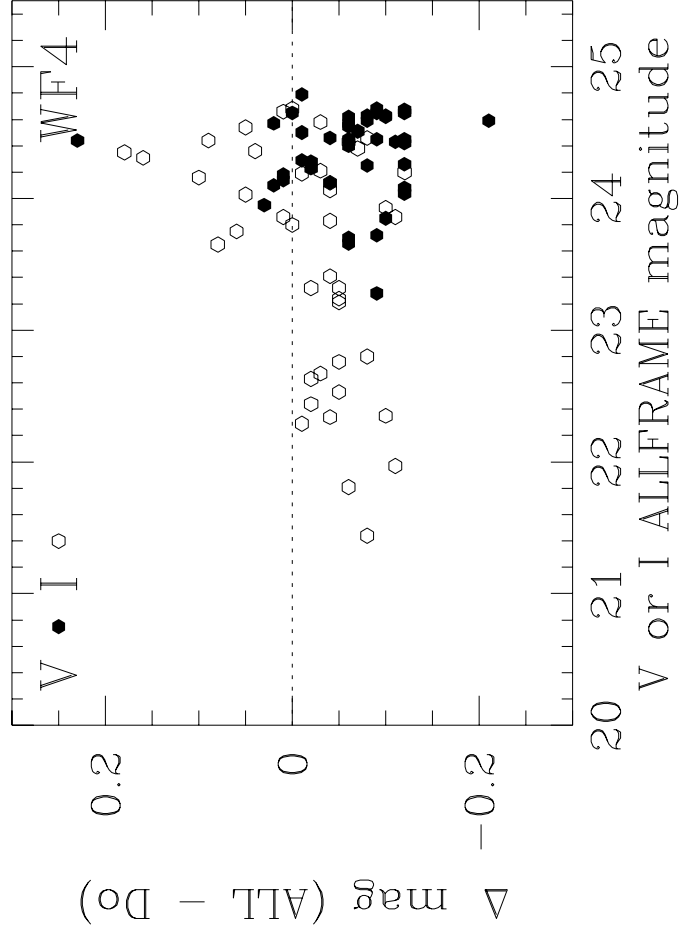
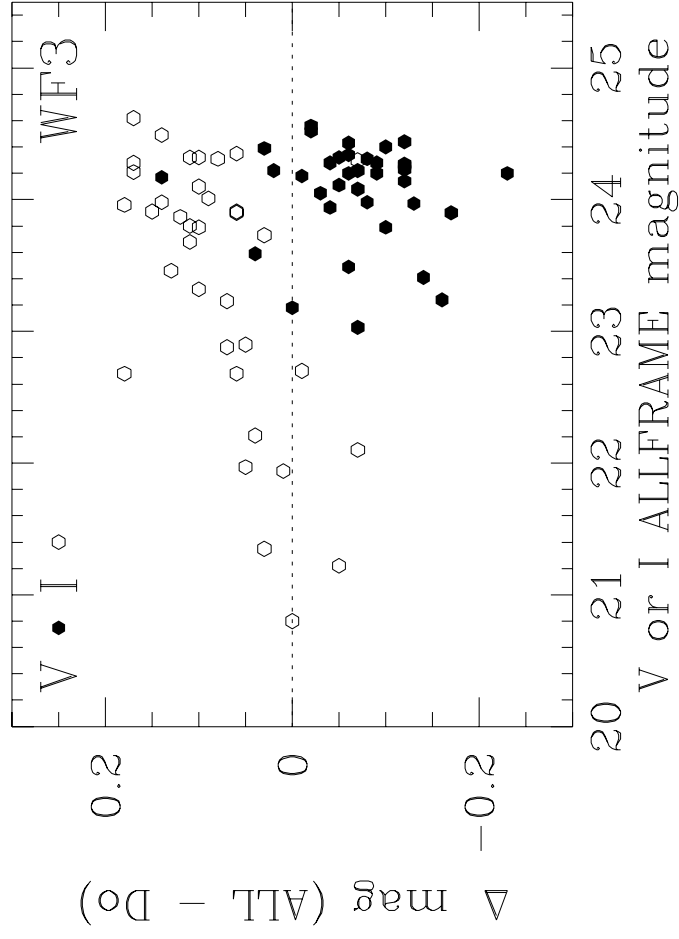
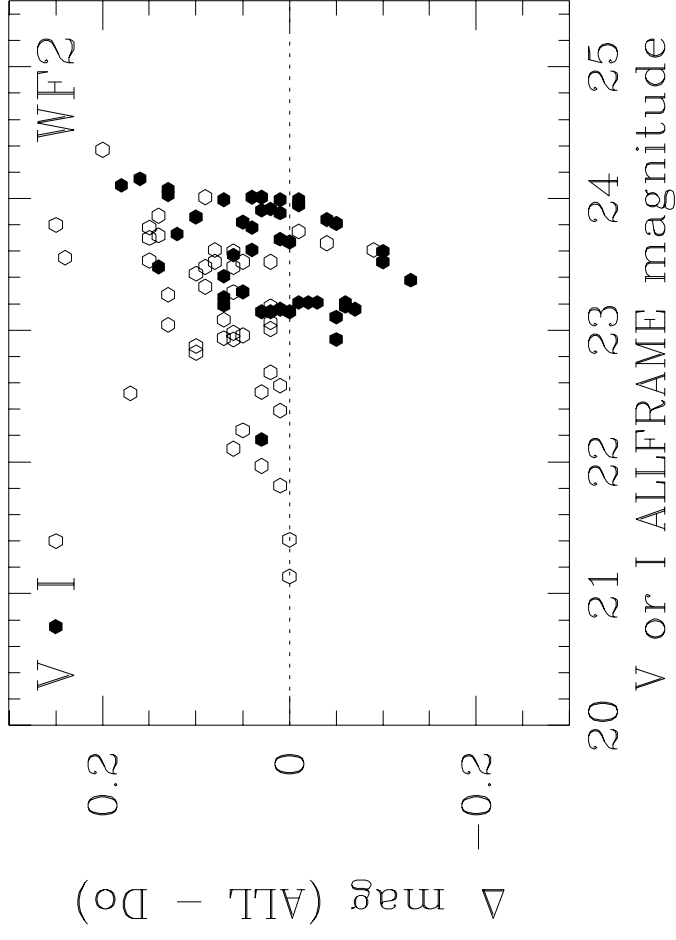
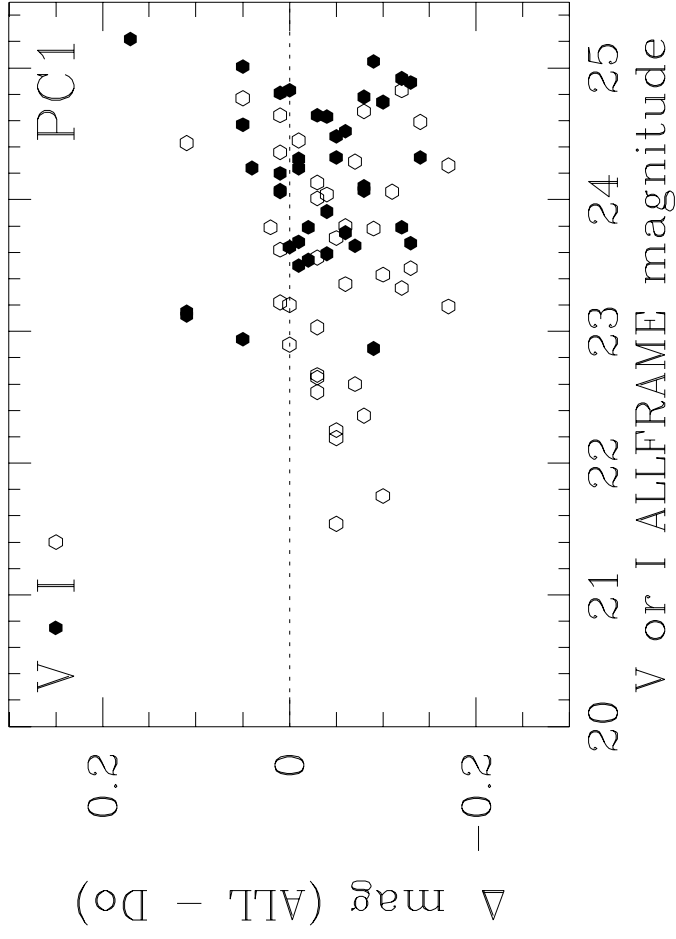
This figure "fig1.jpg" is available in "jpg" format from:

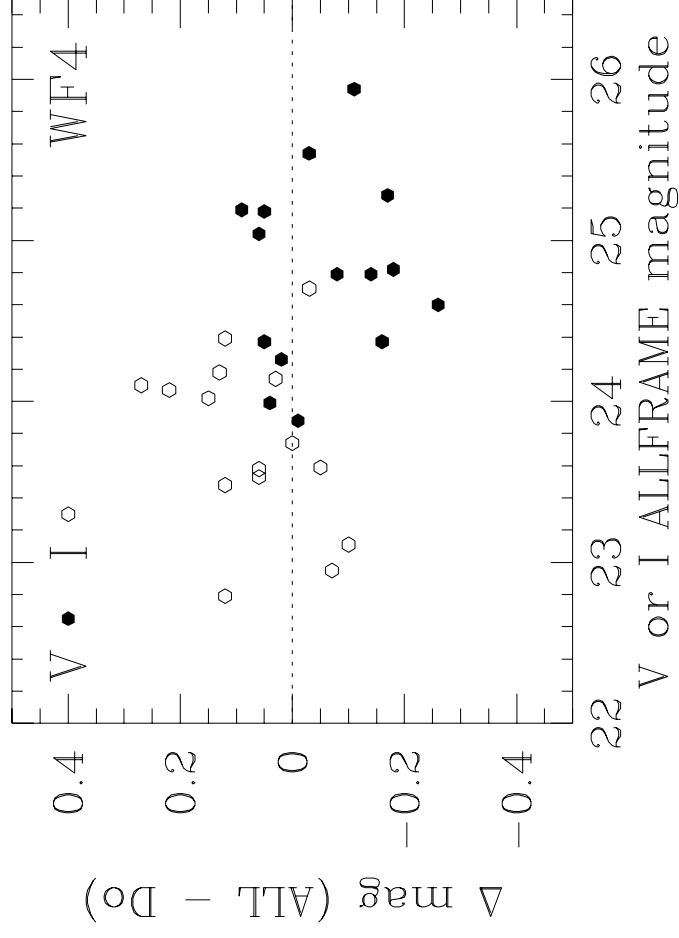
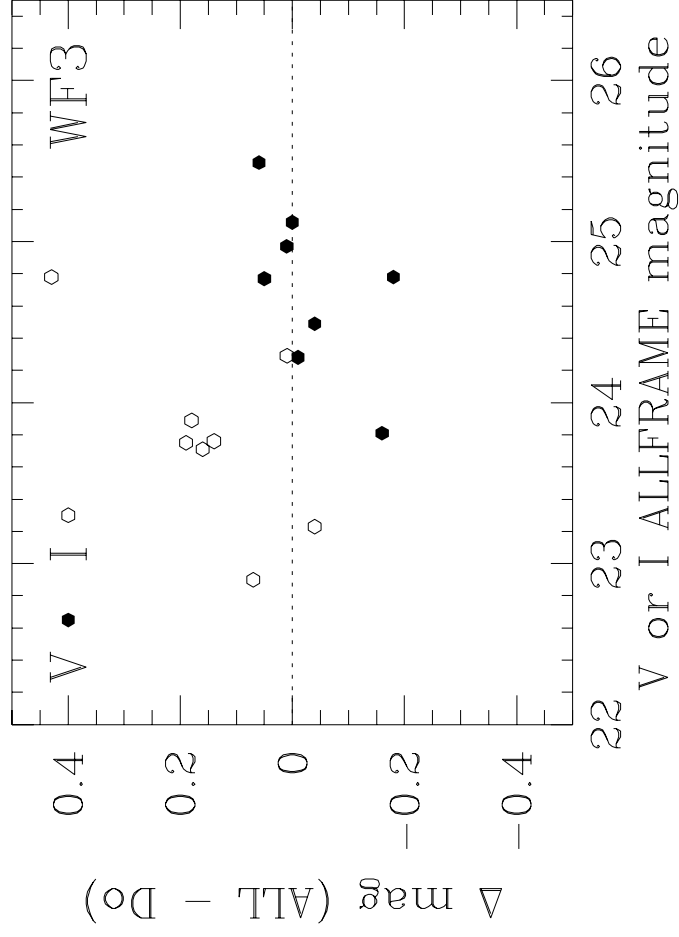
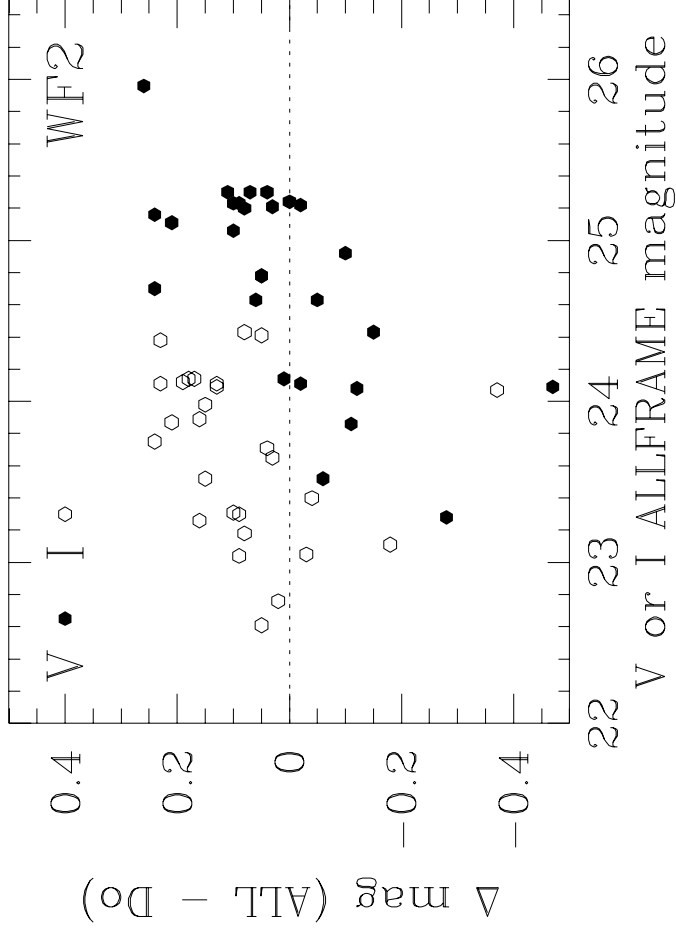
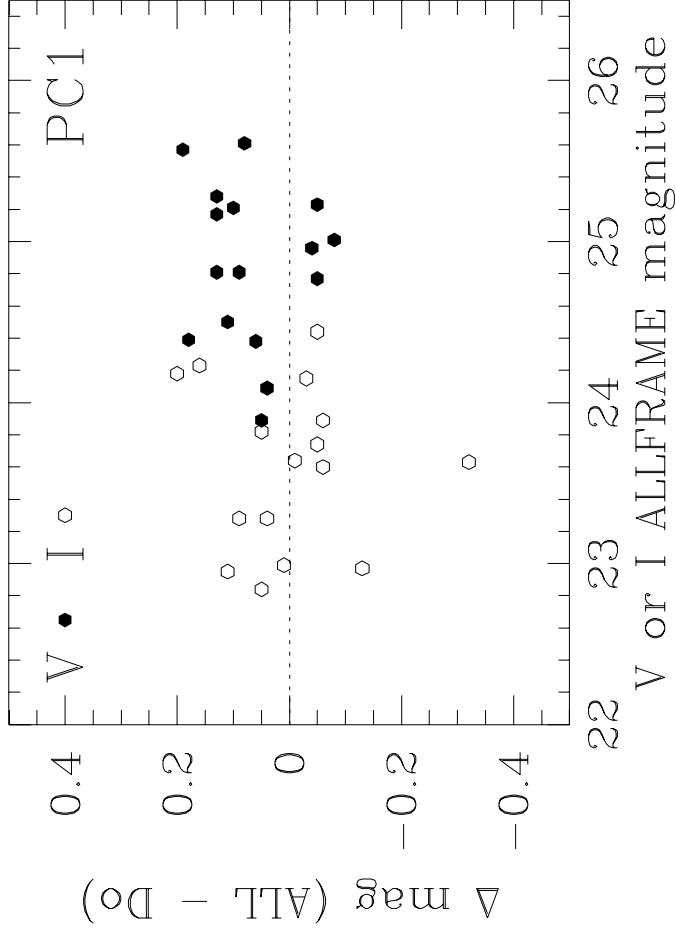
<http://arxiv.org/ps/astro-ph/9705259v1>

This figure "fig2.jpg" is available in "jpg" format from:

<http://arxiv.org/ps/astro-ph/9705259v1>







This figure "fig6a.jpg" is available in "jpg" format from:

<http://arxiv.org/ps/astro-ph/9705259v1>

This figure "fig6b.jpg" is available in "jpg" format from:

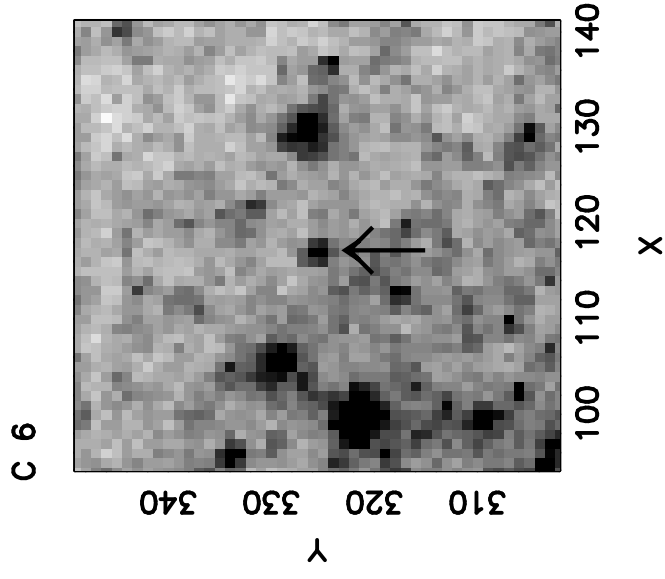
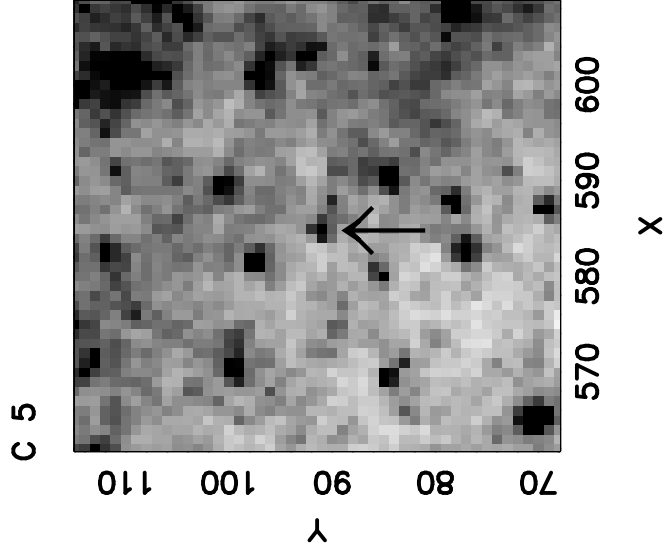
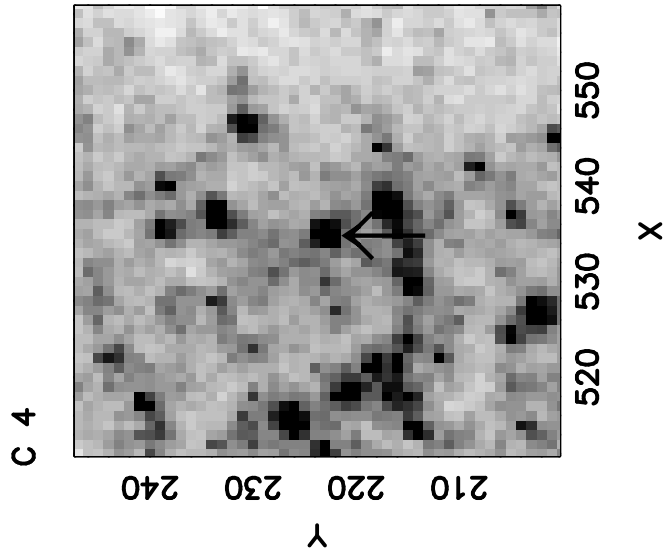
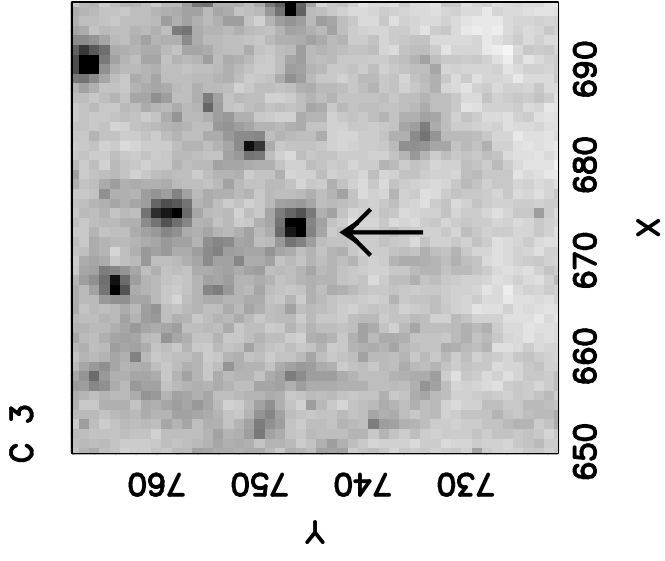
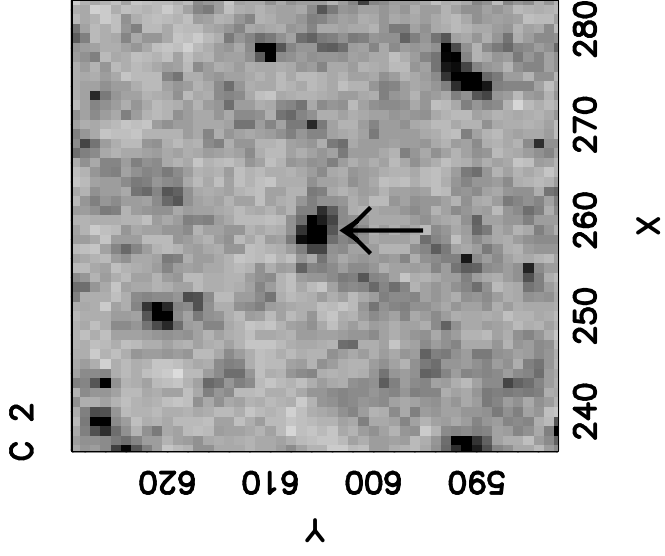
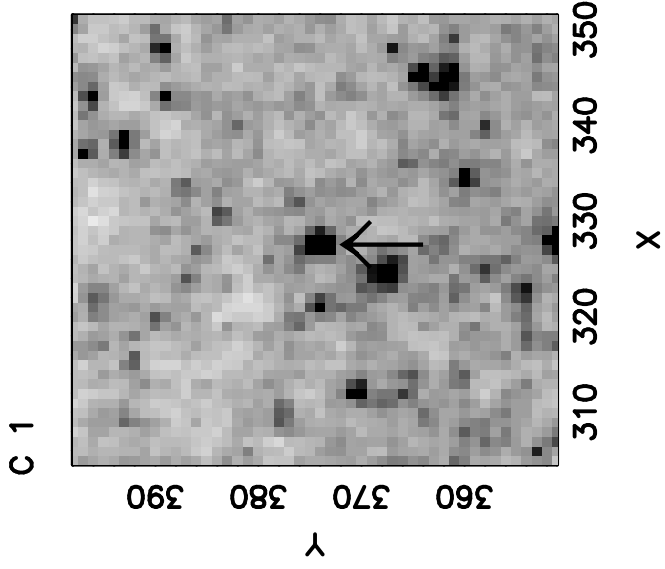
<http://arxiv.org/ps/astro-ph/9705259v1>

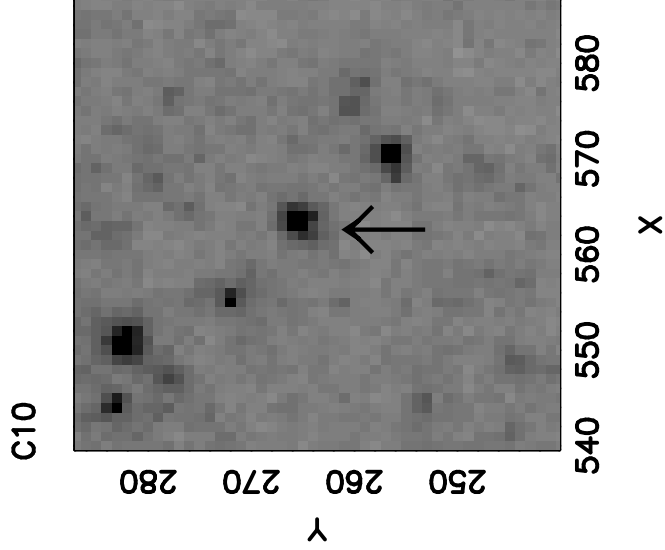
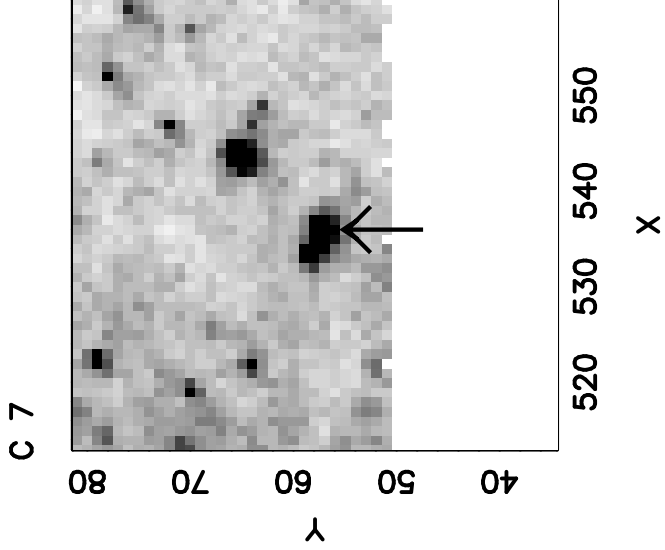
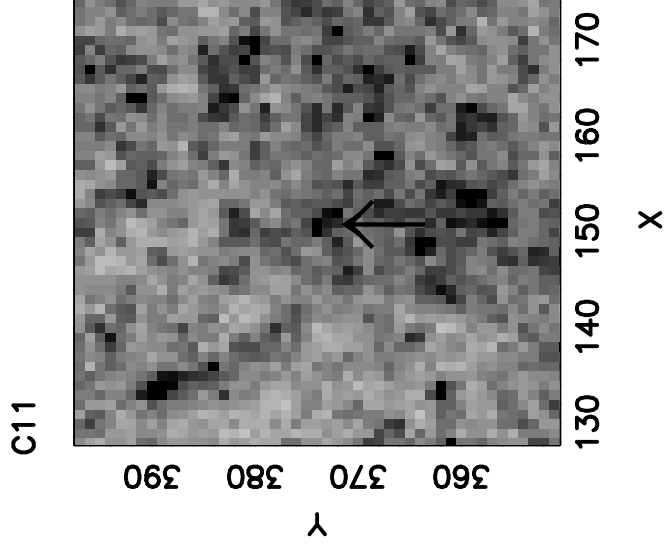
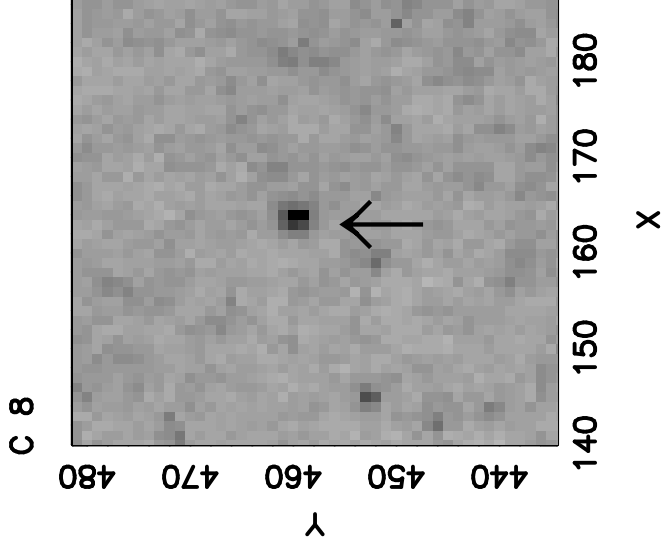
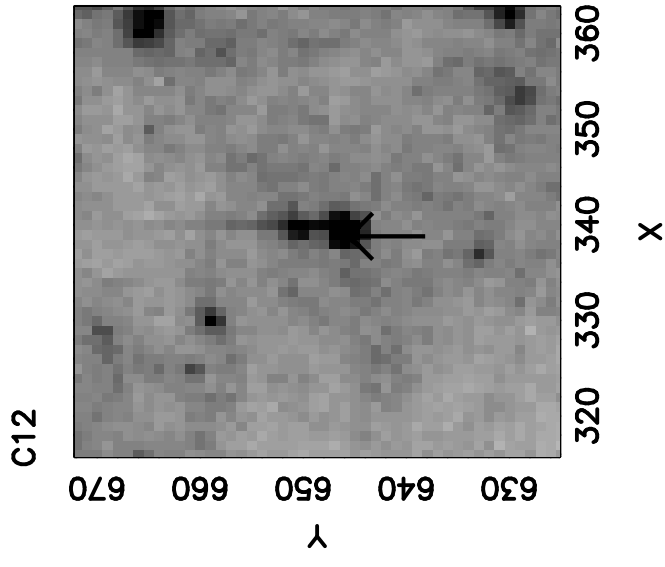
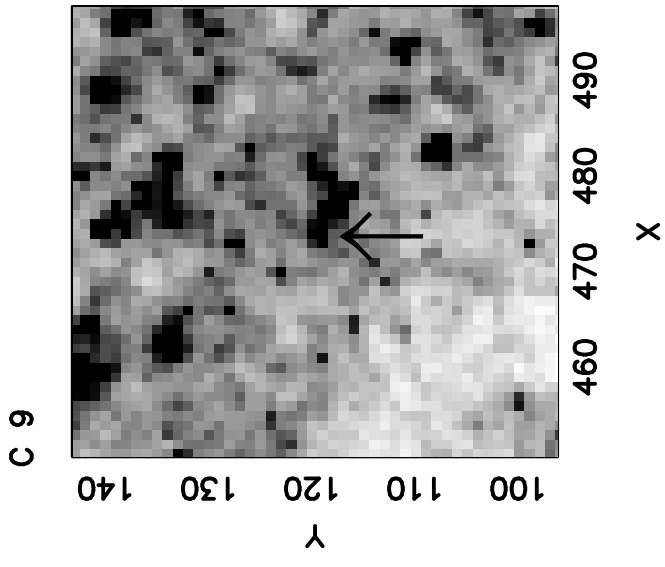
This figure "fig6c.jpg" is available in "jpg" format from:

<http://arxiv.org/ps/astro-ph/9705259v1>

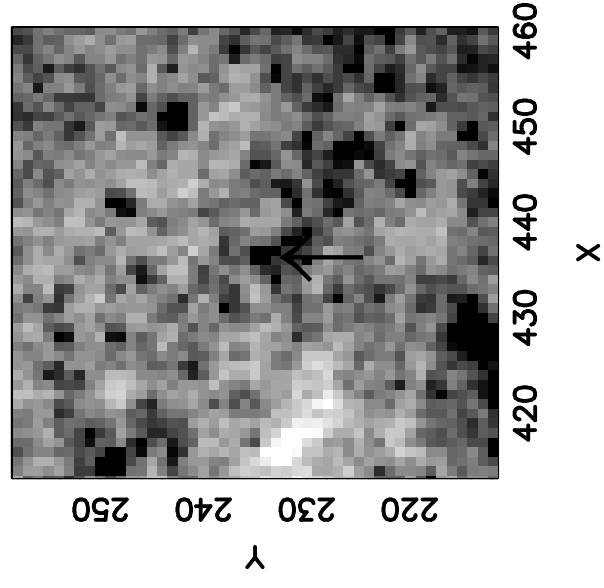
This figure "fig6d.jpg" is available in "jpg" format from:

<http://arxiv.org/ps/astro-ph/9705259v1>

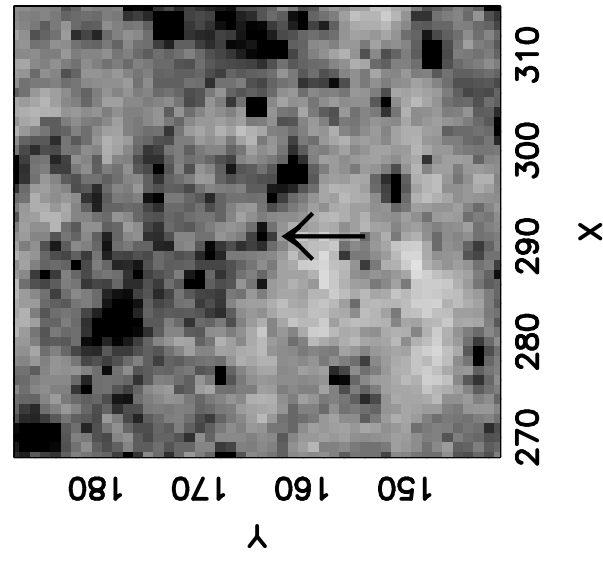




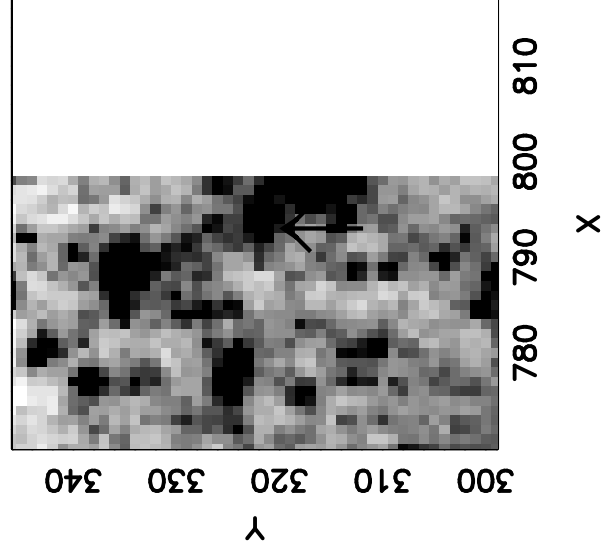
C15



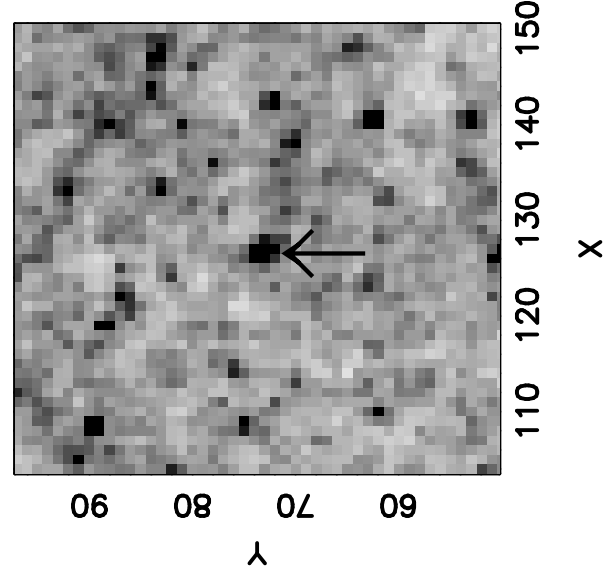
C18



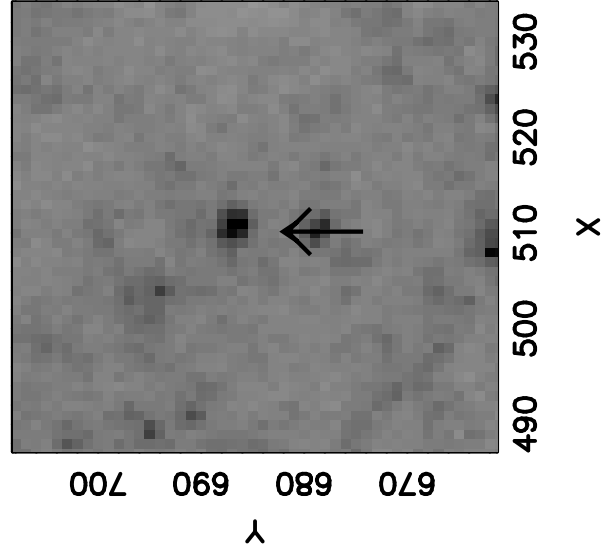
C14



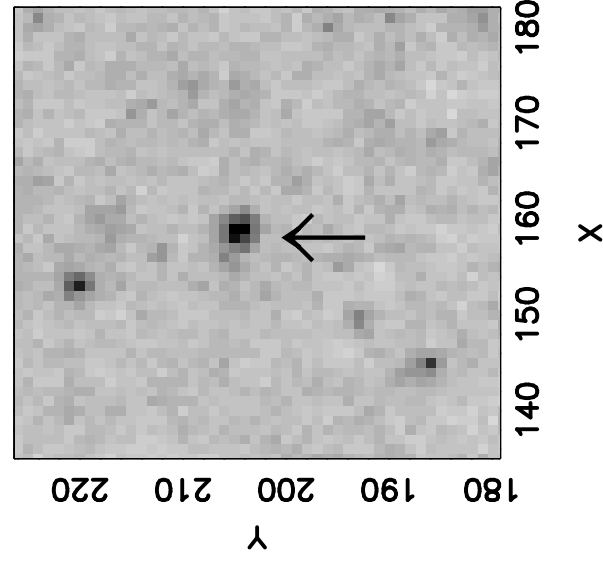
C17

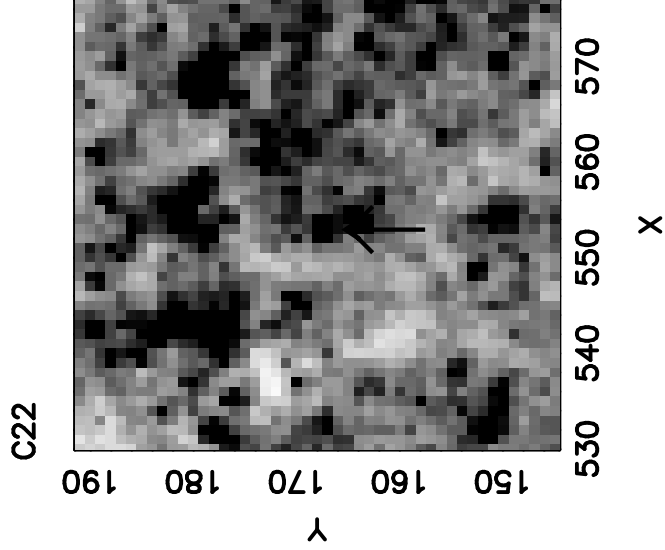
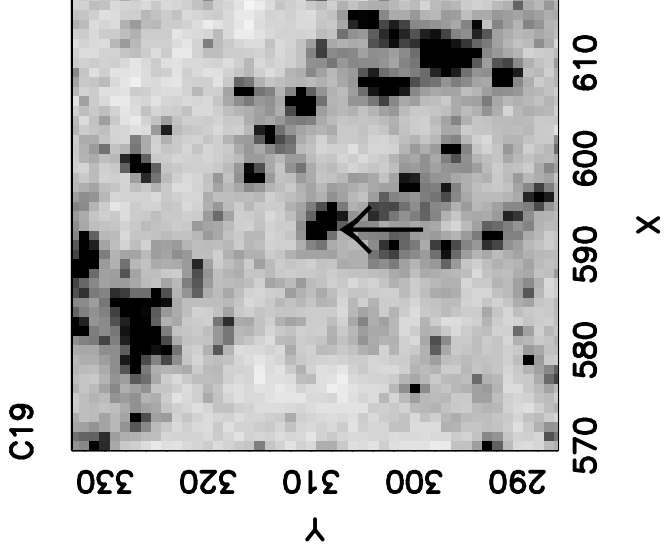
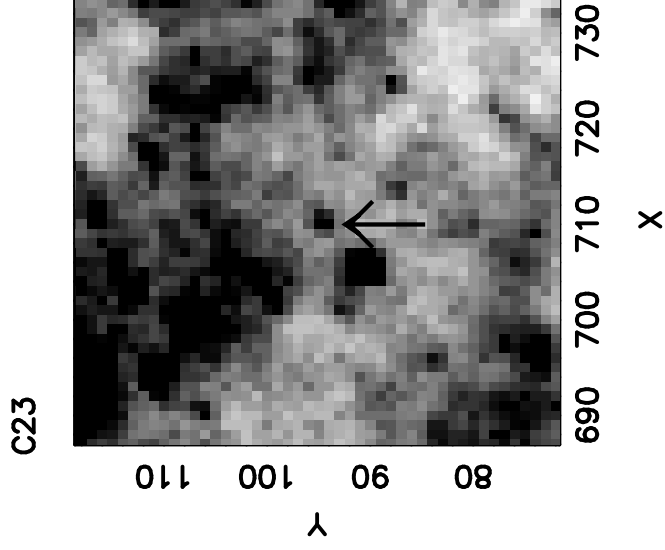
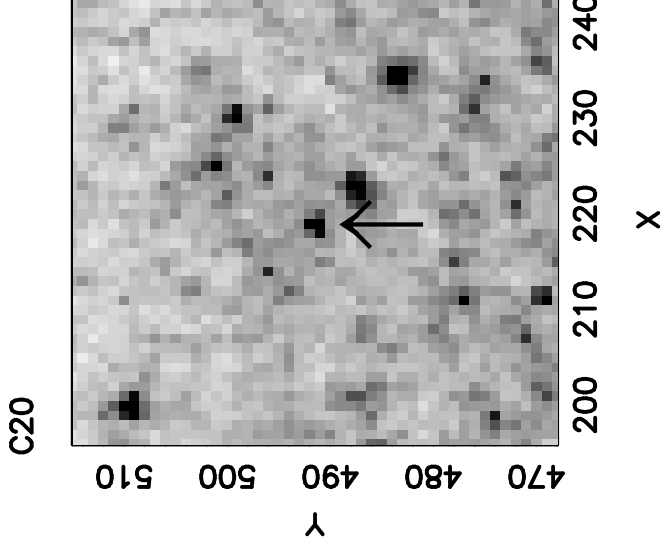
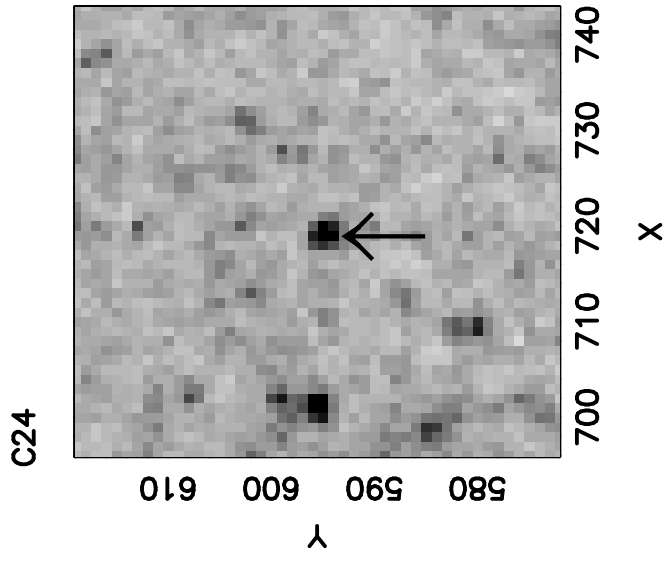
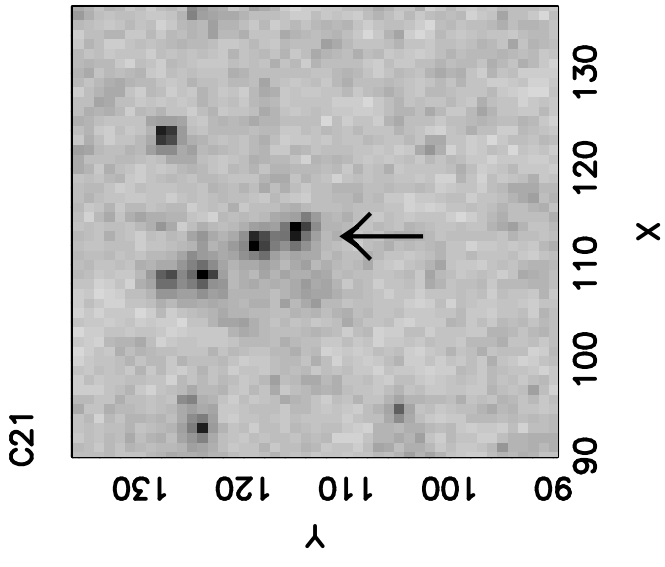


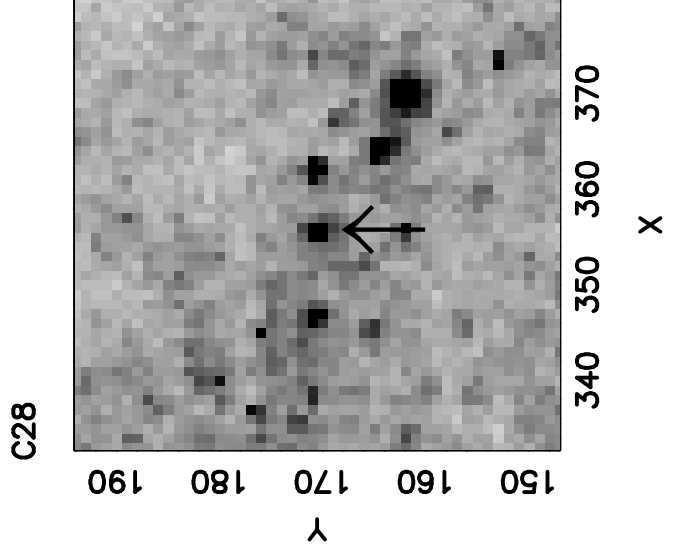
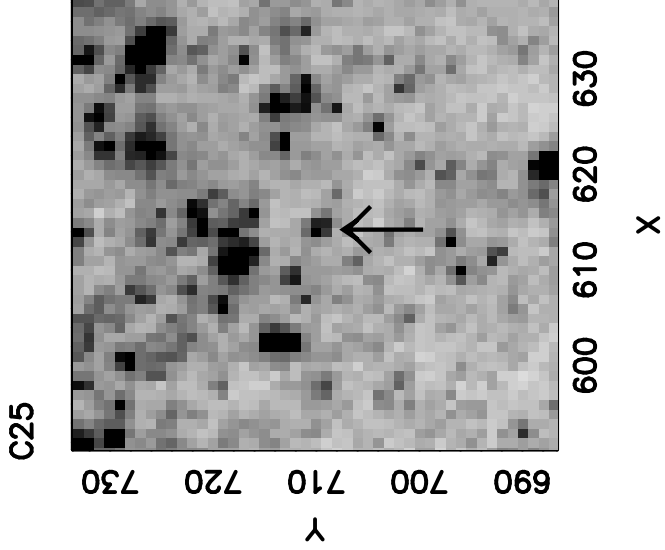
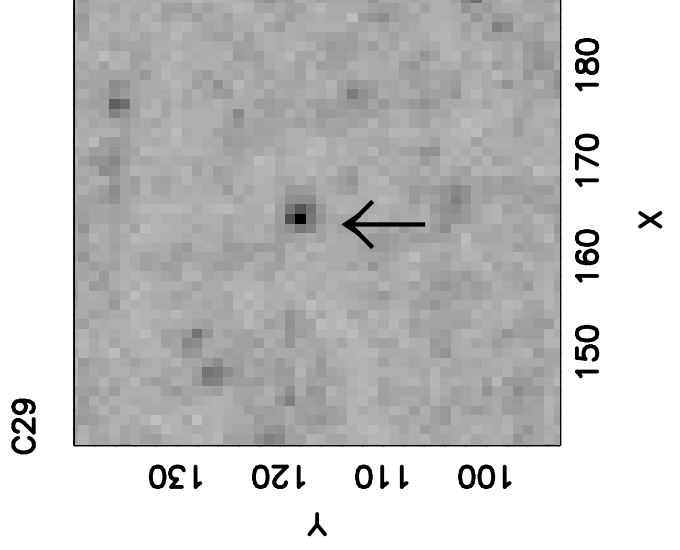
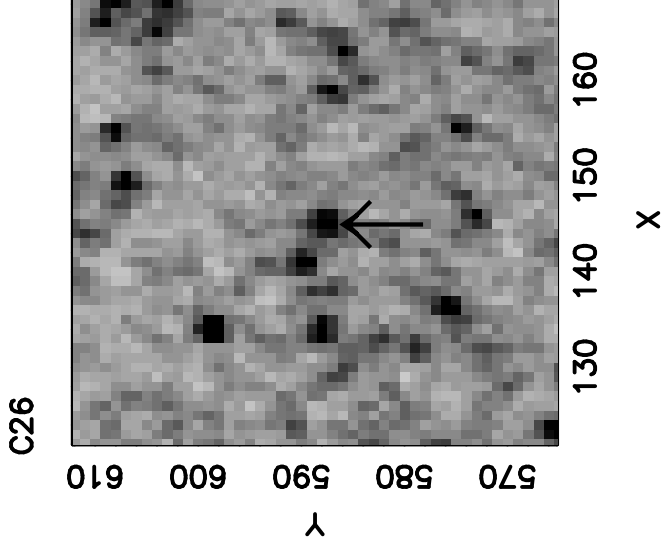
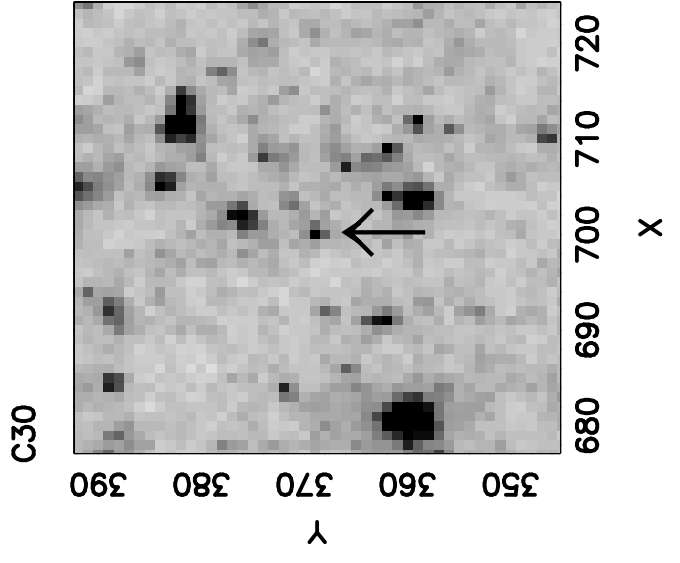
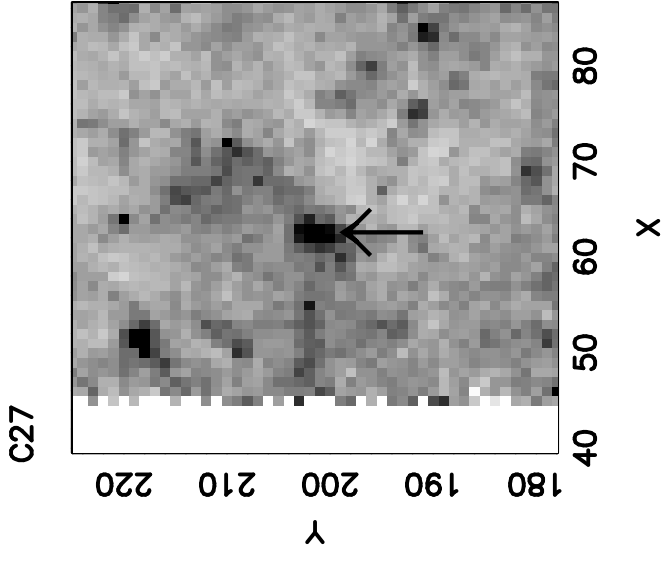
C13



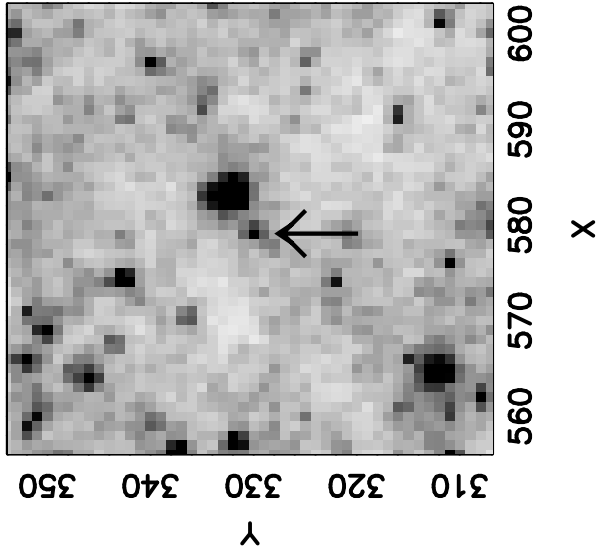
C16



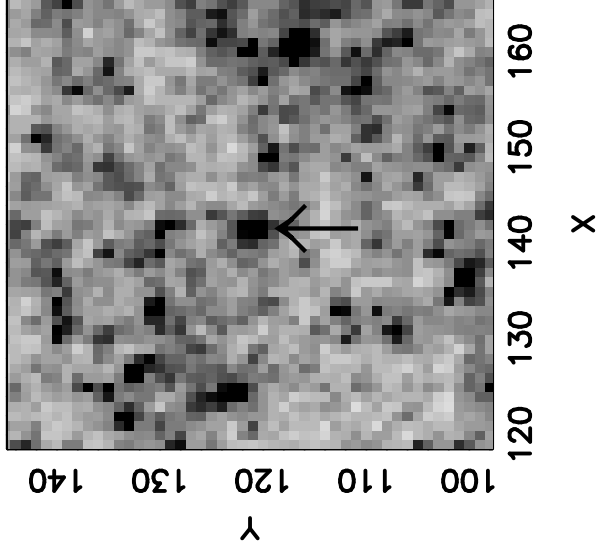




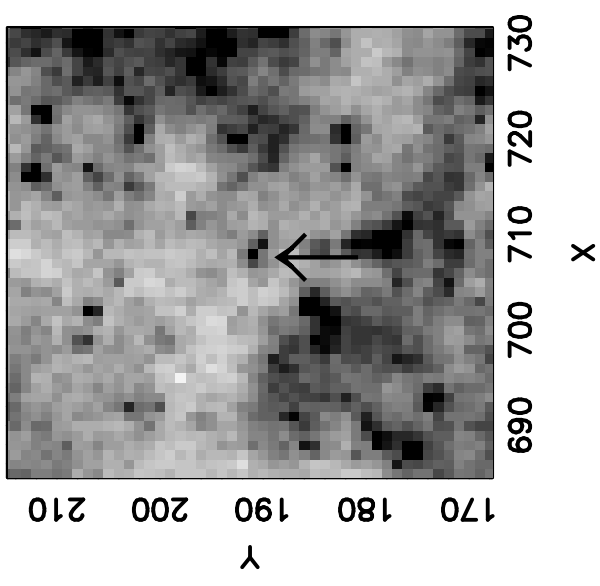
C31



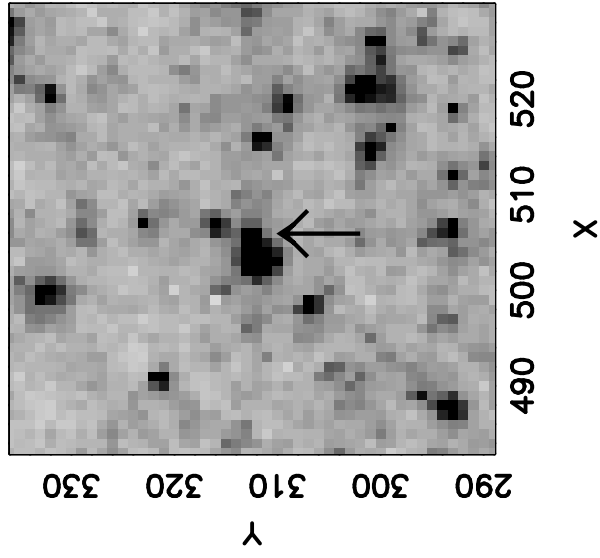
C32



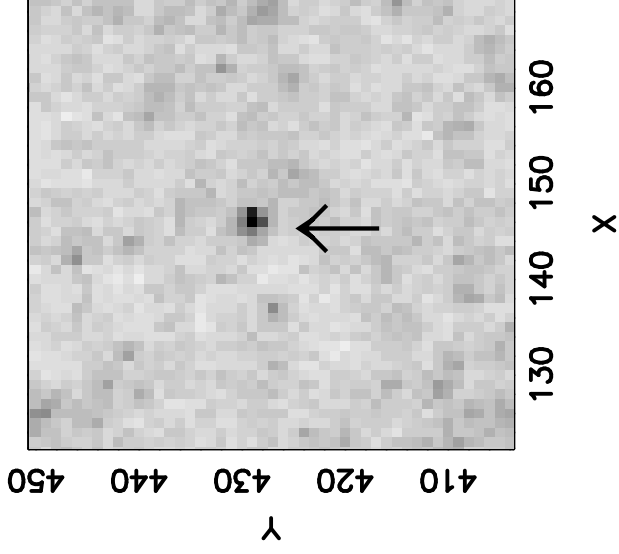
C33



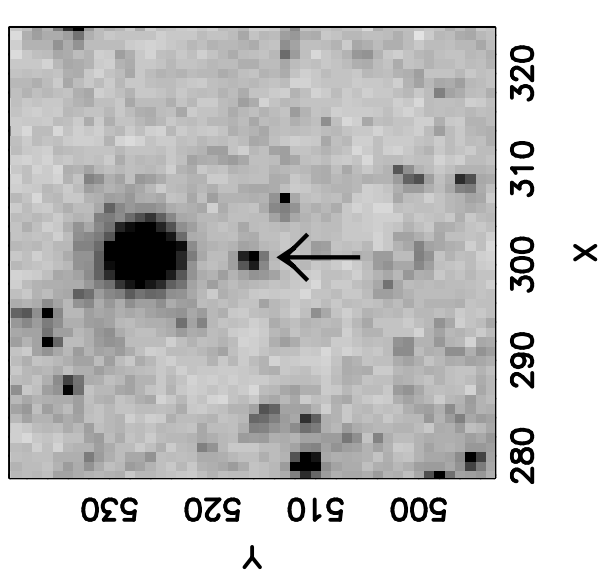
C34



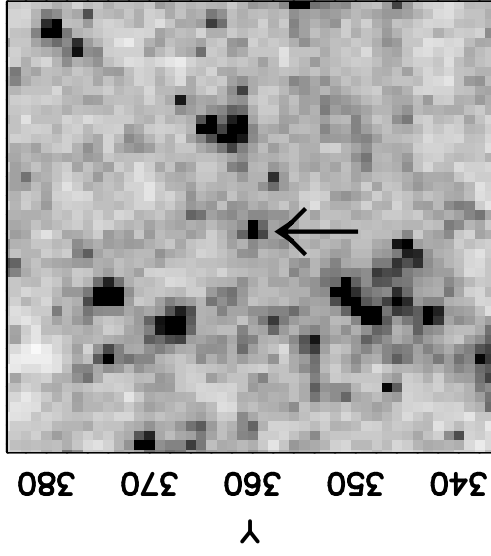
C35



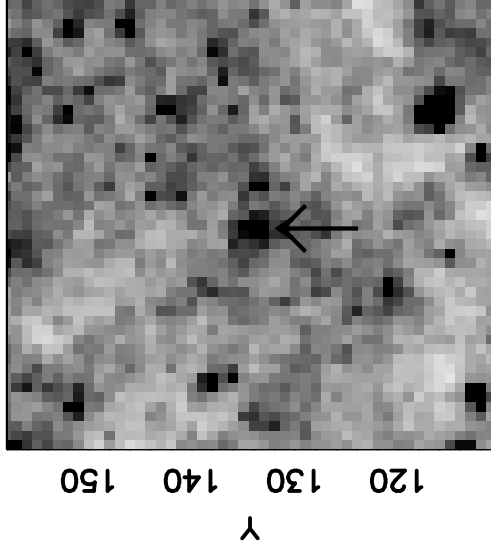
C36



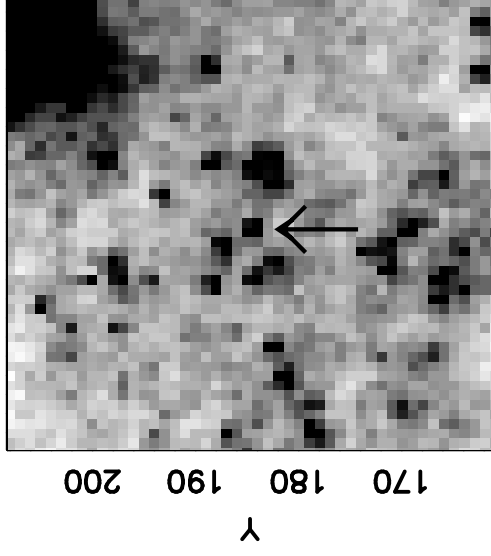
C37



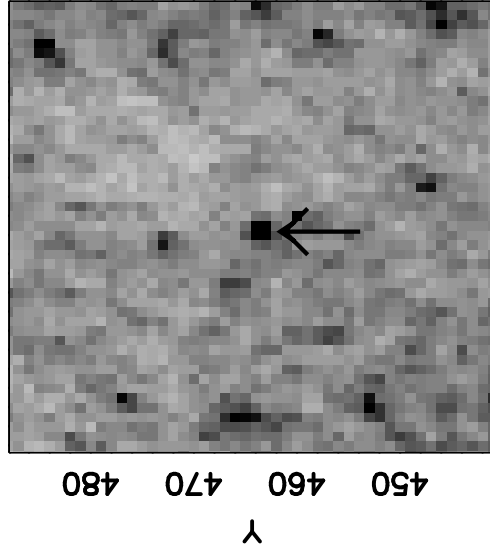
C38



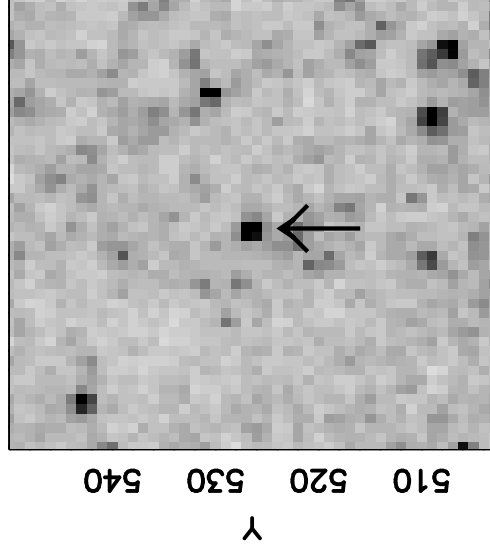
C39



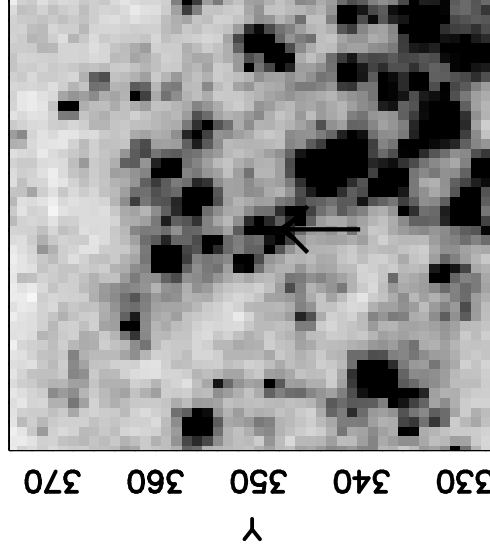
C40



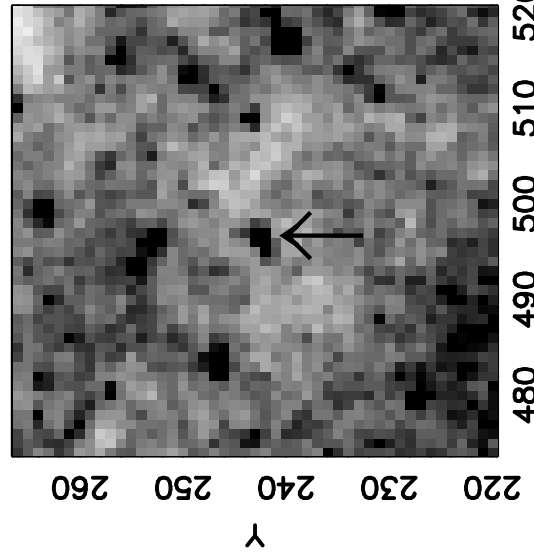
C41



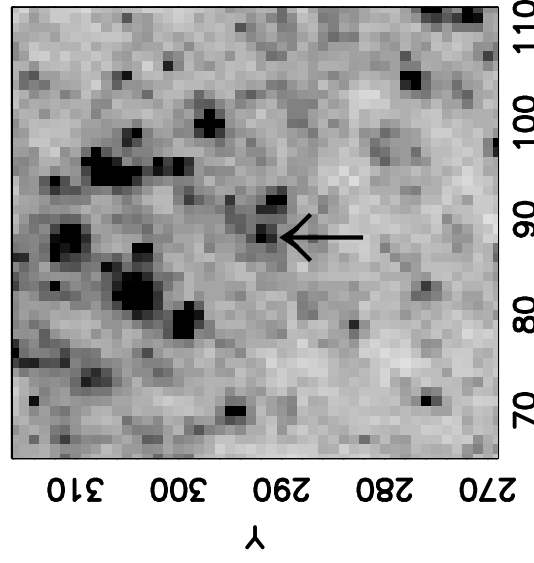
C42



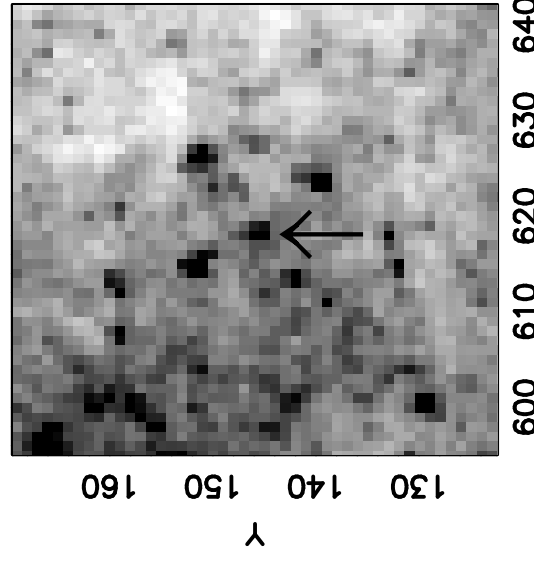
C43



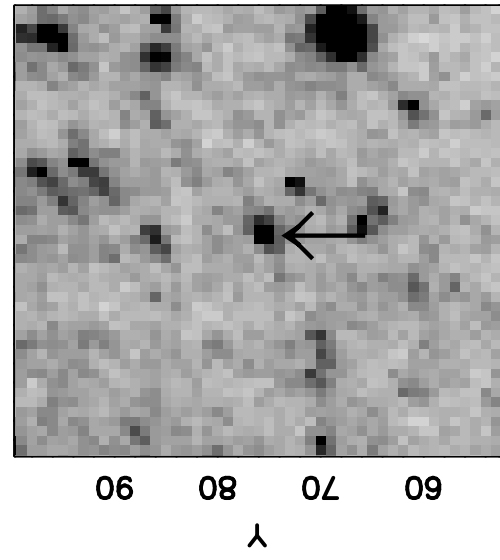
C44



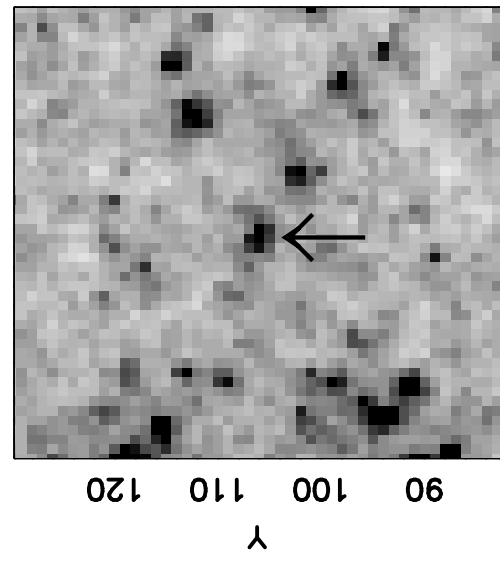
C45



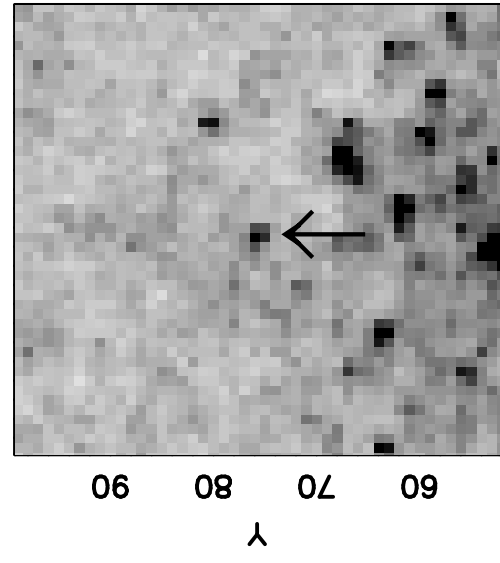
C46



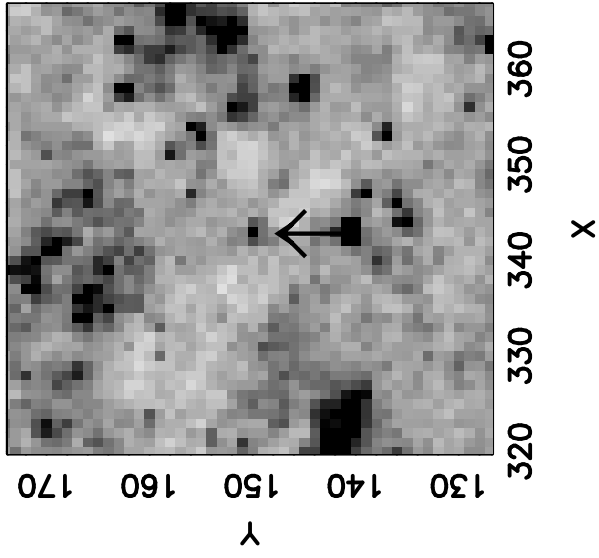
C47



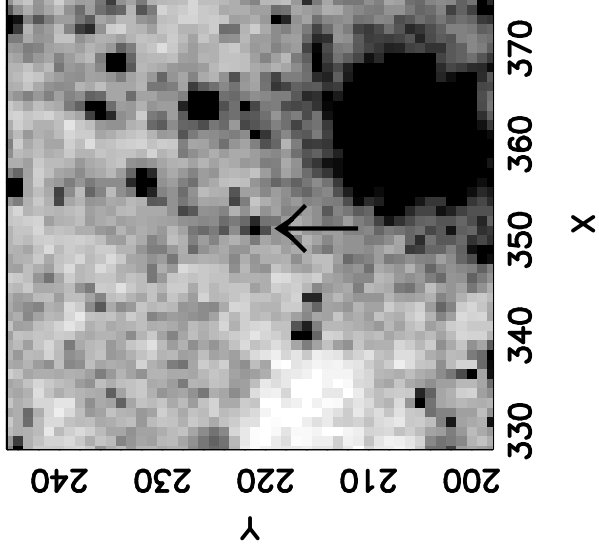
C48



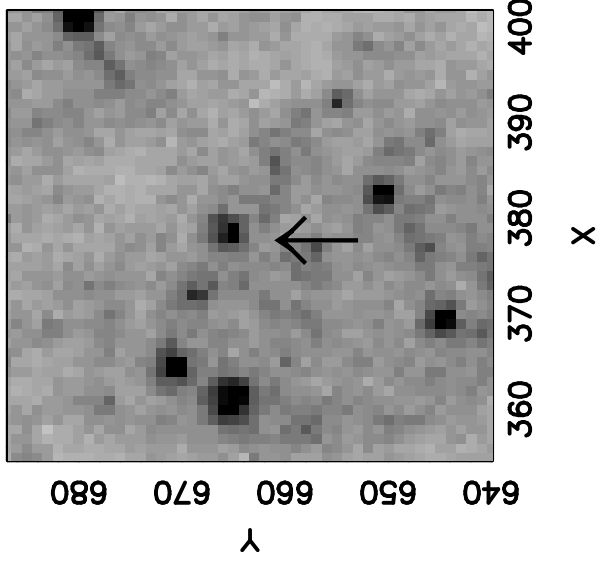
C49



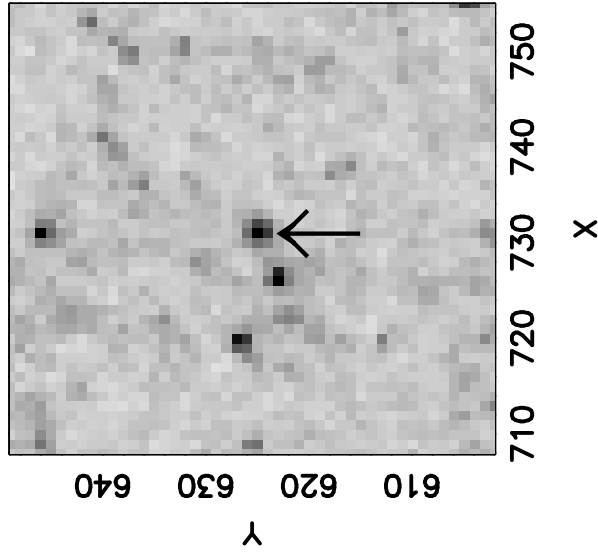
C50



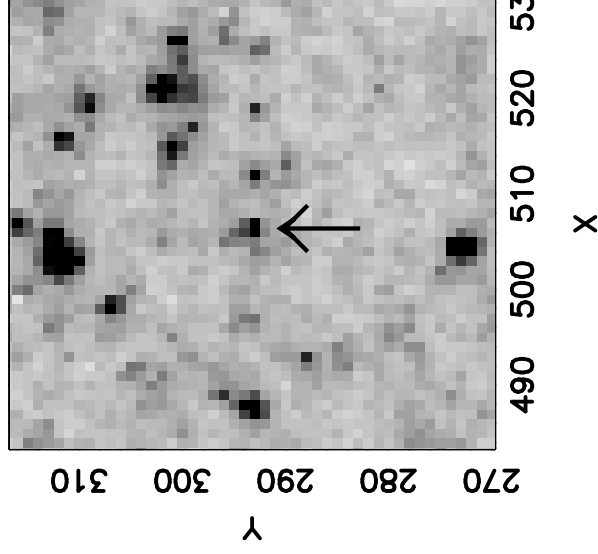
C51



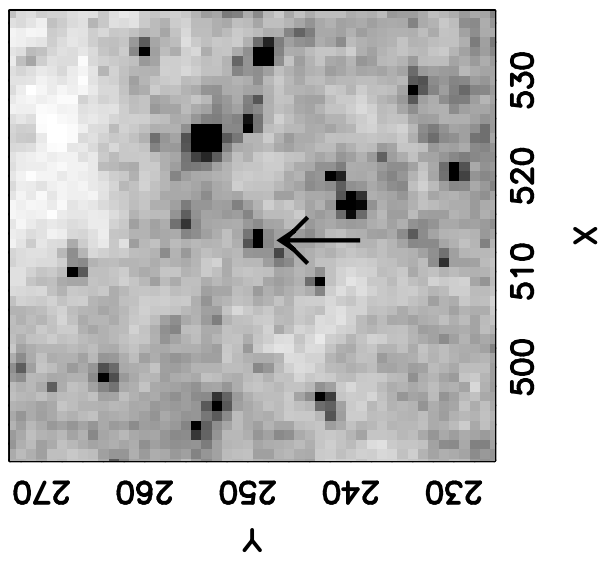
C52

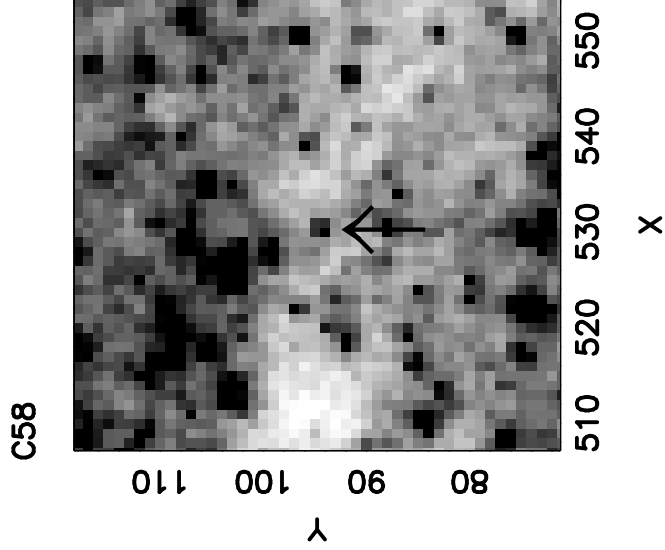
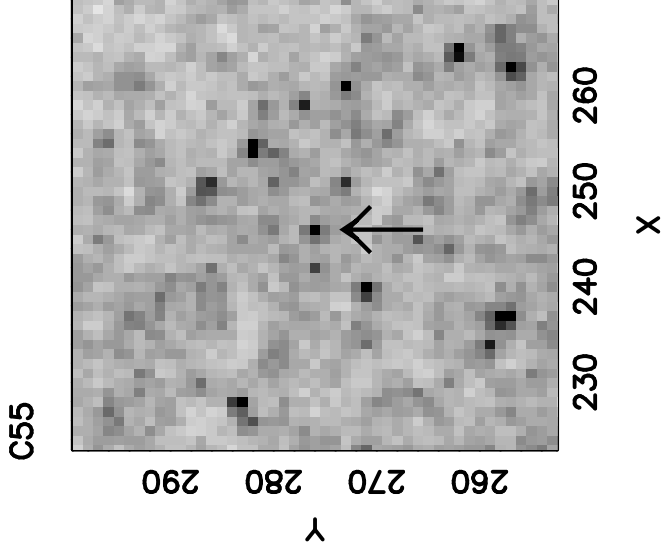
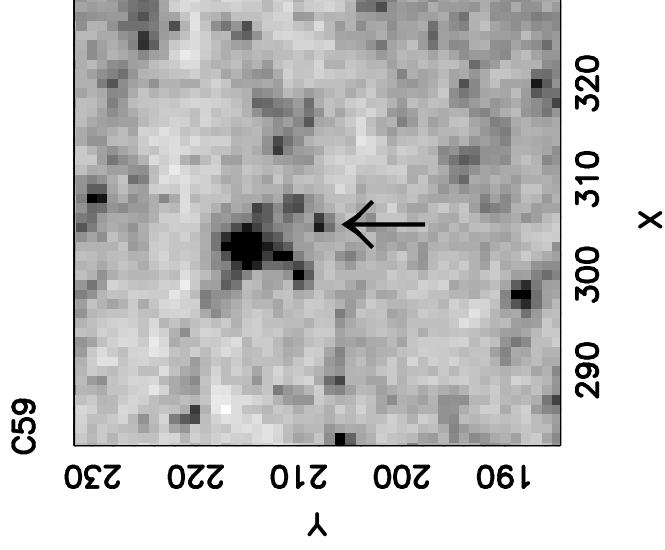
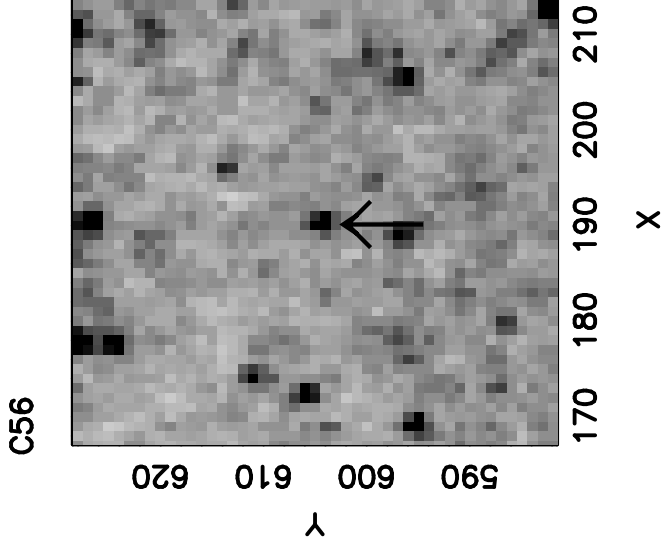
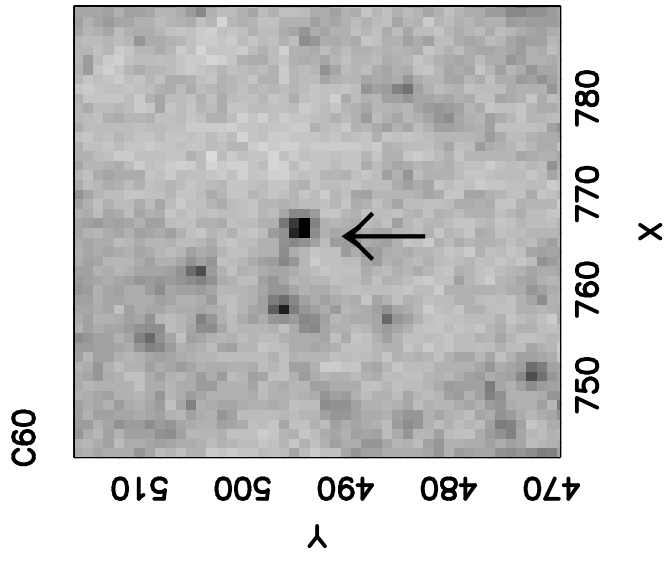
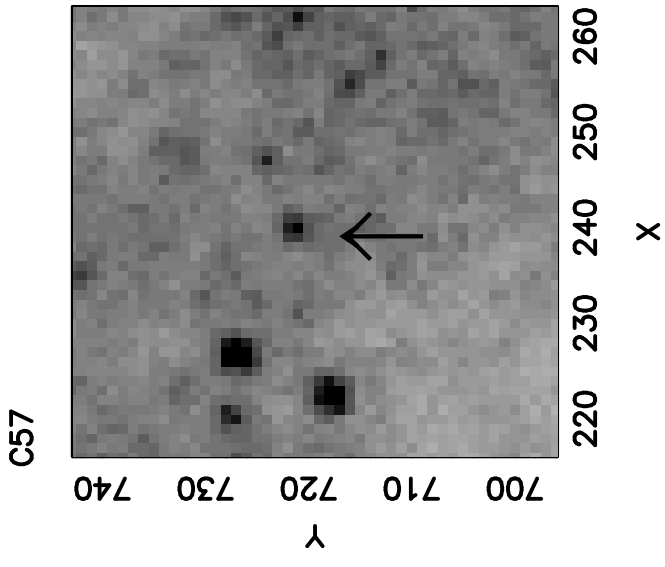


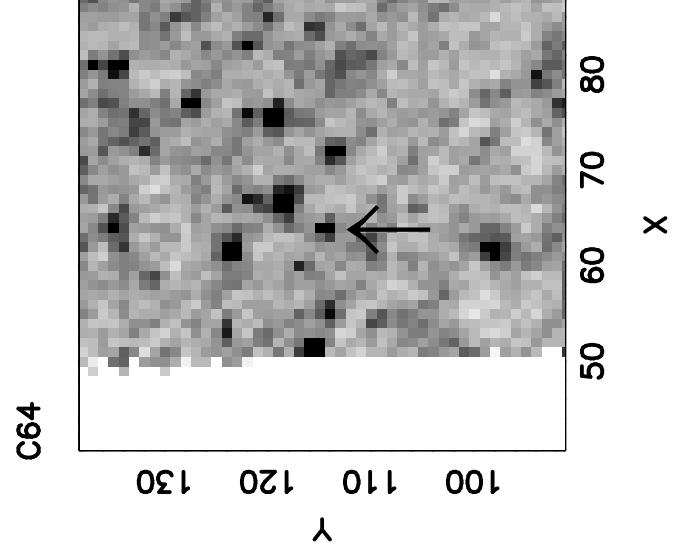
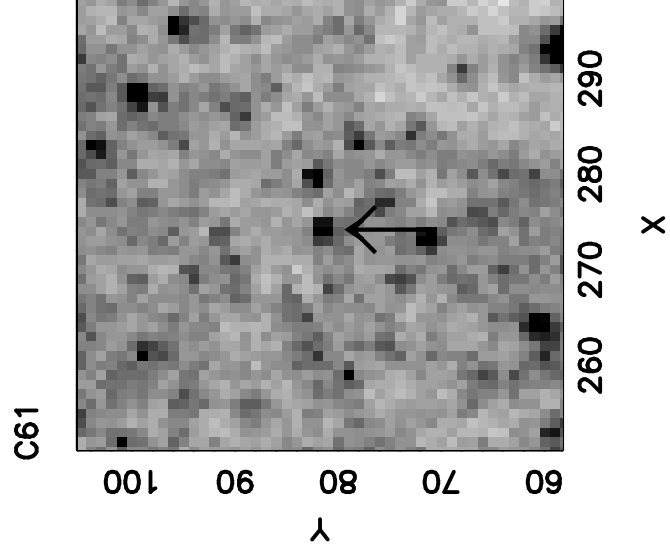
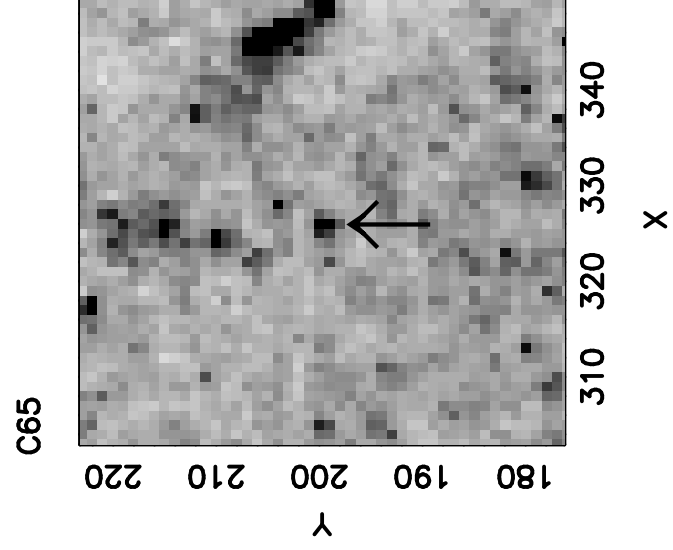
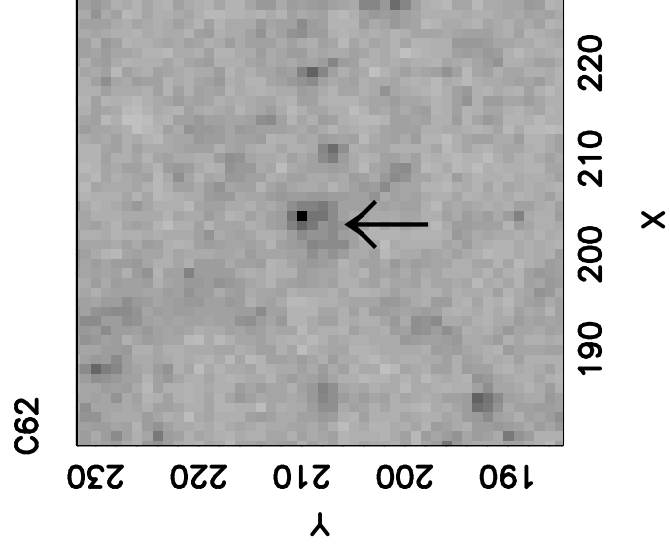
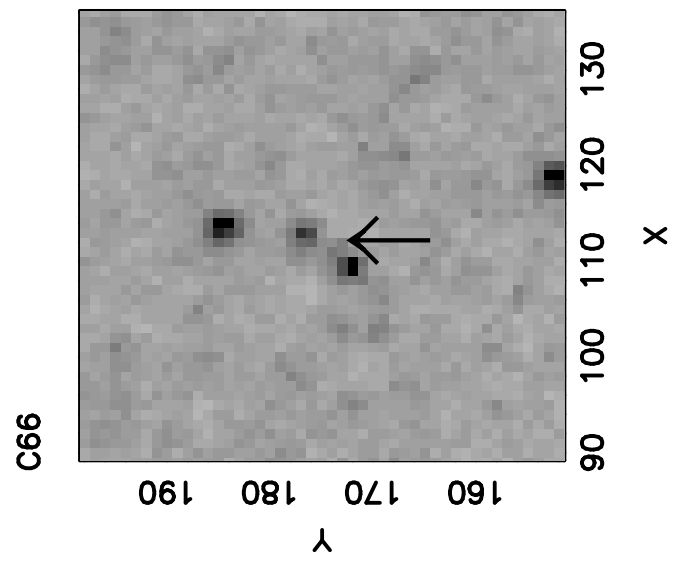
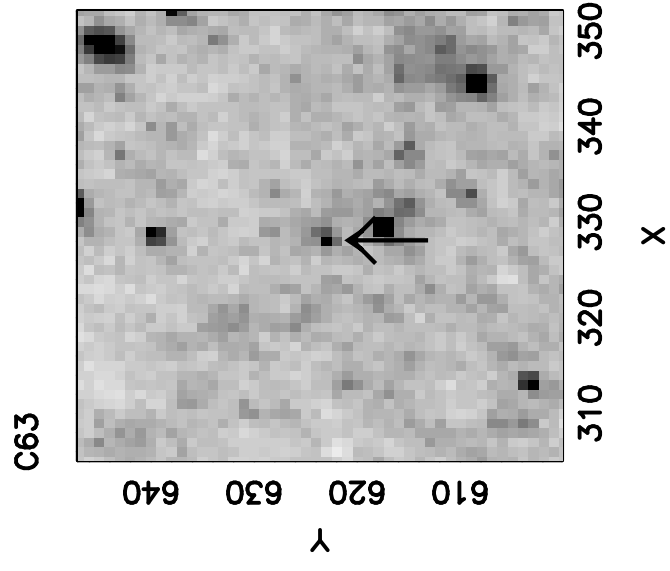
C53

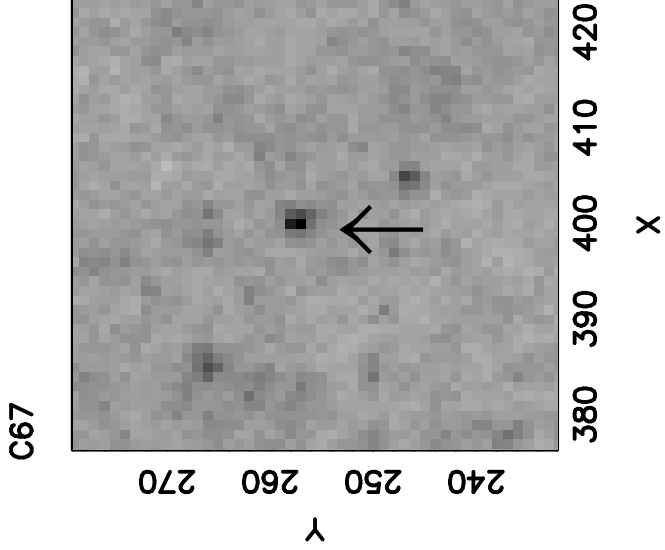
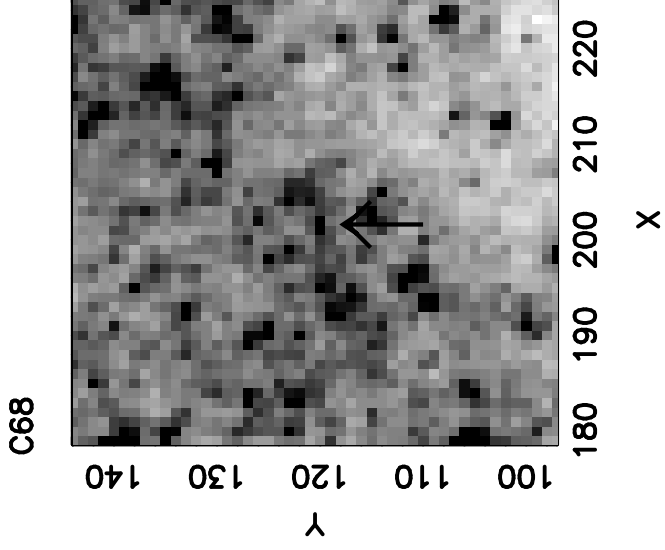
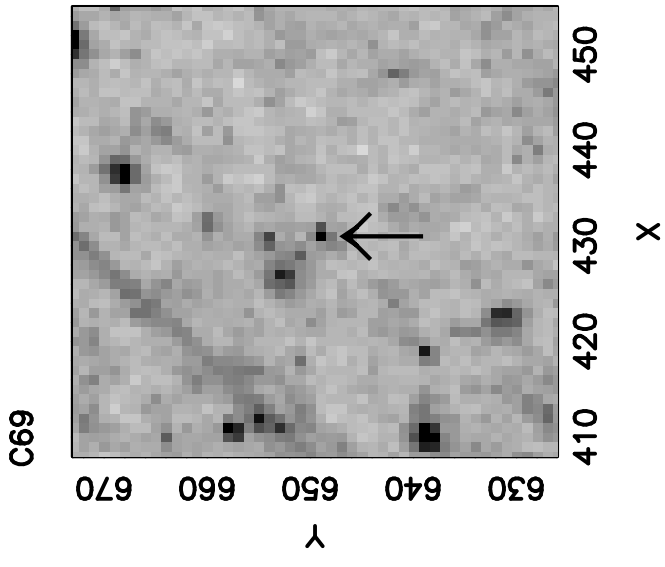


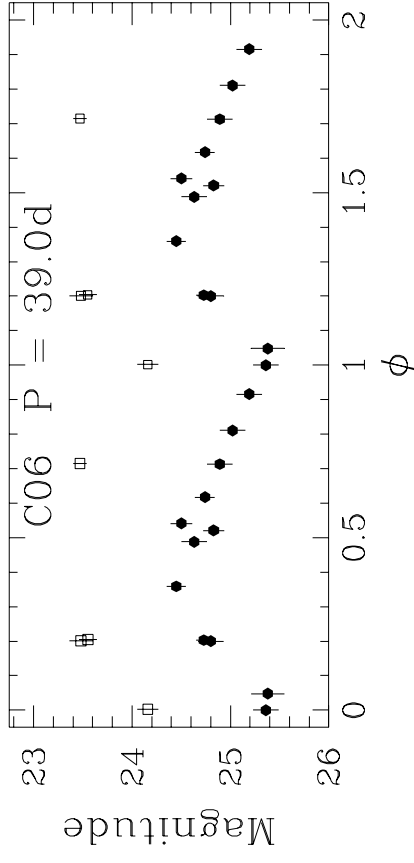
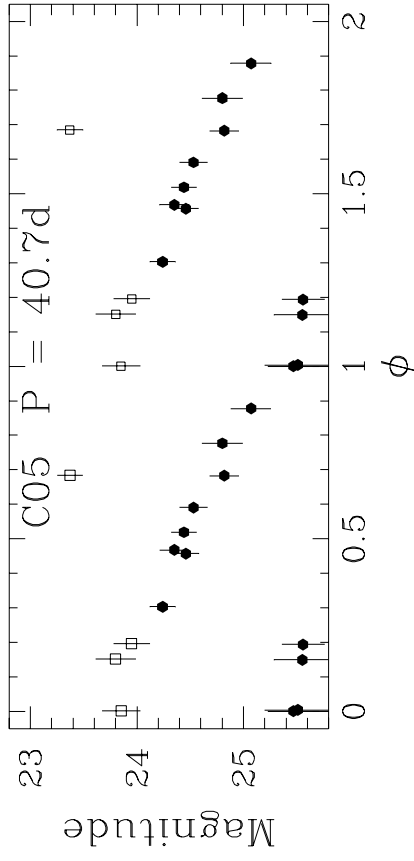
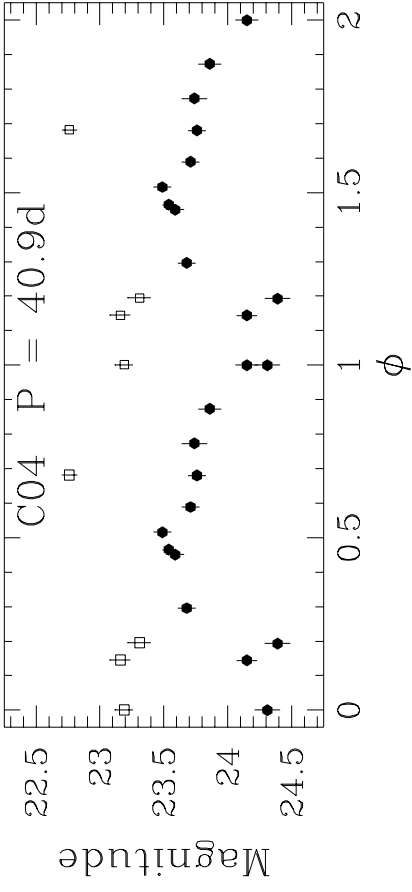
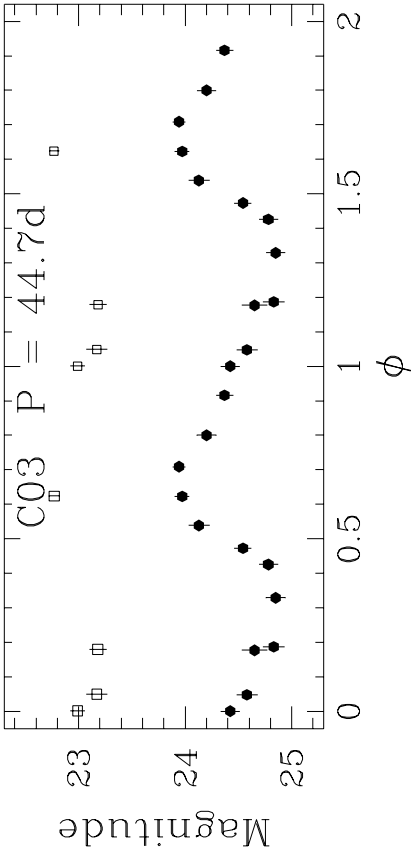
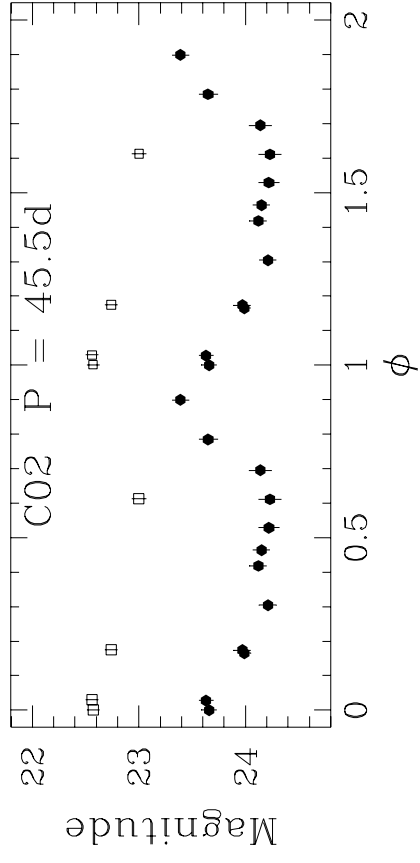
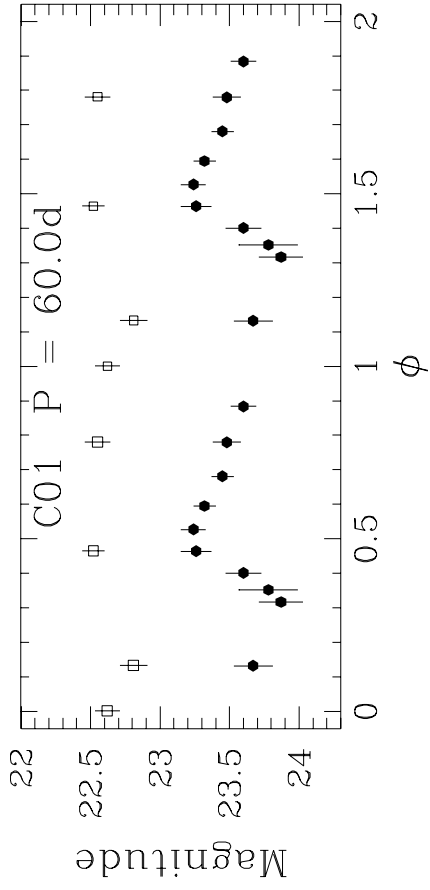
C54

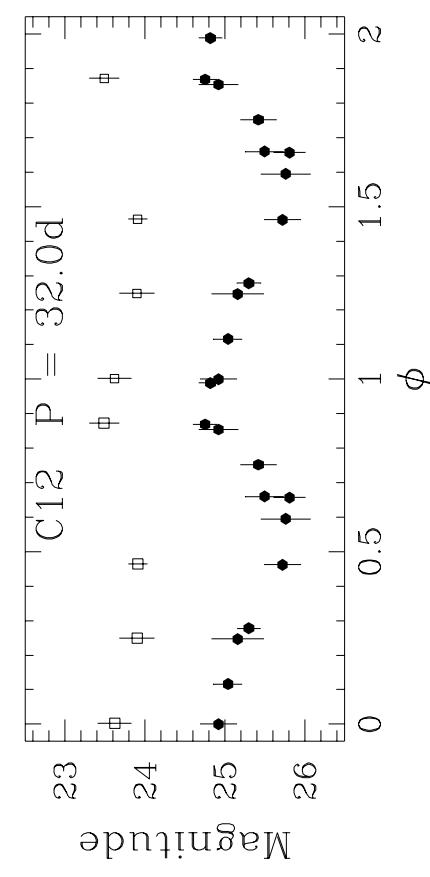
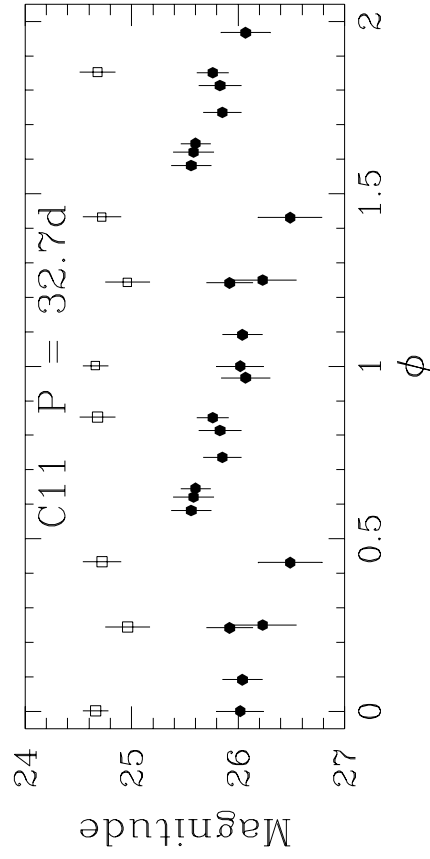
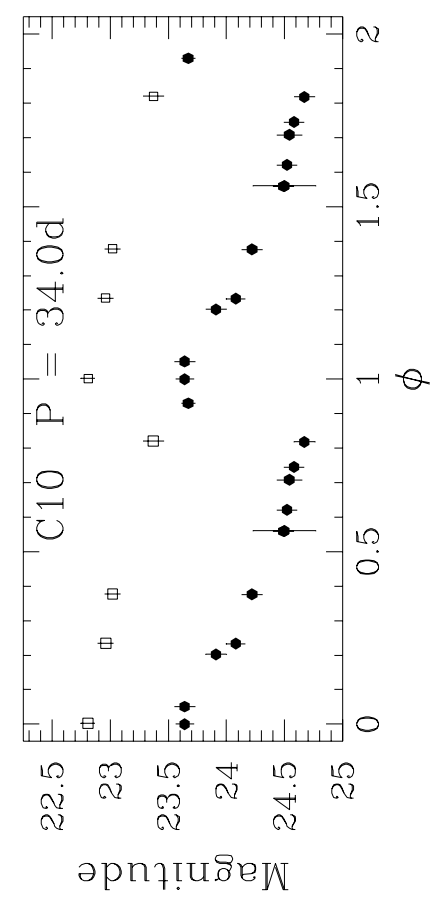
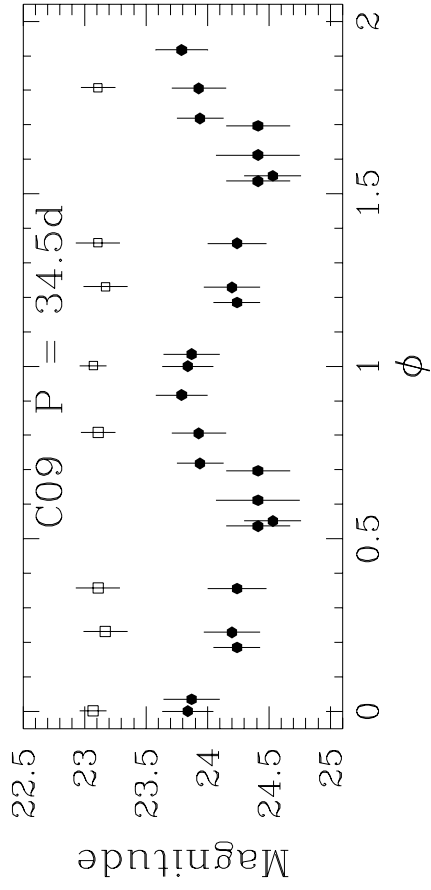
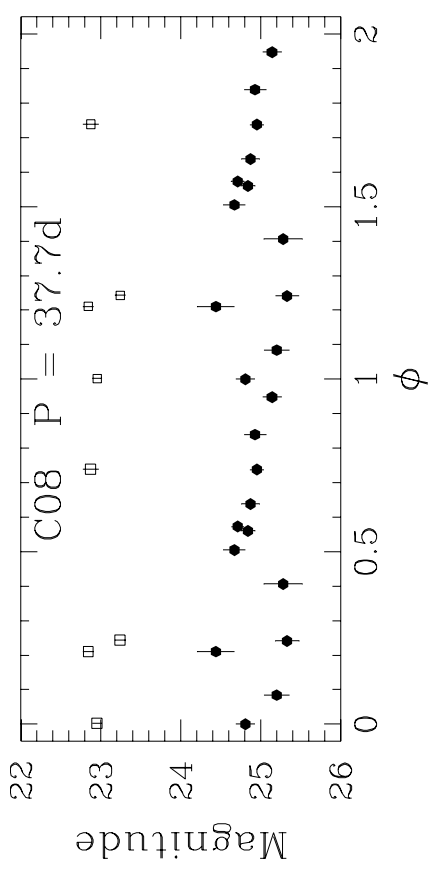
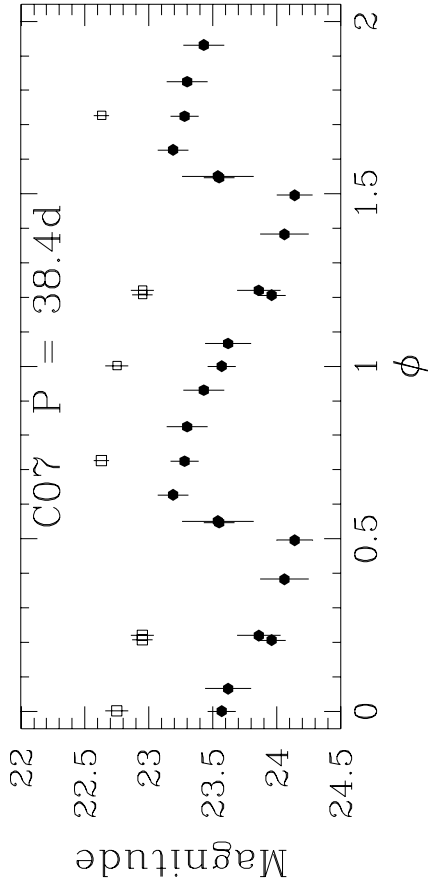


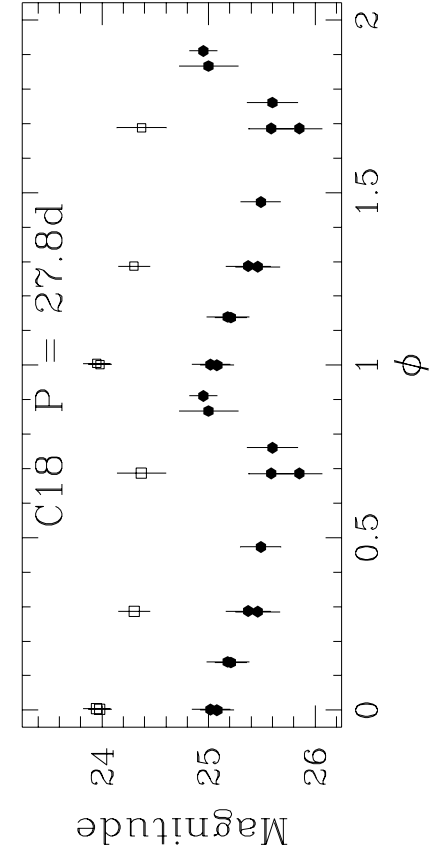
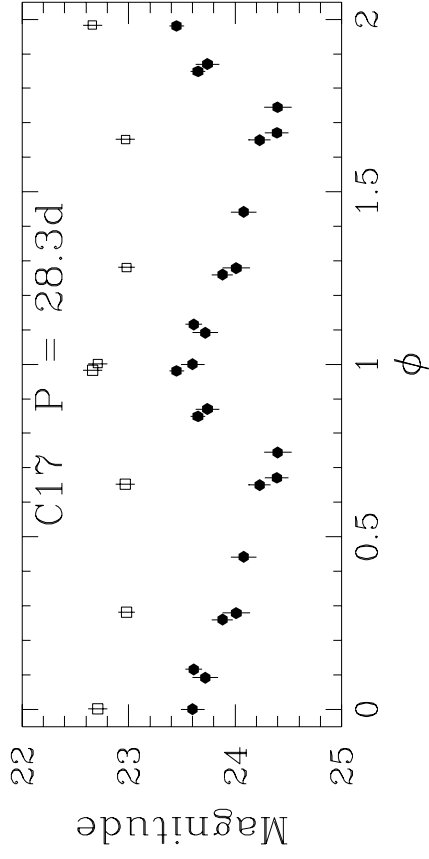
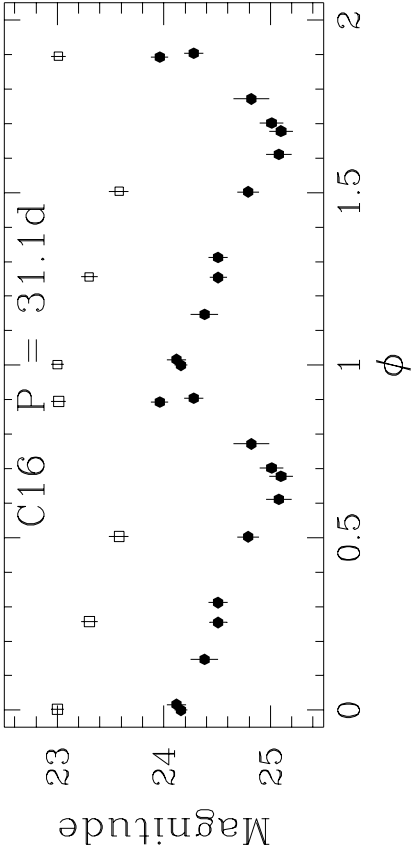
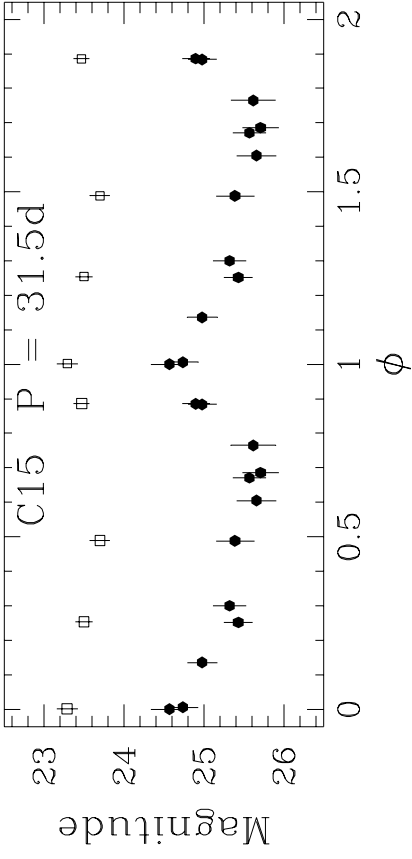
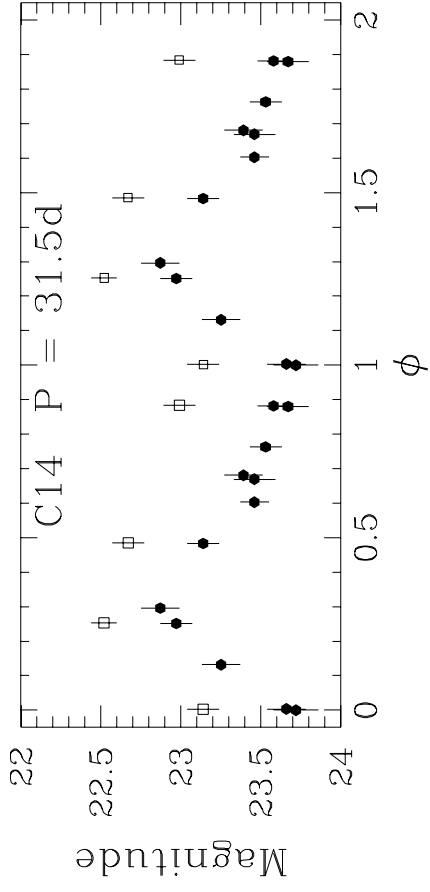
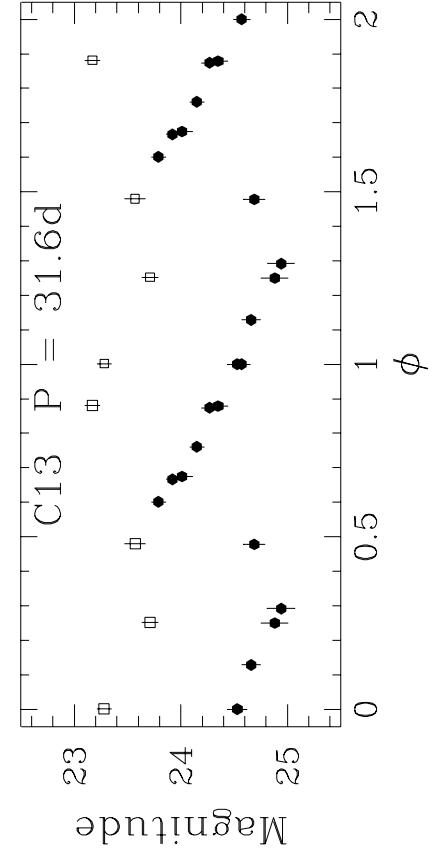


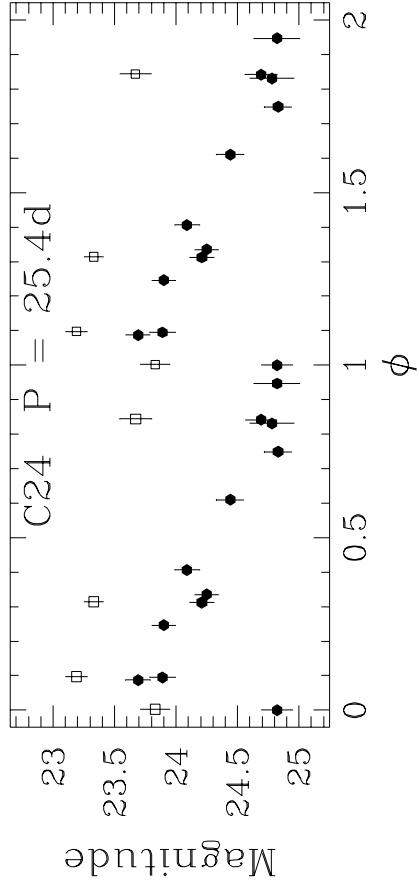
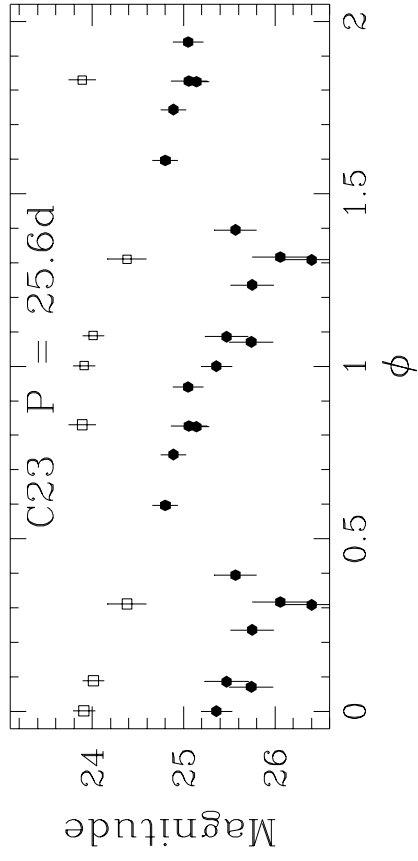
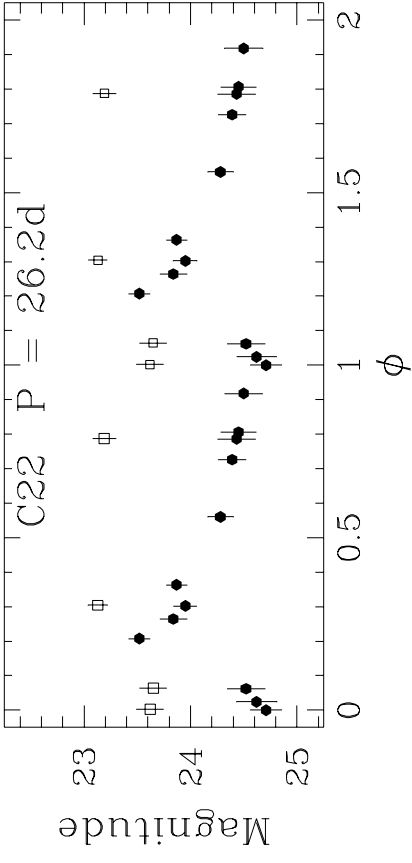
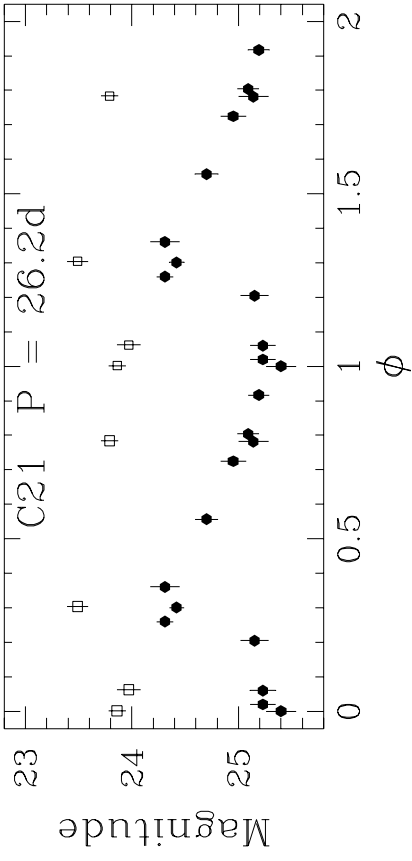
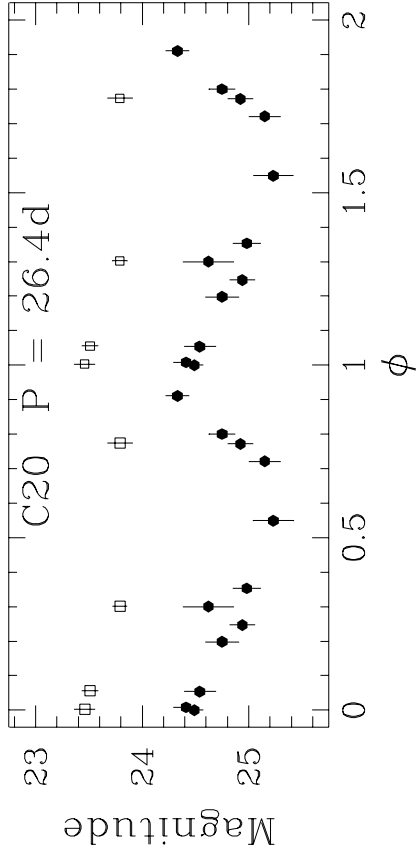
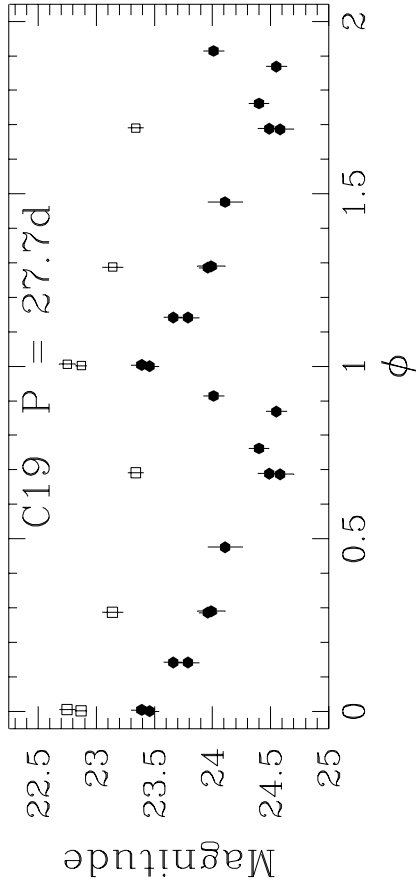


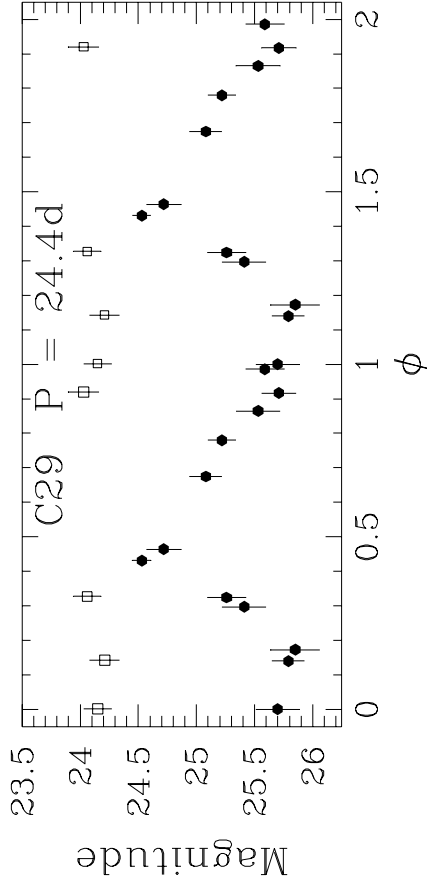
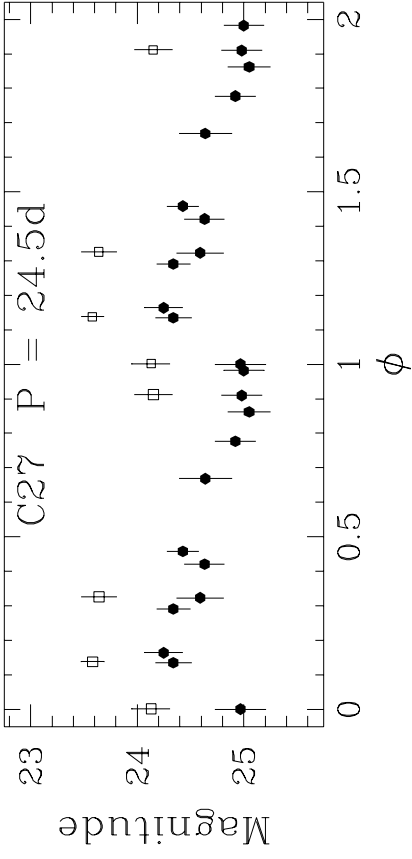
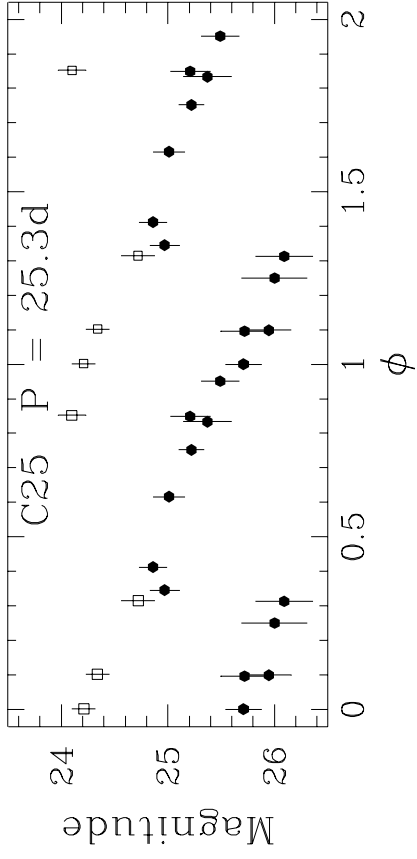
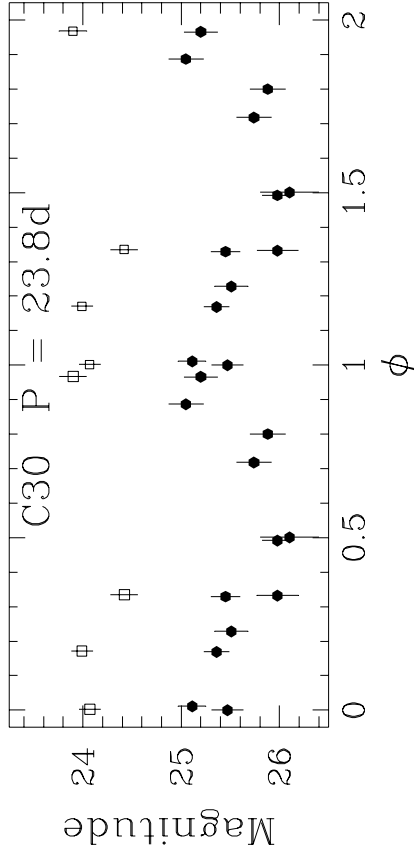
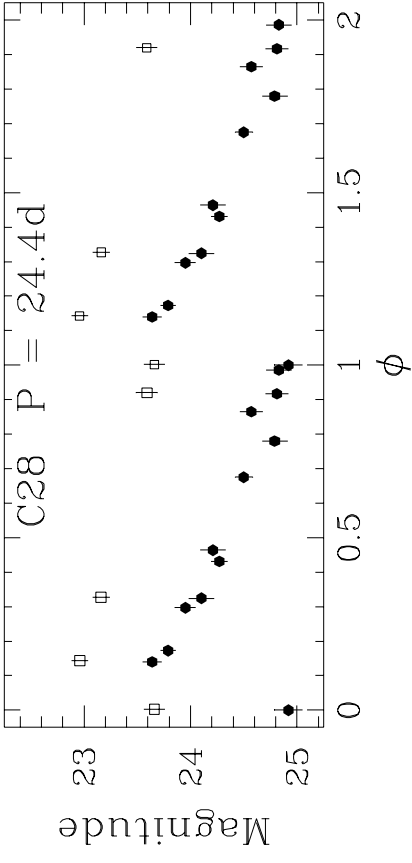
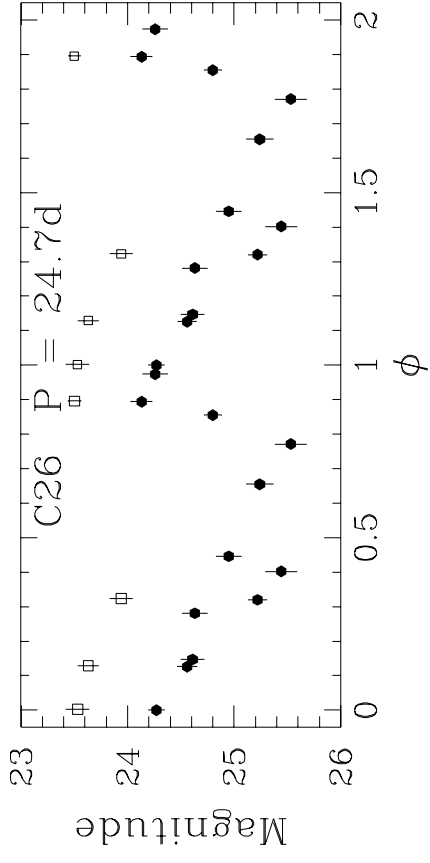


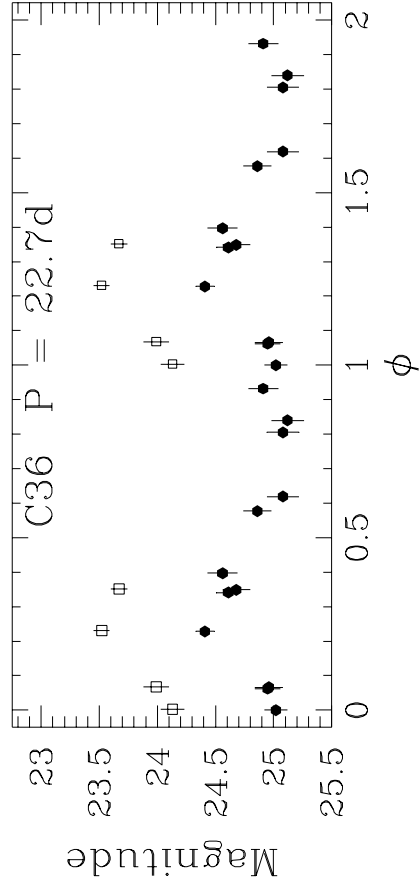
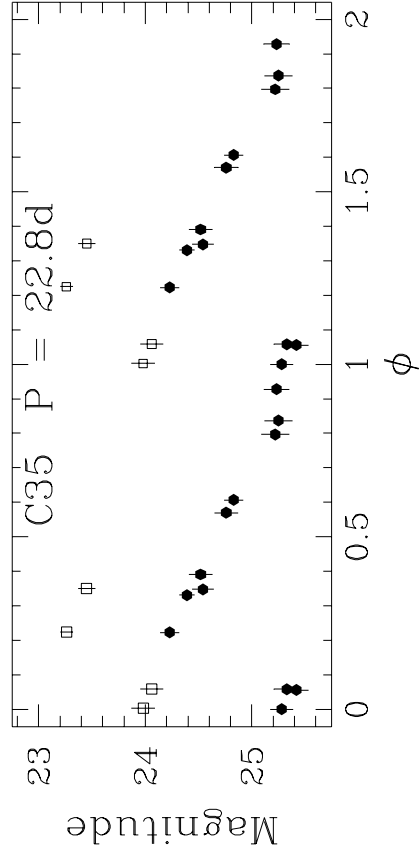
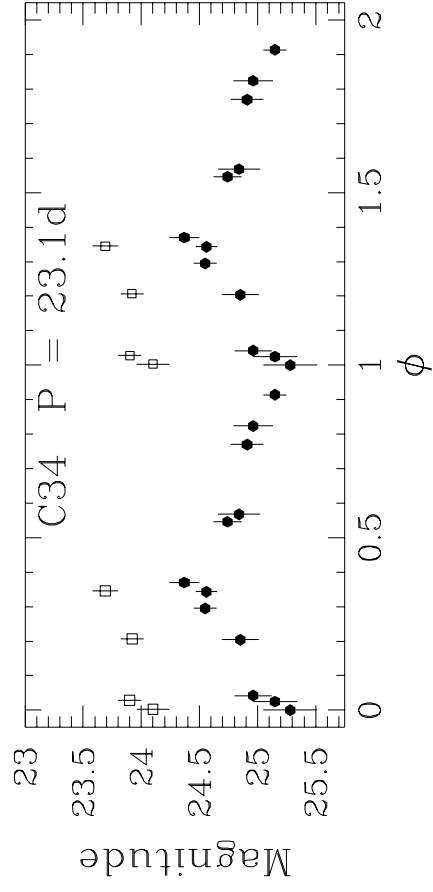
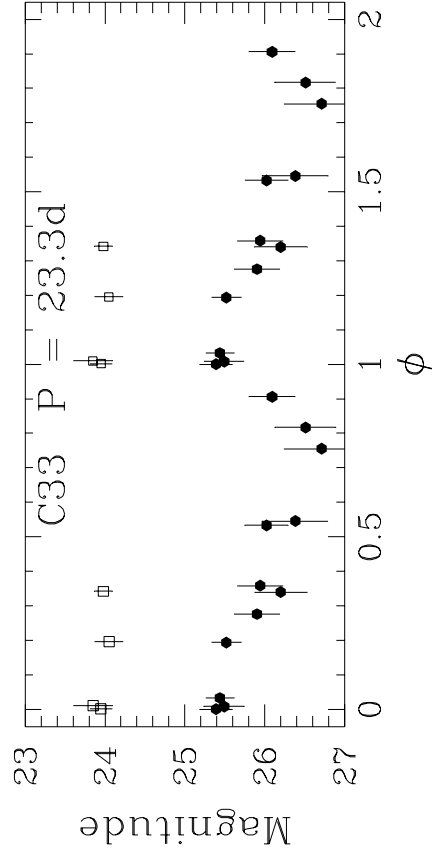
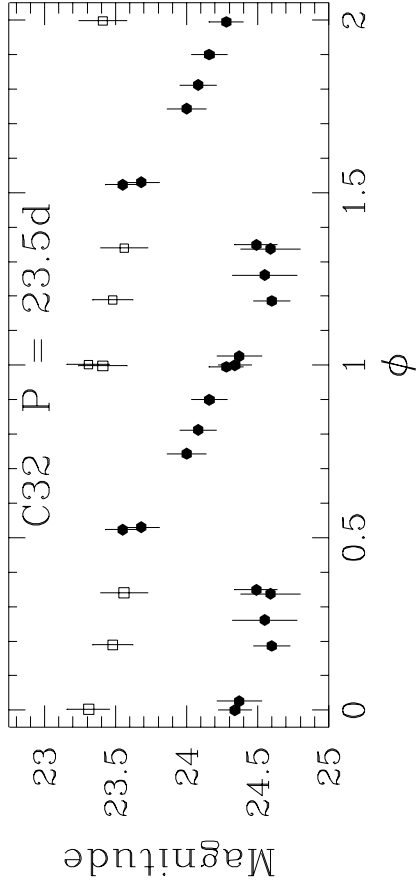
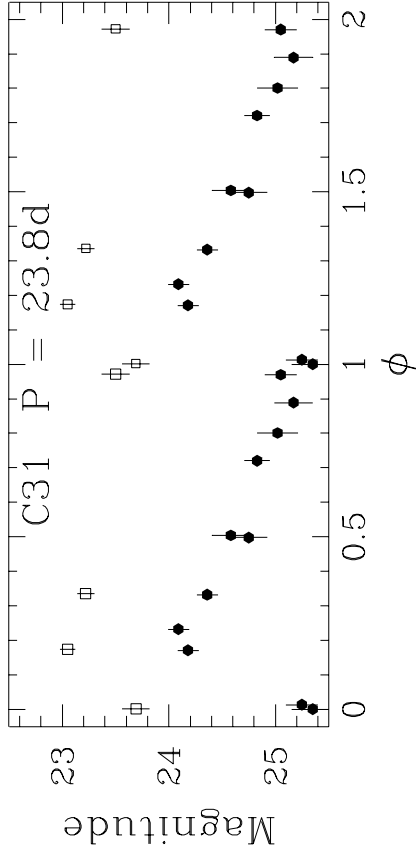


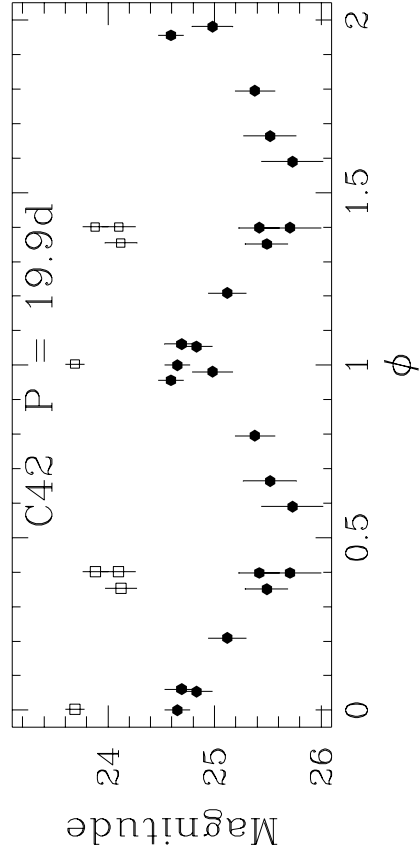
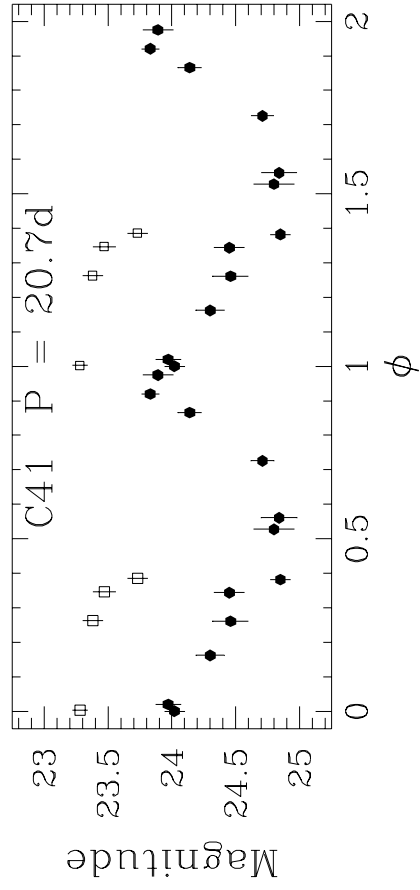
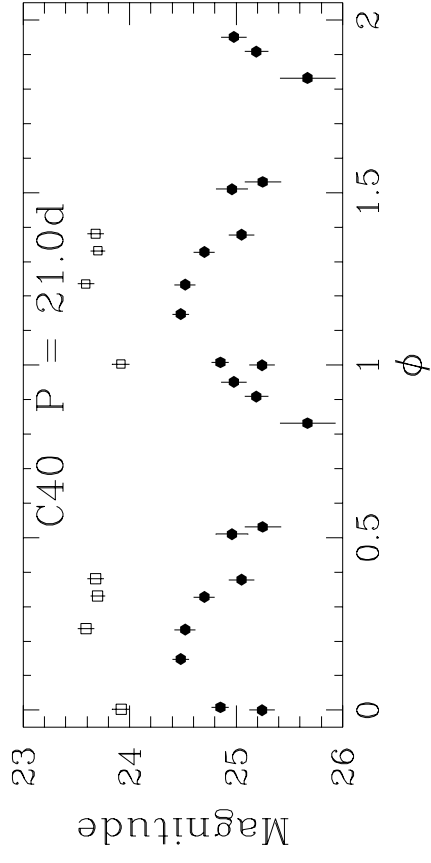
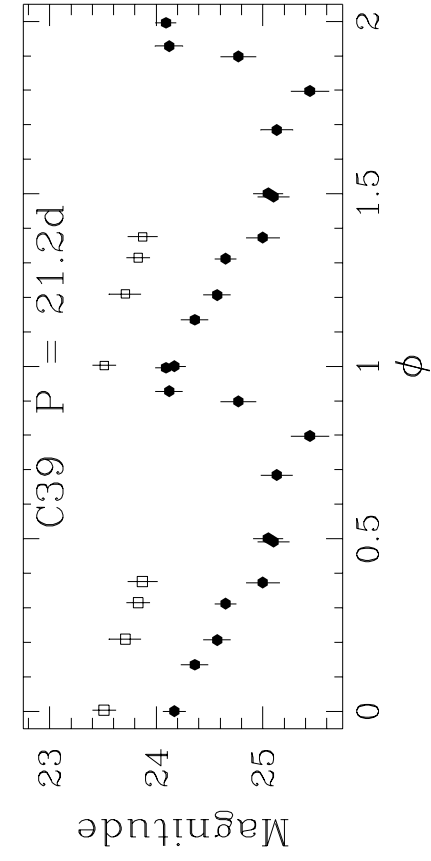
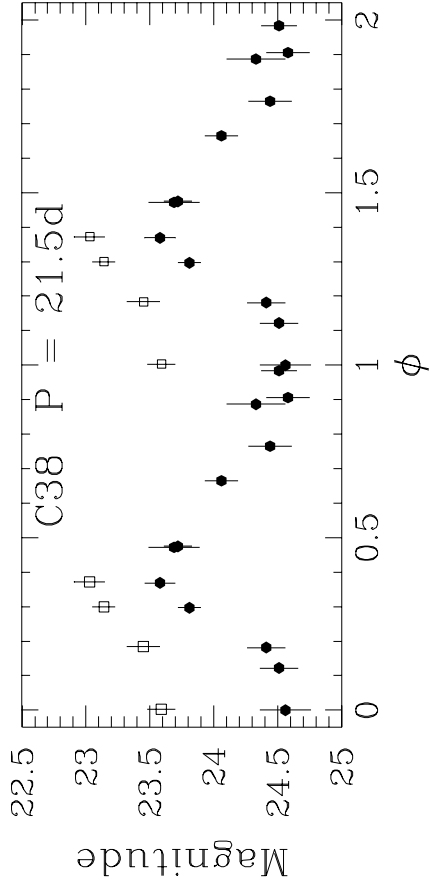
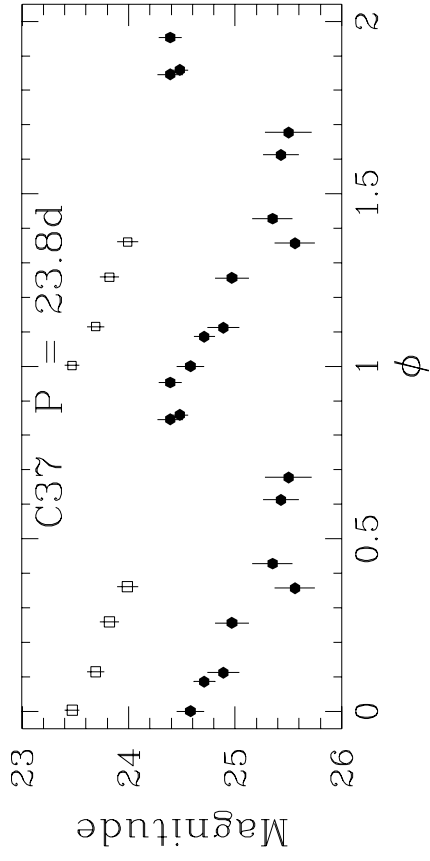


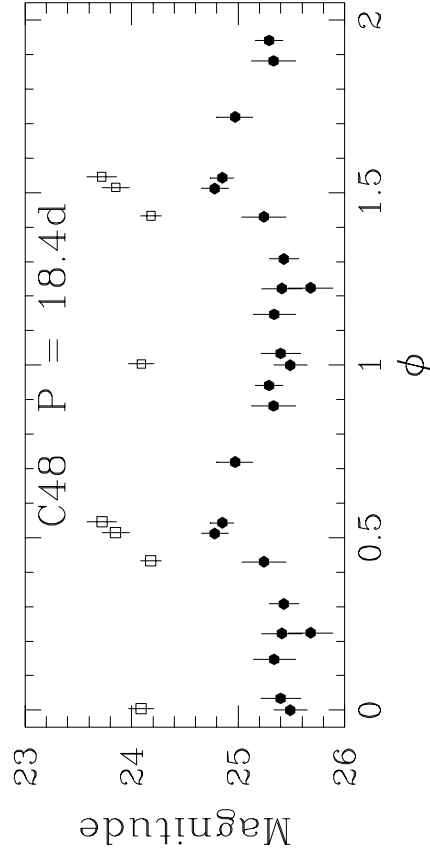
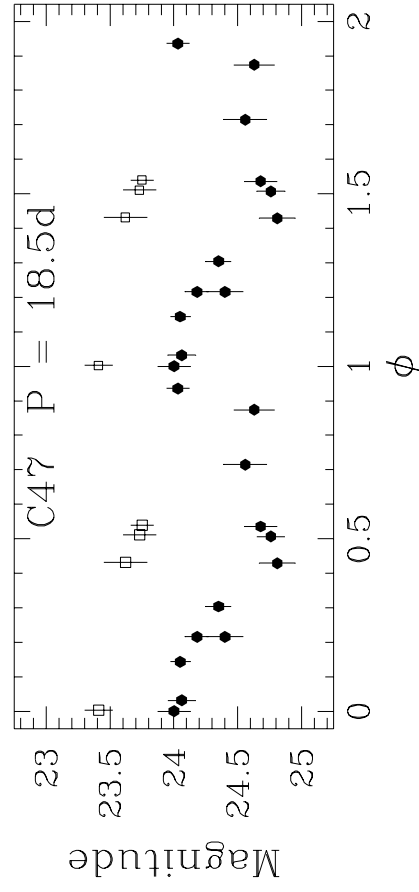
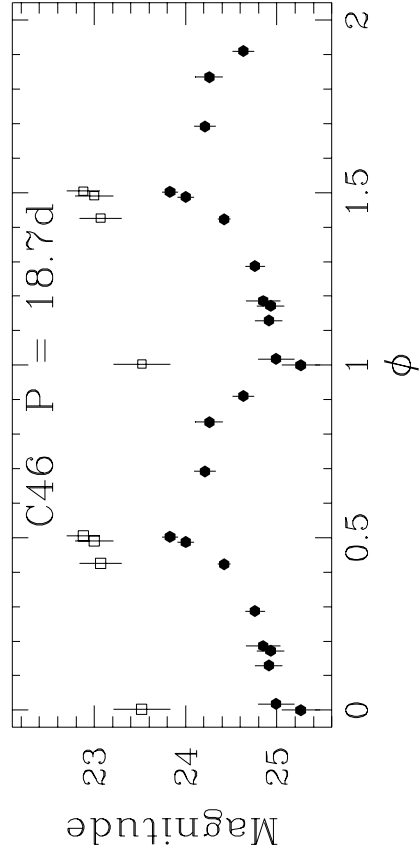
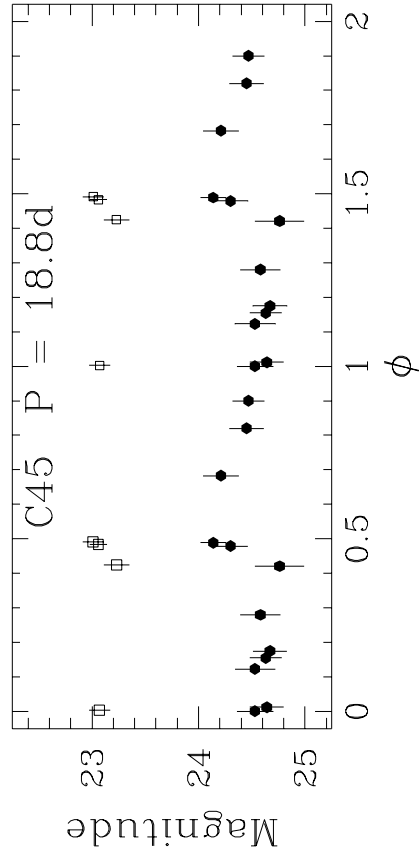
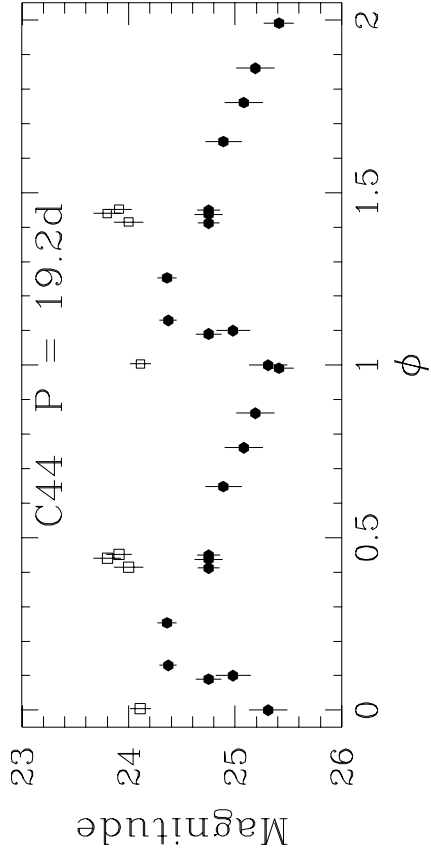
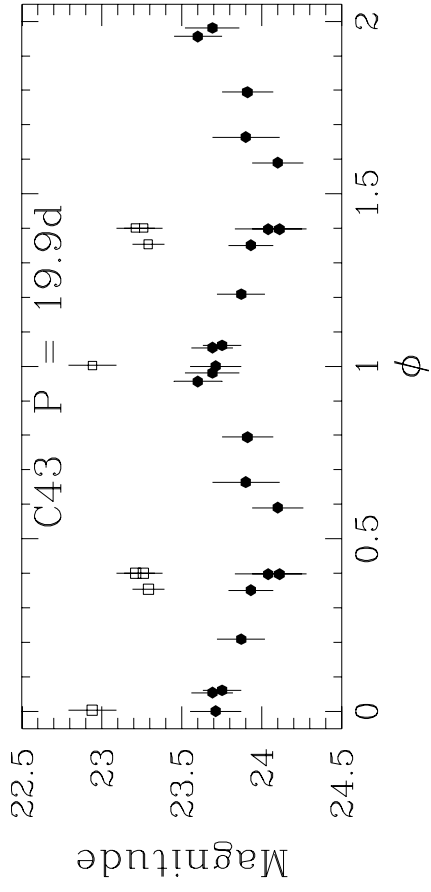


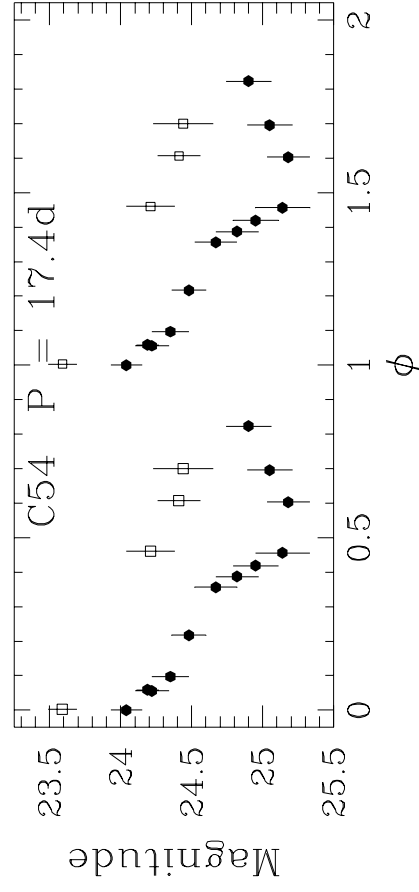
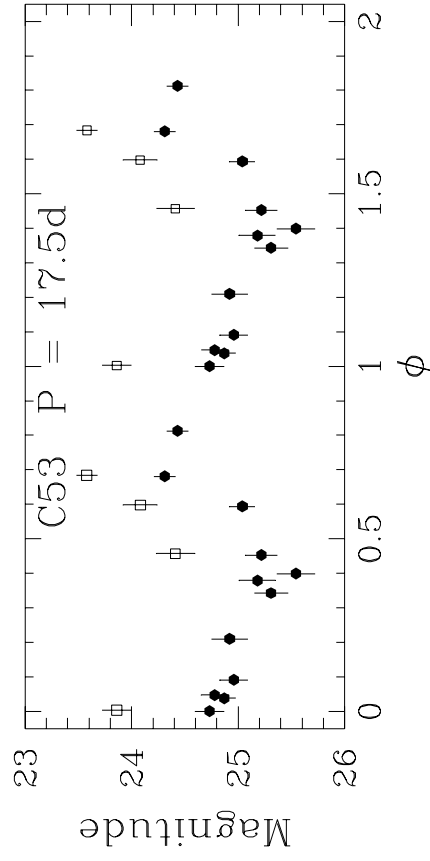
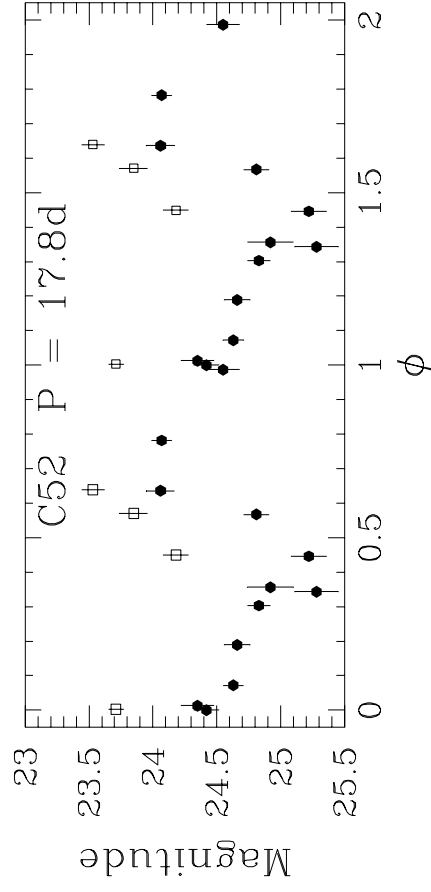
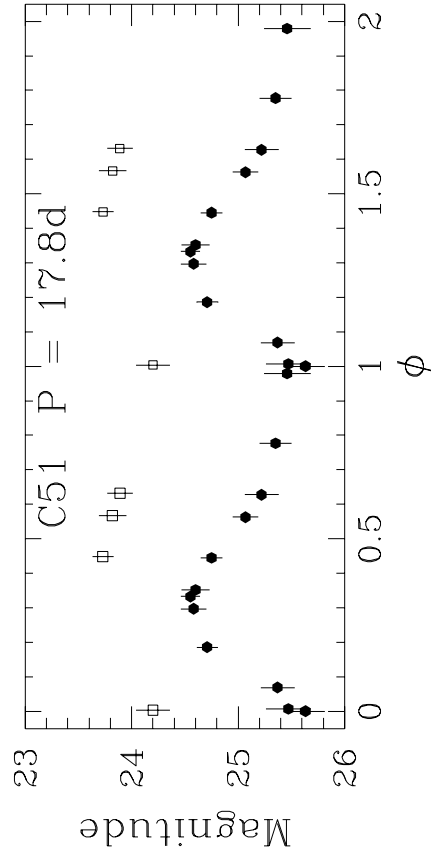
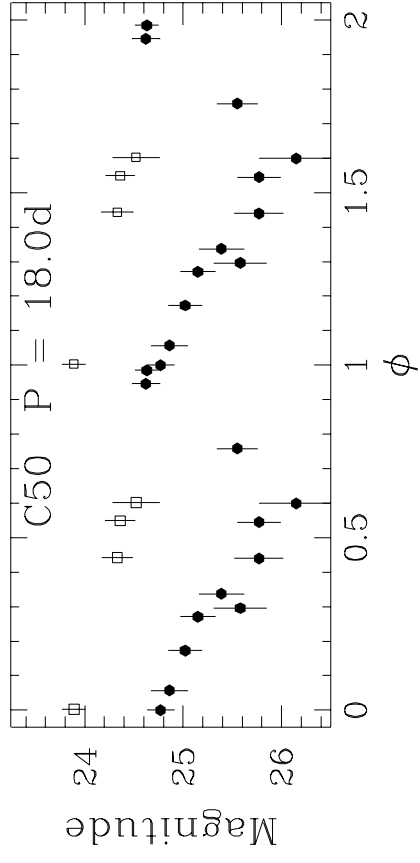
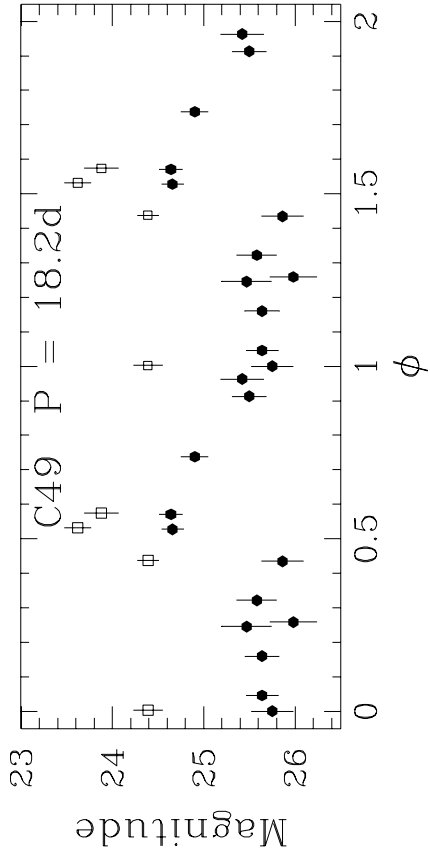


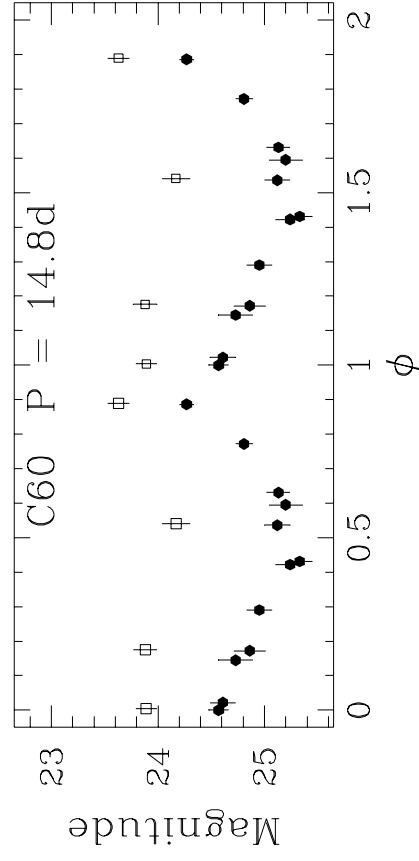
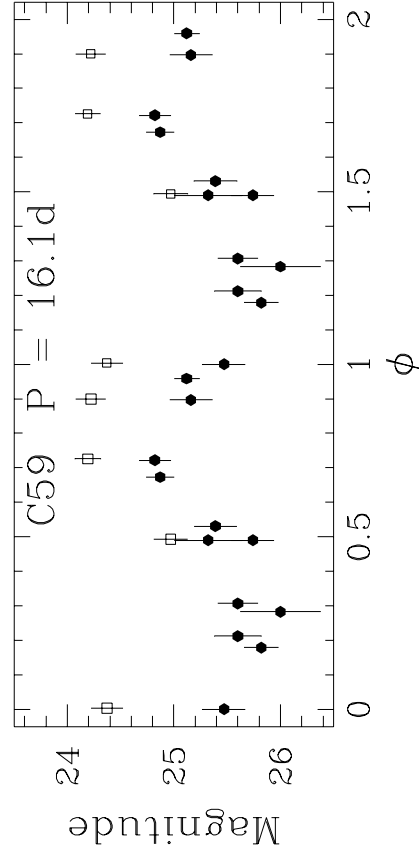
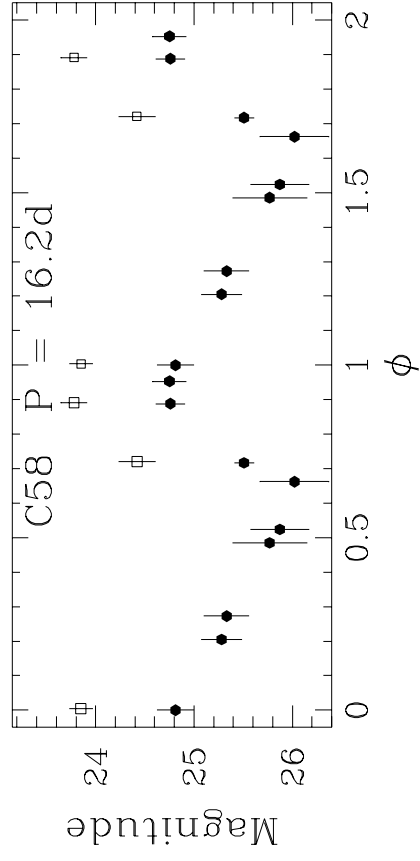
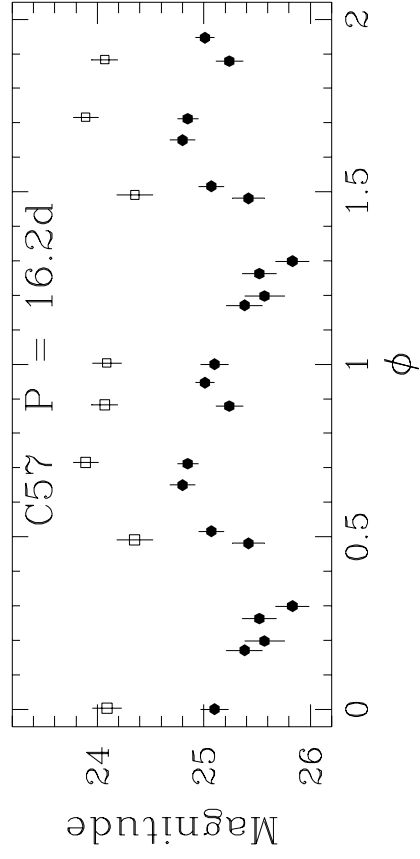
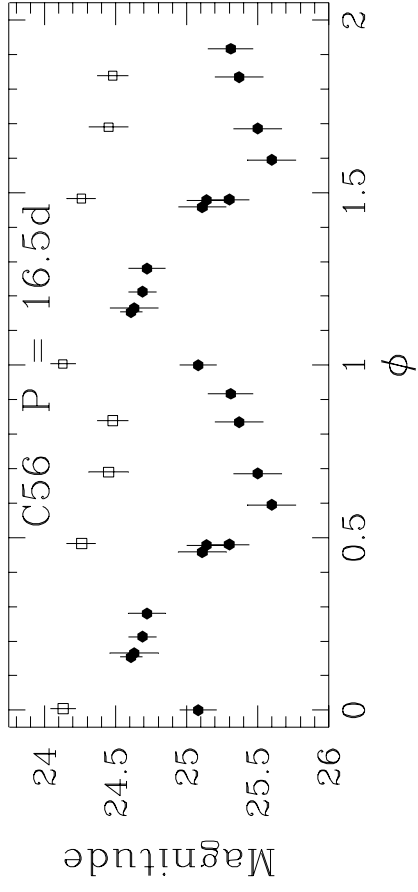
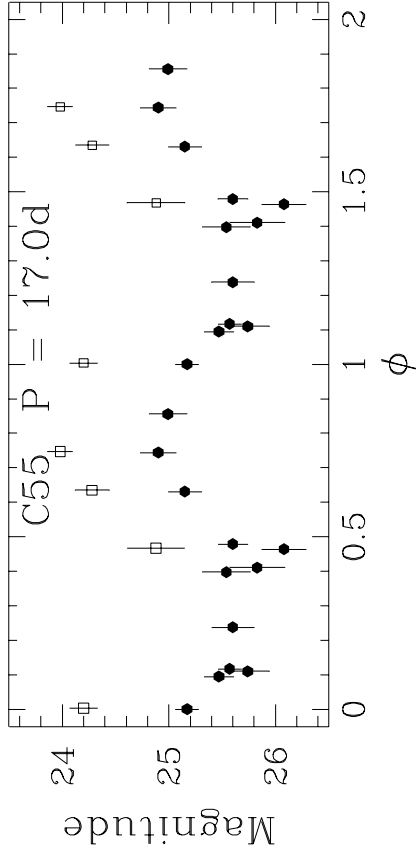


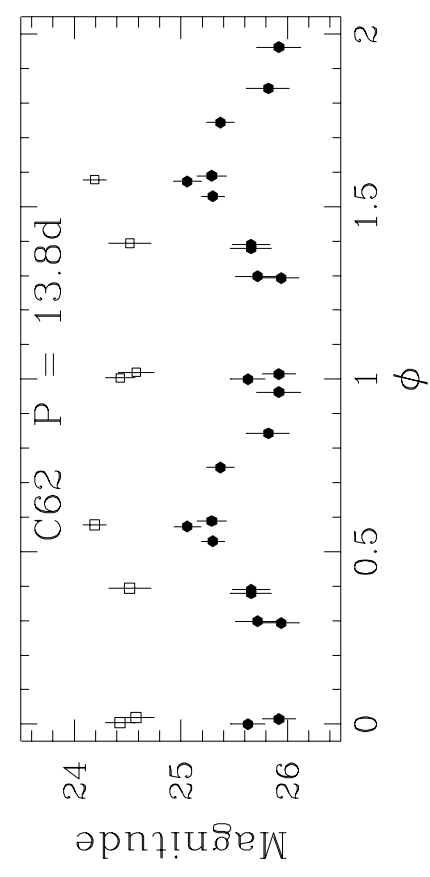
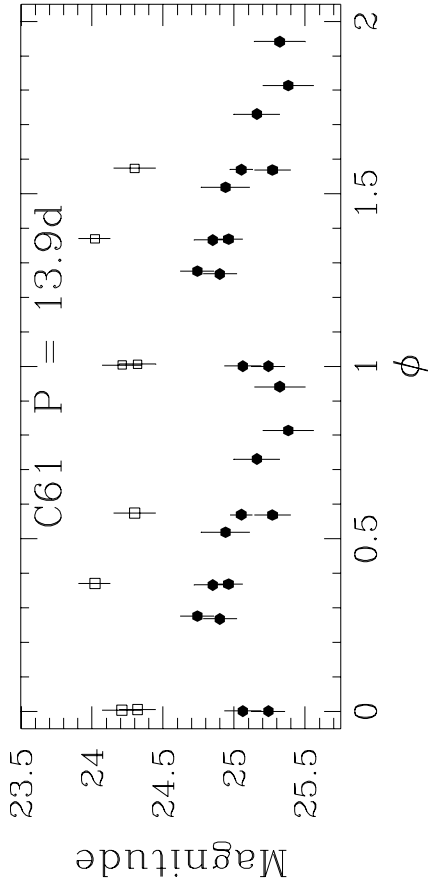












23.5

Magnitude

C61 P = 13.9d

ϕ

2

24

Magnitude

C61 P = 13.9d

ϕ

2

24.5

Magnitude

C61 P = 13.9d

ϕ

2

25

Magnitude

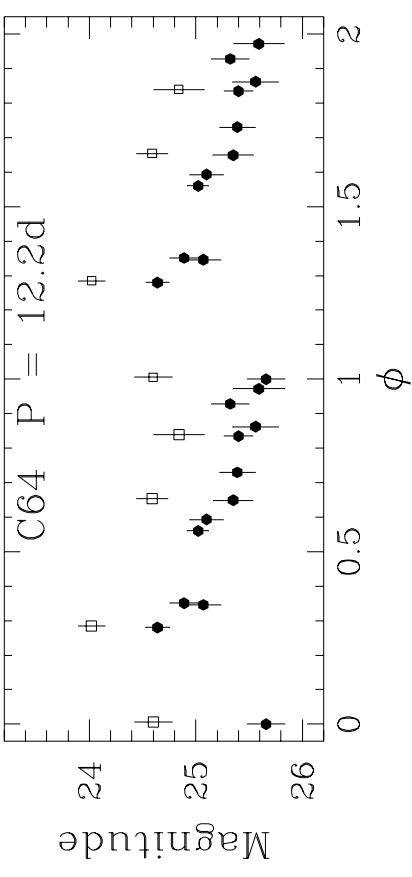
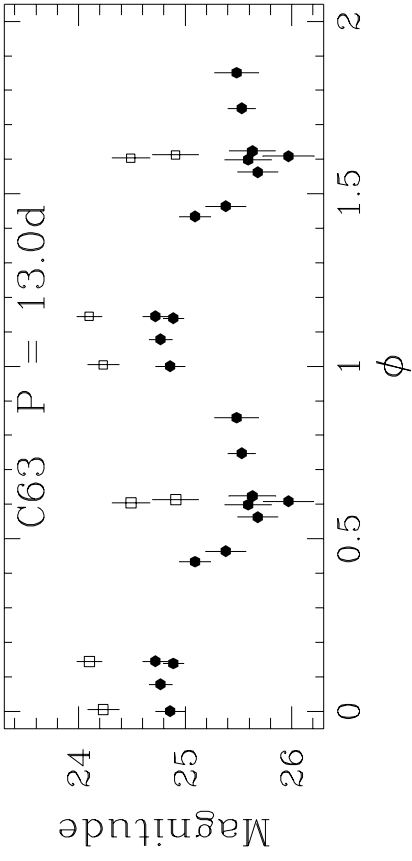
C61 P = 13.9d

ϕ

2

25.5

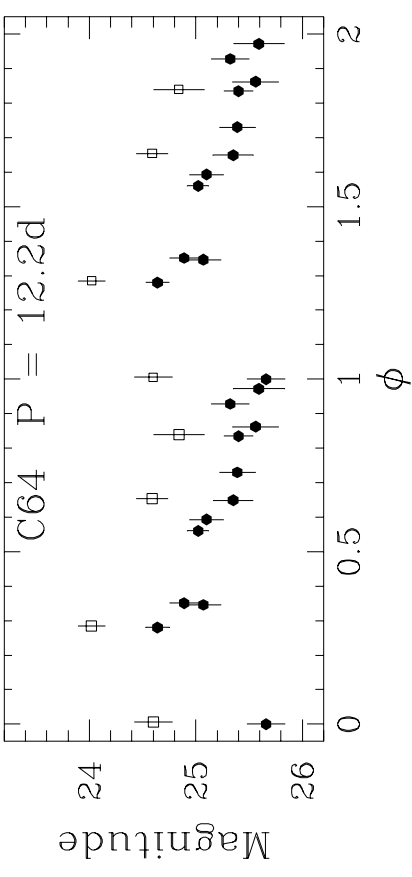
Magnitude



C63 P = 13.0d

ϕ

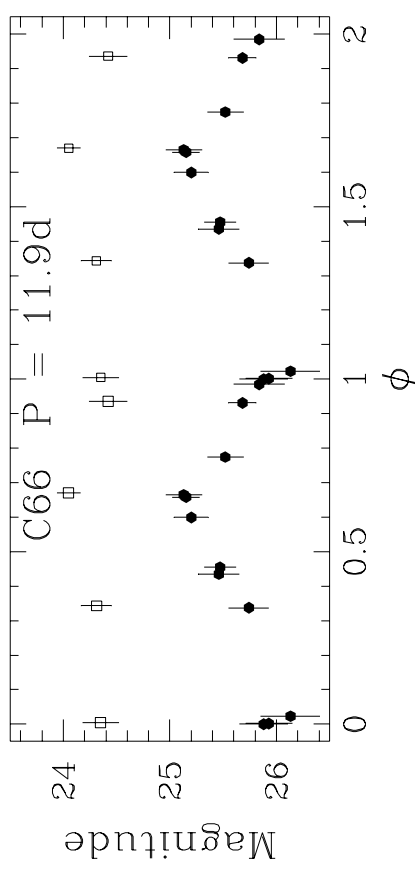
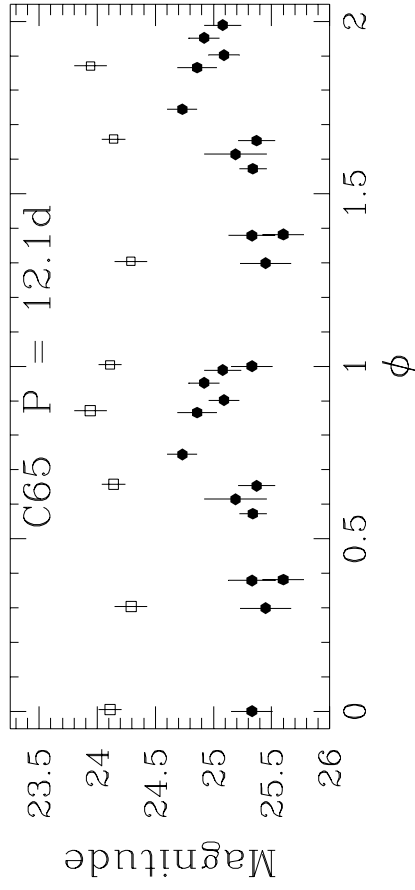
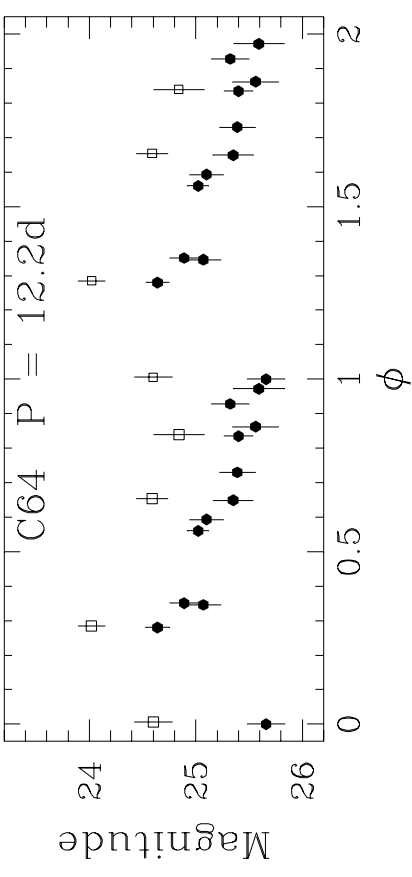
2



C63 P = 13.0d

ϕ

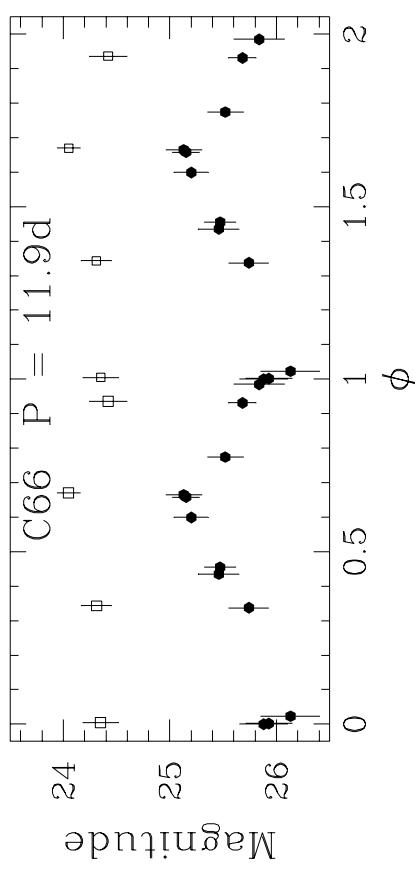
2



C65 P = 12.1d

ϕ

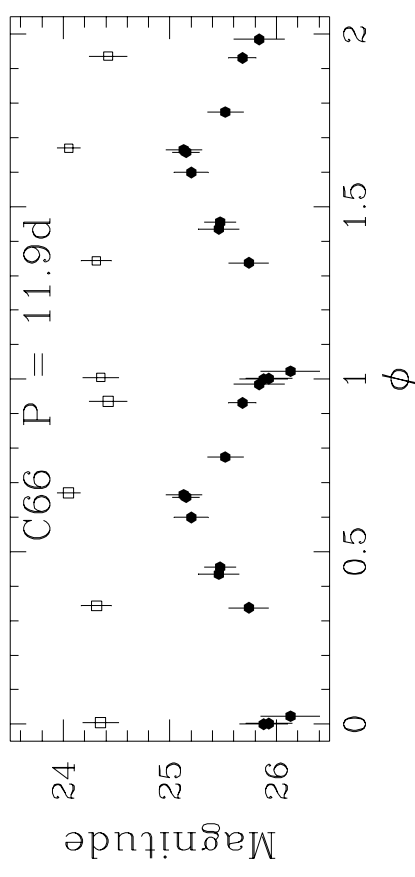
2

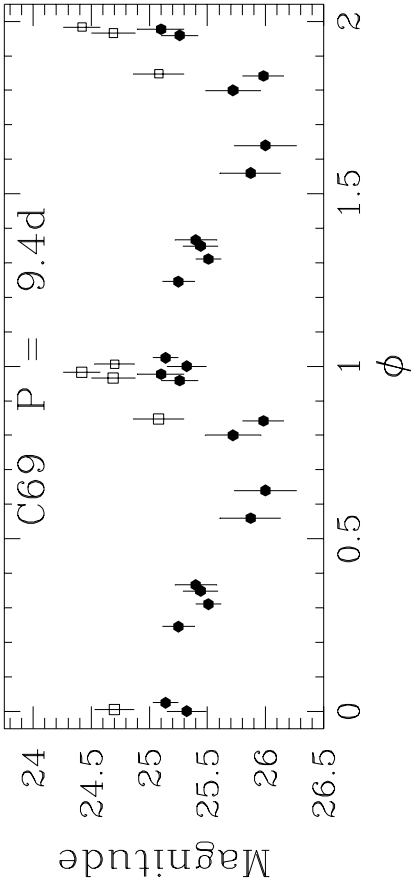
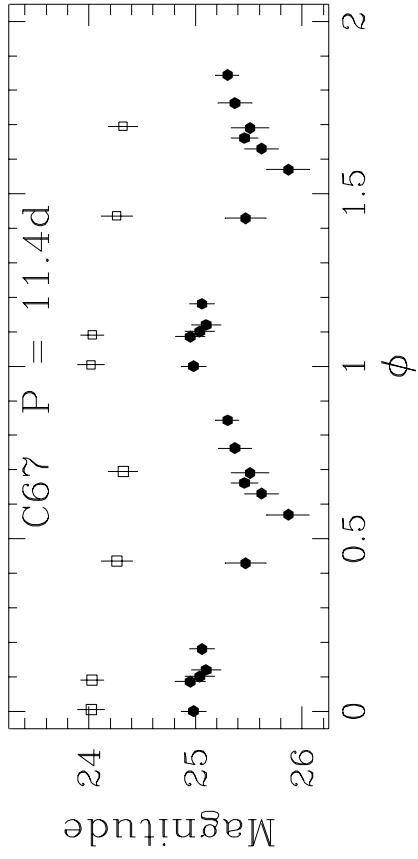
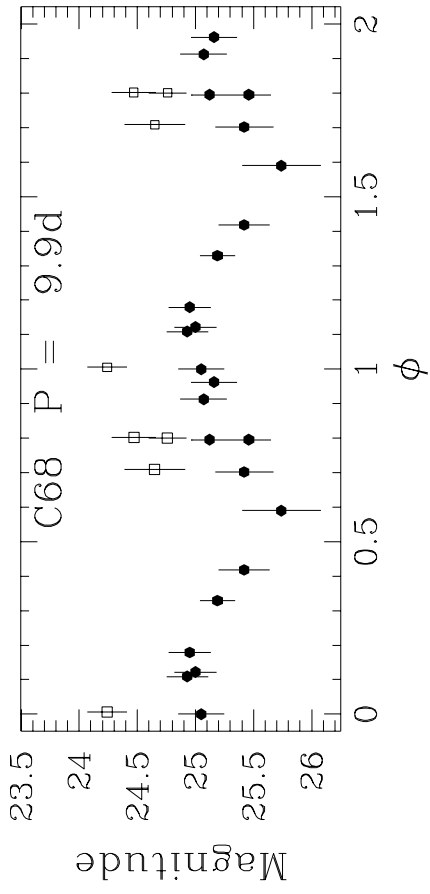


C65 P = 12.1d

ϕ

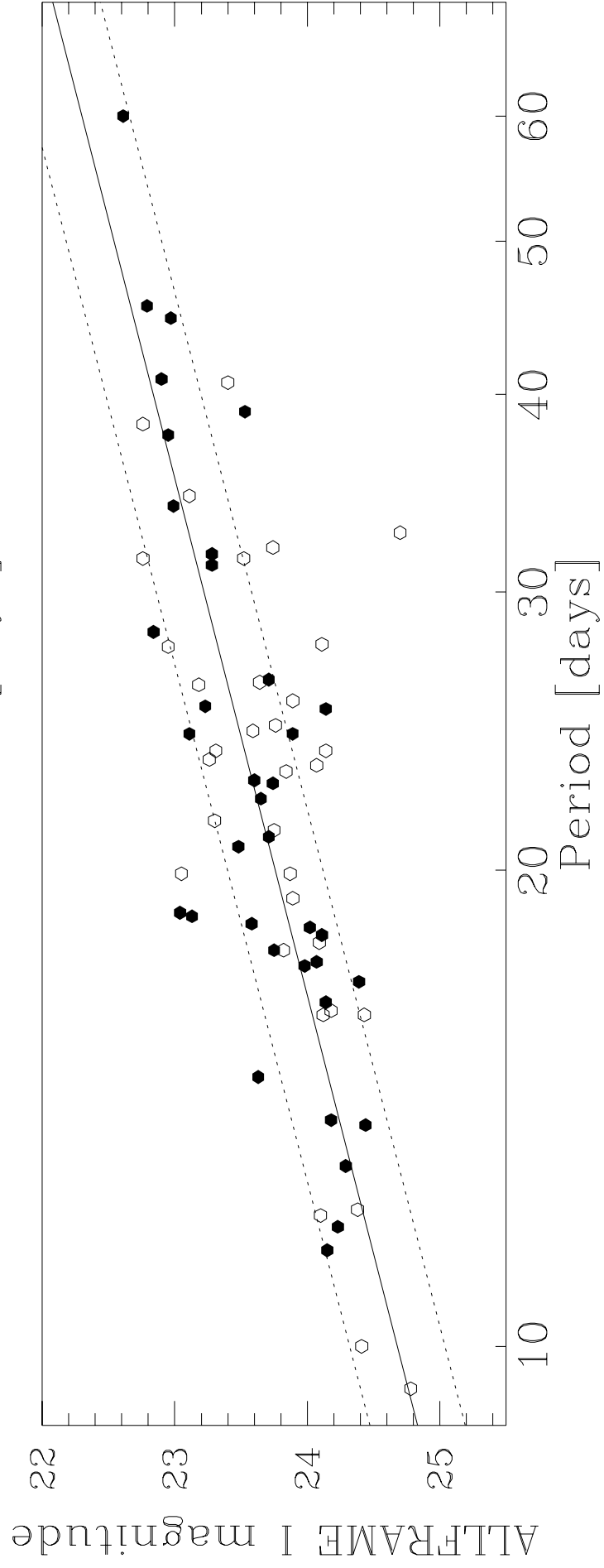
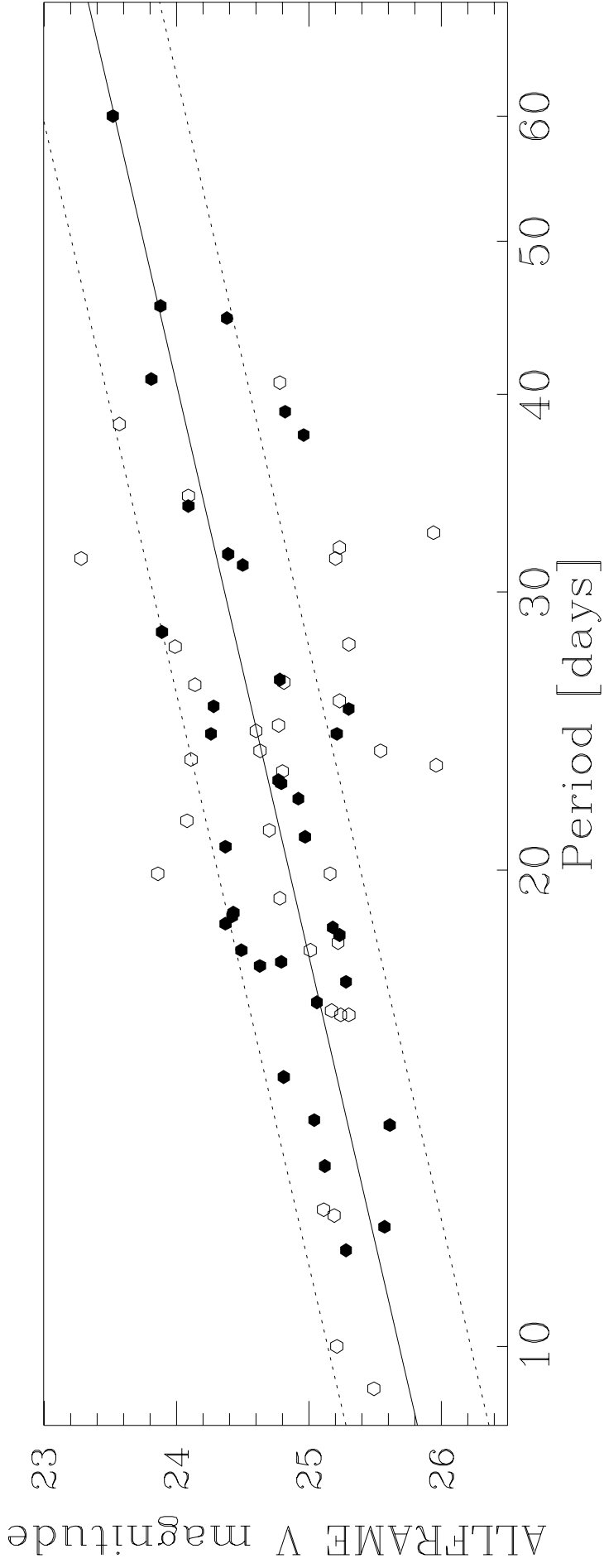
2

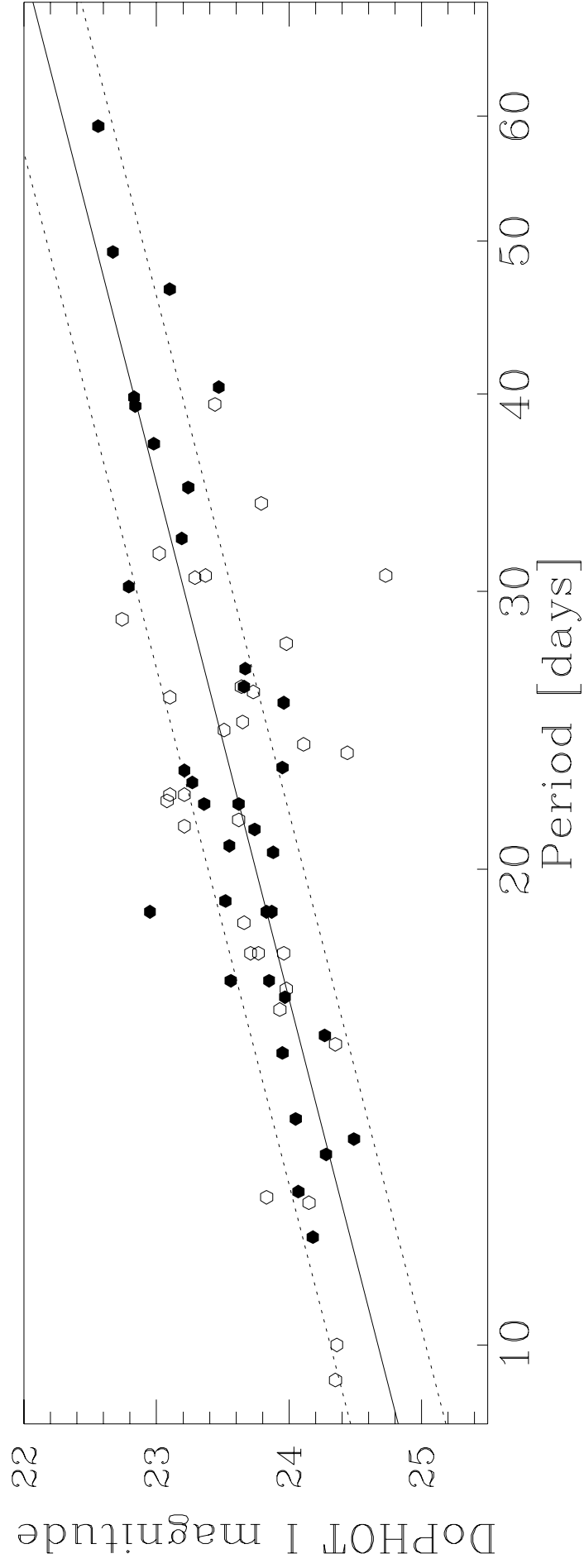
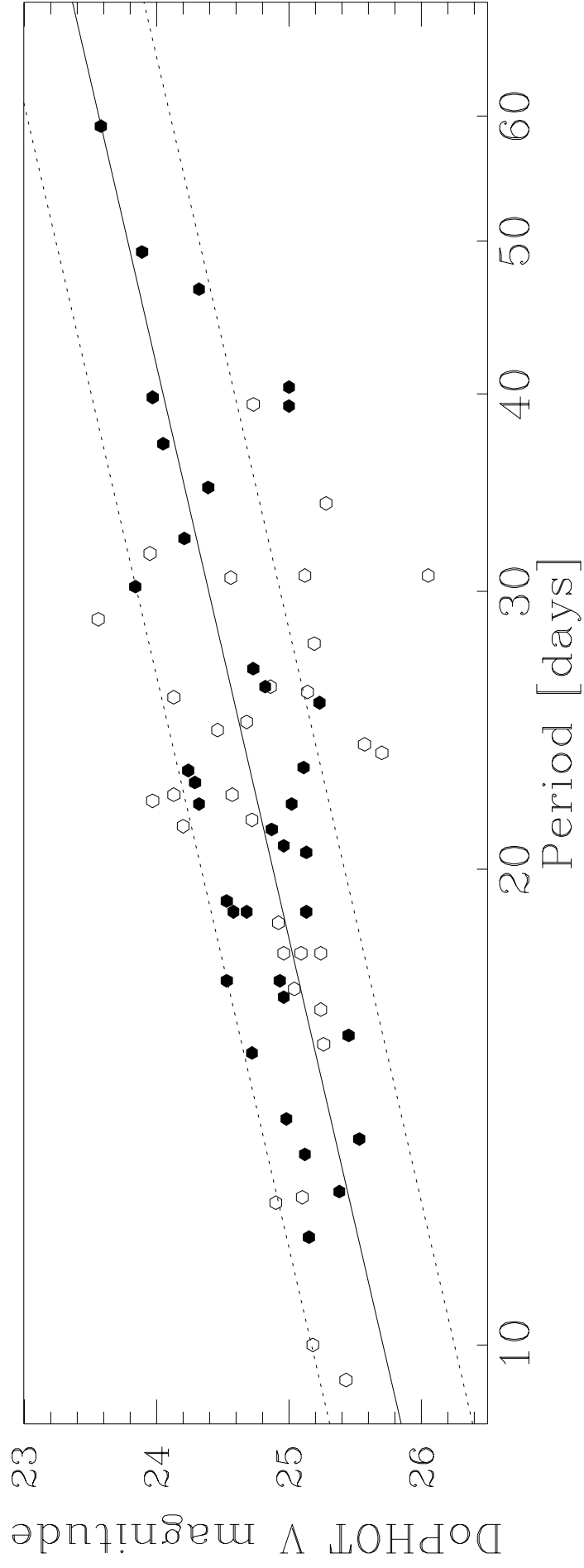




This figure "fig9.gif" is available in "gif" format from:

<http://arxiv.org/ps/astro-ph/9705259v1>





The Extragalactic Distance Scale Key Project VIII. The Discovery of Cepheids and a New Distance to NGC 3621 Using the Hubble Space Telescope[†]

Daya M. Rawson¹, Lucas M. Macri², Jeremy R. Mould¹, John P. Huchra²,
Wendy L. Freedman³, Robert C. Kennicutt⁴, Laura Ferrarese⁵, Holland C. Ford⁶,
John A. Graham⁷, Paul Harding⁴, Mingsheng Han⁸, Robert J. Hill⁹, John G. Hoessel⁸,
Shaun M. G. Hughes¹⁰, Garth D. Illingworth¹¹, Barry F. Madore¹², Randy L. Phelps³,
Abhijit Saha¹³, Shoko Sakai¹², Nancy A. Silbermann¹², & Peter B. Stetson¹⁴

¹Mount Stromlo and Siding Spring Observatories, Institute of Advanced Studies,
Australian National University, Weston Creek, ACT 2611, Australia

²Harvard Smithsonian Center for Astrophysics, Cambridge, MA 02138, USA

³Carnegie Observatories, Pasadena CA 91101, USA

⁴Steward Observatory, University of Arizona, Tucson AZ 85721, USA

⁵Department of Astronomy, California Institute of Technology, Pasadena CA 91125, USA

⁶John Hopkins University and Space Telescope Institute, Baltimore MD 21218, USA

⁷DTM, Carnegie Institution of Washington, Washington, DC 20015, USA

⁸University of Wisconsin, Madison, WI, 53706, USA

⁹Lab. for Astronomy and Solar Physics, NASA GSFC, Greenbelt MD 20771, USA

¹⁰Royal Greenwich Observatory, Cambridge CB3 0EZ, UK

¹¹Lick Observatory, University of California, Santa Cruz CA 95064, USA

¹²IPAC, California Institute of Technology, Pasadena CA 91125, USA

¹³Space Telescope Science Institute, Baltimore MD 21218, USA

¹⁴Dominion Astrophysical Observatory, Victoria, BC V8X 4M6, Canada

[†]Based on observations with the NASA/ESA *Hubble Space Telescope*, obtained at the Space Telescope Science Institute, operated by AURA, Inc. under NASA contract No. NAS5-26555.

Received _____; accepted _____

ABSTRACT

We report on the discovery of Cepheids in the field spiral galaxy NGC 3621, based on observations made with the Wide Field and Planetary Camera 2 on board the *Hubble Space Telescope* (HST). NGC 3621 is one of 18 galaxies observed as a part of *The HST Key Project on the Extragalactic Distance Scale*, which aims to measure the Hubble constant to 10% accuracy. Sixty-nine Cepheids with periods in the range 9–60 days were observed over 12 epochs using the F555W filter, and 4 epochs using the F814W filter. The HST F555W and F814W data were transformed to the Johnson V and Kron-Cousins I magnitude systems, respectively. Photometry was performed using two independent packages, DAOPHOT II/ALLFRAME and DoPHOT.

Period-luminosity relations in the V and I bands were constructed using 36 fairly isolated Cepheids present in our set of 69 variables. Extinction-corrected distance moduli relative to the LMC of 10.63 ± 0.09 mag and 10.56 ± 0.10 mag were obtained using the ALLFRAME and DoPHOT data, respectively. True distance moduli of 29.13 ± 0.18 mag and 29.06 ± 0.18 mag, corresponding to distances of 6.3 ± 0.7 Mpc and 6.1 ± 0.7 Mpc, were obtained by assuming values of $\mu_0 = 18.50 \pm 0.10$ mag and $E(V - I) = 0.13$ mag for the distance modulus and reddening of the LMC, respectively.

Subject headings: Cepheids — distance scale — galaxies: individual(NGC 3621)

1. Introduction

These observations of the spiral galaxy NGC 3621 are part of a Key Project for the *Hubble Space Telescope* (HST). This project, known as *The HST Key Project on the Extragalactic Distance Scale* (Kennicutt, Freedman & Mould 1995), aims to measure the Hubble constant to an accuracy of 10%. By obtaining distances based on Cepheid variable stars to eighteen different galaxies, we will provide a firm basis for the calibration of several secondary distance indicators: the Tully-Fisher relation, surface brightness fluctuations, the planetary nebula luminosity function, the globular cluster luminosity function, type II supernova expanding photospheres, and type Ia supernova standard candles (see Jacoby et al. 1992 for a review of these methods). The HST, with its enhanced resolution over ground-based telescopes and its position in orbit which removes many of the problems plaguing terrestrial observers, is the ideal instrument for the stringent demands of this type of project. Observations of Cepheids in M100 using HST (Ferrarese et al. 1996) have already yielded Cepheid distances to galaxies in the Virgo Cluster, thus displaying the capabilities of the WFPC2 instrument in detecting Cepheids in galaxies well outside of the Local Group. In addition, distances to M81, M101 (Kelson et al. 1996), and NGC925 (Silbermann et al. 1996) have also been determined as a part of the Key Project.

NGC 3621 is a relatively isolated spiral with a morphological classification of Sc II.8 (Sandage & Tammann 1981) or Sc III-IV (de Vaucouleurs et al. 1991) and a low galactocentric redshift of 526 km/s (de Vaucouleurs et al. 1991), indicative of a comparatively small distance relative to that of the Virgo cluster (Mould et al. 1995). Its complex pattern of partially resolved, irregular spiral arms makes it an excellent candidate for the detection of Cepheids, while its high inclination ($i = 51^\circ$) and well-ordered H-I rotation (Gardiner & Whiteoak 1977) indicates that it is an ideal object for the calibration of the Tully-Fisher relation as applied to field spirals.

We describe the observations and preliminary reductions in §2. The photometry and calibration of the instrumental magnitudes is discussed in §3. The search for Cepheids using two independent photometric algorithms and the resulting set of variables are described in §4. Period-luminosity relations and distance moduli are presented and discussed in §5, and our conclusions are given in §6.

2. Observations and Reductions

2.1. Observations

Observations of NGC 3621 using the Wide Field and Planetary Camera 2 (WFPC2) system on the HST commenced on December 27, 1994 with the first of 24 F555W (approximately Johnson V) images. The observations were split over 12 epochs within a 60 day window; 11 of them were cosmic-ray split and one was a single exposure. In addition, 9 F814W (approximately Kron-Cousins I) images divided among four epochs, and 4 F439W images over two epochs were obtained. Given the short total integration time and the very limited phase coverage of the F439W data, it was not included in this data analysis. Single short exposures of 180 seconds were obtained in the F555W and F814W filters to provide a linearity check on the magnitudes derived by the photometric routines (see §3.3 for details). The WFPC2 footprint for the observations, superimposed on a wide-field image of the galaxy (kindly made available by Sandage & Bedke 1985), is shown in Figure 1, while a mosaic of the WFPC2 F555W images can be seen in Figure 2.

The WFPC2 includes four 800×800 CCD detectors. Three of these, the Wide Field Cameras, have a pixel size of 0.1 arcseconds as projected on the sky, for a total field of view of 1.3×1.3 arcminutes each. The remaining CCD, the Planetary Camera, has a pixel size

of 0.046 arcseconds as projected on the sky, for a total field of view of 36×36 arcseconds. A more detailed description of the WFPC2 instrument can be found in *The HST WFPC2 Instrument Handbook* (Burrows et al. 1994). All observations were made with the telescope guiding in fine lock with a stability of approximately 3 mas. The gain and readout noise were $7 \text{ e}^-/\text{DN}$ and 7 e^- , respectively. The CCD was operated at a temperature of -88° C for all observations.

Exposure times and dates for each observation are given in Table 1. The sampling strategy, as discussed by Freedman et al. (1994a), has been designed specifically for the Key Project with the purpose of maximising the probability of detecting a Cepheid with a period in the chosen window of 10–60 days. It follows a power-law distribution in time which provides an optimum sampling of the light curves of Cepheids in this period range and reduces the risk of aliased detections. Figure 3 shows the detection efficiency of our optimum sampling; high values of variance imply a higher probability of detecting Cepheids with those periods while lower values of variance indicate lower probabilities of detection. Note that the variance turnover at 65 days (due to the width of the observing window) implies that this is the longest period that can be reliably determined.

2.2. Data Reductions

The HST data have been calibrated using the pipeline processing at the Space Telescope Institute (STScI). The full reduction procedure, given in Holtzman et al. (1995a), consists of: a correction of A/D errors, the subtraction of a bias level for each chip, the subtraction of a superbias frame, the subtraction of a dark frame, a correction for shutter shading, and a division by a flat field. The names of the STScI reference files used for this calibration are listed in the notes to Table 1. Furthermore, each of the frames was corrected for vignetting

and geometrical distortions in the WFPC2 optics (using files kindly provided by P. Stetson and J. Holtzman, respectively). Lastly, the images were multiplied by four and converted to integers, to reduce disk usage and allow image compression. This conversion led to an effective readout noise of $4e^-$ and a gain of $1.75e^-/\text{DN}$. A more complete description of the calibration steps can be found in Hill et al. (1997) and Stetson et al. (1997).

Holtzman et al. (1995b) have described the effect on photometry of charge transfer inefficiency (CTI) in the Loral WFPC2 chips. The principal effect at very low light level is a loss of sensitivity from bottom to top of each chip amounting to 0.04 mag for a star at row 800 relative to an equivalent star at hypothetical row 0. Subsequent investigations (Holtzman, private communication) have made use of the pre-flash capability built into WFPC2 (but not a user commandable facility). Pre-flash intensities from $30 e^-$ to $1000 e^-$ were added to observations of standard stars in ω Centauri, and aperture photometry was carried out systematically as a function of pre-flash level and y-coordinate. This demonstrated that data with $0 e^-$ background show a 0.04 mag ramp relative to $30 e^-$ (and brighter) background levels. For our purposes, this confines the CTI problem to the calibration results of Holtzman et al. and implies that no ramp correction is required for any of our observations, where the background level is always greater than $70 e^-$. Similarly, the observations of NGC 2419 and Pal 4 used in the determination of the ALLFRAME PSF (see below) have high background levels and are not affected by CTI.

Hill et al. (1997) have described a difference in the photometric zero points of the WFPC2 depending on the exposure time of the observations that are used for their determination. For exposures lasting less than about sixty seconds, the zero points are systematically higher by ~ 0.05 mag (on average) than those of exposures lasting more than 1300 seconds. The effect seems to arise from a loss of $2 e^-/\text{pixel}$ per exposure (Casertano & Baggett 1997), which significantly affects the magnitudes of faint stars on images with

low background levels. Given the length of our exposures and their high background levels, we use the long-exposure zero points in this paper.

3. Photometry and Calibration

3.1. Photometric Reductions

Photometry of NGC 3621 was obtained by two groups implementing independent software packages; D.M.R. and J.R.M. at Mount Stromlo Observatory, Australia used DAOPHOT II/ALLFRAME (Stetson 1994), while L.M.M. and J.P.H. at the Harvard-Smithsonian Center for Astrophysics, Cambridge, USA used a version of DoPHOT (Schechter, Mateo & Saha 1993) specially modified to deal with HST WFPC2 data (Saha et al. 1996). The reader is referred to those respective publications for a detailed description of each photometry package. Each package performs photometry using independent techniques, and a comparison of results yields a fundamental check on the validity of the software and the photometry. This provides a powerful tool for detecting the presence of errors and biases which might go undetected if only one package were used.

3.1.1. DAOPHOT II and ALLFRAME

Both the DoPHOT and ALLFRAME software packages use profile-fitting procedures to measure magnitudes. DoPHOT constructs a PSF (Point Spread Function) using the brightest stars in the frame being reduced, while DAOPHOT II/ALLFRAME has the ability to construct PSFs from bright stars in the frame being reduced or from independent

images of un-crowded fields. The PSFs used for the ALLFRAME reductions were made using images of un-crowded regions of NGC 2419 and Pal 4 (Hill et al. 1997), with the implicit assumption that any long-term temporal variation of the PSF for a given filter/chip combination can be absorbed into the aperture correction term (see below). Because of the very high degree of crowding, with few, if any un-crowded stars in the NGC 3621 frames, this is the preferred approach for the DAOPHOT II/ALLFRAME reduction track. These globular cluster PSFs have significant levels of background light, and should be free of low light level CTI problems in the wings.

The ALLFRAME reduction followed the same steps described in previous papers of this series (Kelson et al. 1996, Ferrarese et al. 1996, Silbermann et al. 1996, Hill et al. 1997), and we give only a brief description here. The FIND routine in DAOPHOT II is initially applied to all of the images. This routine looks for stellar-like objects in each image, and provides a filter against cosmic-rays, and non-stellar objects. This filter basically screens against objects which deviate from a circularly symmetric shape (their “roundness”), and also against objects whose profile deviates substantially from that of a gaussian, by being too sharp, or flat (their “sharpness”). These parameters can be set to allow more or less flexibility in the filter. By imposing hard limits in this first stage of the reduction we obtain the positions for about 1000 stars in each image, although many of these will still be cosmic rays which have passed through the filter described above. These positions are used by the DAOMASTER program to derive coordinate transformations between each of the images. These are further refined using the ALLFRAME package on this limited set of stars, which improves the accuracy of the transformations. Using these transformations, a very deep image is obtained by mosaicing all of the images together. FIND is then run on this image, which should be free of contaminating cosmic rays. ALLSTAR is then used to subtract each of these stars, and FIND is run again. This process is repeated until no new stars are found. A final visual examination of the image reveals a few remaining stars (typically

around 30), which are also included in the list. Using this final list of stars, ALLFRAME is used to obtain a final list of photometric data. Using the epoch-epoch coordinates derived above, ALLFRAME simultaneously fits a PSF to each star in each image, thus ensuring a self-consistent determination of the magnitude across the window of observations. The calculation of the sky background from an annulus around each star is made only after *all* stars have been removed from the image.

3.1.2. DoPHOT

A brief description of the DoPHOT reduction steps is given in this section; Saha et al. (1996) contains a detailed account of the process. The DoPHOT reduction started by combining each pair of cosmic-ray split images to produce a single, cosmic-ray-free image. This was done using a special algorithm (developed by A. Saha and described in Saha 1996) that co-adds the cosmic-ray split images and identifies pixels that exhibit a large variation between the two frames. Special care is taken to bring both frames to the same background level and to ensure that the program does not trigger on small, sub-pixel shifts of the cores of bright stars. Once the contaminated pixels are identified, they can be replaced with the corresponding pixels from the other frame or set to a mask value so that they are not used at later stages of the processing.

The version of DoPHOT optimised for HST photometry was developed by A. Saha to address some aspects of WFPC2 data that are quite different from ground-based CCD data, such as a point-spread function with a tight core and flared wings and the removal of faint cosmic-ray hits and hot pixels, which is complicated by the under-sampled nature of the data. A DoPHOT reduction starts with the automatic identification of the brightest non-saturated stellar objects in the frame, which are used to construct an

analytic point-spread function (PSF). DoPHOT then proceeds to examine every object whose central pixel is above a certain threshold (which is lowered after each iteration). Every object in the frame is analysed to determine if it is best fit by the stellar PSF, by two close stellar PSFs (appropriate for blended stars), by an extended PSF (appropriate for background galaxies or other extended objects), or by a cosmic-ray profile. Once the best fit is determined, it is applied to the object and used to remove it from the frame. At the end of an iteration, the PSF is improved by using the information obtained from the newly identified stars, and the program goes on to identify objects of lower threshold.

DoPHOT was run a first time on the cleaned images to identify bright objects, which were used to derive coordinate transformations between the epochs. The epochs with negligible shifts (i.e., less than one pixel in each direction) were processed with the same algorithm described above to create deep master frames. These master frames have several advantages, not only in terms of signal-to-noise but also due to the fact that the co-addition of several epochs dithers the sub-pixel profile of the PSF core into a gaussian and allows DoPHOT to determine the centroid of an object with greater accuracy. This reduces the uncertainty in the photometry, which is greatly affected by centering uncertainties in the case of under-sampled data.

The object lists obtained from the reduction of the master frames were transformed into the coordinate systems of each epoch and used by DoPHOT to obtain photometric information for each object from each frame. The magnitudes obtained by DoPHOT are “fitted” magnitudes, which need to be tied to the standard 0.5-arcsecond magnitude system described in Holtzman et al. (1995b). This calibration is described next.

3.2. Calibration

The calibration of photometry for NGC 3621 was achieved using the method outlined in Holtzman et al. (1995b) and Hill et al. (1997). The general equations which convert the “flight-system” instrumental magnitudes into the standard system (Johnson V and Kron-Cousins I) are:

$$V = F555W - 0.052(V - I) + 0.027(V - I)^2 \quad (1)$$

$$I = F814W - 0.063(V - I) + 0.025(V - I)^2. \quad (2)$$

The preceding equations refer to instrumental magnitudes ($F555W$ and $F814W$) that have been fully calibrated and corrected for exposure time and for changes in the gain state of the camera. This is due to a change in the gain state of the camera from $14 \text{ e}^-/\text{DN}$ for the calibration data to $7 \text{ e}^-/\text{DN}$ for the NGC 3621 observations. The gain ratio terms (from Holtzman et al. 1995b) are 1.987, 2.003, 2.006 and 1.955 for the PC1, WF2, WF3 and WF4 chips, respectively, and have uncertainties of order 1%.

The calibration of ALLFRAME photometry involves the corrections listed in the preceding paragraph as well as an aperture correction to bring the fit magnitudes to the 0.5-arcsecond magnitude system. This correction is obtained by comparing photometric magnitudes for the brightest isolated stars in the field of each chip within a 0.5-arcsecond radius calculated using DAOGROW (Stetson 1990) and the corresponding ALLFRAME magnitudes for those stars. The number of stars used in this calculation were 22, 31, 32, and 27 in the PC1, WF2, WF3, and WF4 chips, respectively. These aperture corrections are averages over all our NGC 3621 frames. This local determination of the aperture corrections allows one to correct the effect of any temporal variation in the PSFs over the duration of cycle 4. Variation in these results from image to image is negligible, if the uncertainty in their calculation is taken into account. Comparison with the results for other galaxies in our cycle 4 series show a similar result with typical aperture correction changes of 0.02 mag

from galaxy to galaxy, changes which are barely significant ($\sim 2\sigma$) compared with their measuring errors. The final equations used to calibrate the ALLFRAME photometry are listed in Table A1.

The calibration of DoPHOT photometry also involves an aperture correction, but this coefficient is calculated using a different approach (see Hill et al. 1997 and Saha et al. 1996 for a complete description of the process). It is known that the PSF of stellar cores in the WFPC2 chips varies slightly as a function of position within the chip, while the aperture magnitudes calculated using radii of five pixels or more are constant over the field of view (Holtzman et al. 1995b). Since DoPHOT uses a PSF that does not vary with position, its fitted magnitudes will exhibit a variation of less than 0.15 mag peak to peak due to this effect. These variations are removed by transforming the magnitudes into 5-pixel aperture magnitudes, using correction coefficients derived by A. Saha (Saha et al. 1996) from observations of the Leo I dwarf galaxy (Mateo et al. 1997). The transformation to 0.5-arcsecond aperture magnitudes is achieved using correction coefficients derived from the Leo I data and the NGC 3621 master images. These coefficients vary from frame to frame, and have values between 0.01 mag and 0.13 mag, with uncertainties of ~ 0.03 mag.

3.3. Comparison of ALLFRAME and DoPHOT Photometry

A comparison of the ALLFRAME and DoPHOT photometric systems was conducted for all chip/filter combinations using a visually-selected subset of stars with no bright neighbours within five pixels. Their coordinates (obtained with SAOIMAGE from the plate solutions provided by STScI in the image headers) and V and I ALLFRAME and DoPHOT magnitudes are listed in Tables A2-A5 for future comparisons of our photometry with other observations of NGC 3621 Cepheids. Figure 4 shows plots of Δ mag

(ALLFRAME-DoPHOT) versus ALLFRAME magnitude for these stars. The mean offsets between the two photometric systems are as follows: PC1, $\Delta V = -0.026 \pm 0.011$ mag and $\Delta I = -0.039 \pm 0.014$ mag; WF2, $\Delta V = +0.020 \pm 0.010$ mag and $\Delta I = +0.071 \pm 0.010$ mag; WF3, $\Delta V = -0.066 \pm 0.011$ mag and $\Delta I = +0.077 \pm 0.011$ mag; WF4, $\Delta V = -0.057 \pm 0.010$ mag and $\Delta I = -0.018 \pm 0.010$ mag. This zero-point difference has been seen in other galaxies observed as part of this Key Project; it reflects uncertainties in the aperture corrections of different filter/chip combinations as well as the different treatments of the sky background by the two photometry packages. A full description of the differences is outside the scope of the present paper; this will be analysed in a forthcoming paper employing artificial stars to examine the systematics of both photometry packages. Based on our results, we estimate a photometric uncertainty of ± 0.07 mag in both bands for bright ($m < 24$), isolated stars. See §4.3 for a comparison of Cepheid magnitudes.

A linearity check was conducted using the 180-second V -band image taken on JD 2449746. Fully-calibrated magnitudes of the brightest stars ($V < 23.5$ mag) were compared with the mean magnitudes of the same stars. The zero-point difference was found to be $\Delta V = 0.010 \pm 0.015$ mag and $\Delta V = 0.066 \pm 0.094$ mag for ALLFRAME and DoPHOT respectively.

4. Identification of Cepheid Candidates

4.1. Search for Cepheids

The search for Cepheid variables using ALLFRAME and DoPHOT data was conducted using similar but slightly different approaches. In both cases, the first step was a classification of all objects as either variable or non-variable. In the ALLFRAME search,

this step involved a sigma-like classification of all objects as either variable or non-variable, using a robust estimate of σ , called σ_F (Hughes 1989; Hoaglin, Mosteller & Tukey 1983), that is insensitive to large outliers caused, for example, by cosmic rays. One obtains σ_F by sorting all points in a light-curve in order of magnitude, and calculating the spread (in magnitudes) of the middle 50% of the sorted points. A star was considered a variable if its σ_F was greater than 2 times the mean σ_F of stars with similar magnitudes. This method thus screens against cosmic ray hits, producing a robust list of likely variables.

The first step in the DoPHOT search was performed using a χ_ν^2 variability statistic,

$$\chi_\nu^2 = \sum_i^n \frac{(m_i - \bar{m})^2}{\nu \sigma_i^2}, \quad (3)$$

(Saha & Hoessel 1990), where n is the number of data points available, \bar{m} is the mean magnitude of the star, m_i and σ_i are the individual magnitude measurements and their uncertainties, and $\nu = (n - 1)$. All objects with $\chi_\nu^2 \geq 1.75$ were flagged as variable.

The second step in both searches consisted of a periodicity test of the objects flagged as variables. The ALLFRAME search used a phase dispersion minimisation (PDM) technique (Stellingwerf 1978), which is a variant on the Lafler & Kinman (1965) method. The algorithm bins the light curve into multiple phase and frequency bins, to compare the resultant dispersion with that obtained for the un-binned light-curve. For a periodic variable, this ratio will then be a minimum at the relevant period and phase. This technique is ideal for detecting periodic, but minimally sampled, light-curves of any shape.

The second step in the DoPHOT search used the original Lafler & Kinman method. A “goodness of periodicity” statistic $\Theta(P)$ is calculated,

$$\Theta(P) = \sum_i^n \frac{(m_{i+1} - m_i)^2}{(m_i - \bar{m})^2}, \quad (4)$$

where P is a trial period, \bar{m} is the mean magnitude of the star, and the m_i ’s are the individual magnitude measurements, ordered by phase according to the trial period. Θ

reaches a local minimum when P equals the period or an alias of the period; we chose the deepest minimum as the variable period. Next, the Λ parameter (defined as the ratio of Θ away from the period to Θ at the period) was calculated; only stars with $\Lambda \geq 3$ were considered *bona fide* periodic variables.

The third and last step in both searches involved a visual examination of the remaining objects to identify the Cepheid candidates. Period uncertainties were estimated by visually inspecting the phasing of the light-curve for nearby periods in the case of ALLFRAME, and the variation of Λ with trial period in the case of DoPHOT. To calibrate these estimated period uncertainties, we adopted a Monte Carlo technique in which the light curves were perturbed by the photometric uncertainties, and the periods re-derived. The output period distributions of these simulations tend to be normal distributions with sidelobes of widely varying amplitude due to aliasing. Within the main peak of the distribution, the uncertainties quoted in column (2) of Table 3 are approximately 2.5σ error bars. But to divide these quoted uncertainties by 2.5 to obtain *rms* errors would be to ignore the incidence of aliasing.

Both searches returned the same Cepheid candidates, with the exception of two variables that are located in very crowded regions, and another located close to the edge of the chip. For these three variables, only ALLFRAME photometry is available. See § 4.3 for details.

4.2. Mean Magnitudes

Phased light curves that are evenly sampled can be used to calculate mean magnitudes by simply obtaining an intensity-averaged magnitude,

$$m = -2.5 \log_{10} \frac{1}{N} \sum_{i=1}^N 10^{-0.4 \times m_i}. \quad (5)$$

However, when the sampling is not uniform it is better to use a more elaborate approach and obtain a phase-weighted magnitude,

$$m = -2.5 \log_{10} \sum_{i=1}^N 0.5 \times (\phi_{i+1} - \phi_{i-1}) \times 10^{-0.4 \times m_i}, \quad (6)$$

where N is the total number of epochs and m_i and ϕ_i are the magnitude and phase of the i -th epoch, in order of increasing phase. Typical differences between the two methods are of the order a few hundredths of a magnitude, which do not impact significantly the determination of the distance modulus.

In the case of cosmic-ray split pairs of observations, the two magnitude measurements of a single epoch were combined using weights given by the inverse square of the uncertainty in their photometry. This greatly reduces contamination due to cosmic rays and spurious magnitude estimates. In practice, obvious cosmic ray hits were removed from the data, their presence being identifiable by a major increase in intensity for one of the cosmic-ray split frames and a large uncertainty in the resulting photometry.

The I -band photometry consists of only four epochs of data, which gives rise to under-sampling of the light curves and decreases the precision of both methods of averaging. One way to compensate for this is to make use of the correspondence between V and I light curves for Cepheids, as discussed by Freedman (1988). This takes advantage of the fact that, as a first approximation, one light curve can be mapped onto the other by simple numerical scaling. The ratio of V to I amplitude is found to be 1:0.51. Using this result, we can make an estimate of the correction to the average I magnitude that is required by the under-sampling. This is achieved by calculating the difference between the V -band average for all epochs and for just those epochs with both V - and I -band observations.

This result is rescaled by the 1:0.51 amplitude ratio and applied to the mean I magnitude. The correction is calculated using both methods of averaging and it amounts to no more than ± 0.1 magnitudes, with an average of approximately 0.04 magnitudes.

4.3. The Cepheids Found in NGC 3621

The ALLFRAME and DoPHOT variable searches produced a total of sixty-nine Cepheids (identified as C01-C69). Table 2 lists, for each variable, its identification number, the chip in which it is found, its J2000.0 coordinates (obtained with SAOIMAGE from the plate solution provided by STScI in the image headers) and comments on its quality. The comments describe the degree of crowding (C, f, F, or FF), sampling of the light curve (A, a, or D) and amplitude of the variability (B or E), and indicate the presence of other irregularities such as high sky gradients (s), image defects (I) and cosmic rays (d). A full key to these comments is given in the notes to the table. Using this scheme, a Cepheid with high quality photometric data would have the classification of ABC. This system was applied uniformly across the entire sample of Cepheids to achieve a consistent determination of the best variables to use in the final fit to the Period-Luminosity function.

Table 3 lists, for each variable, the ALLFRAME and DoPHOT periods and phase-weighted magnitudes for the V and I bands. The individual photometric measurements are listed in Tables A6 and A7 for ALLFRAME $F555W$ - and $F814W$ -band data, and in Tables A8 and A9 for DoPHOT $F555W$ - and $F814W$ -band data, respectively. No DoPHOT data is available for variable C07 (located close to one edge of one chip, in an area not searched by DoPHOT), and for variables C34 and C46 (located within very crowded regions). DoPHOT data is also unavailable for most variables in the epoch of JD 2449767 due to problems with image registration.

A comparison of the ALLFRAME and DoPHOT V - and I -band phase-weighted magnitudes for the Cepheids is presented in Figure 5. The mean offsets (ALLFRAME - DoPHOT) are as follows: PC1, $\Delta V = +0.07 \pm 0.02$ mag and $\Delta I = 0.00 \pm 0.03$ mag; WF2, $\Delta V = +0.01 \pm 0.03$ mag and $\Delta I = +0.09 \pm 0.03$ mag; WF3, $\Delta V = -0.03 \pm 0.03$ mag and $\Delta I = 0.14 \pm 0.05$ mag; WF4, $\Delta V = -0.06 \pm 0.03$ mag and $\Delta I = 0.07 \pm 0.03$ mag. While the V -band differences are consistent with those derived from bright, isolated field stars (§3.3) except for the case of PC1 which is a three-sigma result. The I -band offsets also agree well within their uncertainties. These differences between the ALLFRAME and DoPHOT photometry sets are under investigation using experiments involving the insertion of artificial stars in the data. It reflects no more than a 5% discrepancy in the distance, and is included in the error budget.

The Cepheids are identified in the field of each of the WFPC2 chips in Figures 6a-d. Finding charts for each of the stars are displayed in Figures 7a-l; each of the charts encompasses a 50 by 50 pixel area around each variable. V - and I -band light curves based on the ALLFRAME data are presented in Figures 8a-l. Figure 9 shows the location of all Cepheids in a color-magnitude diagram of NGC 3621 stars. The Cepheids are shown to have colors consistent with those expected for Cepheids.

5. Period-Luminosity Relations and Distance Moduli

5.1. Methodology

The method used to derive V - and I -band apparent distance moduli is the same as that was used in other papers in this series. The period-luminosity relations of LMC Cepheids (Madore & Freedman 1991) are scaled to an assumed true distance modulus of $\mu_{0,\text{LMC}} =$

18.50±0.10 mag (total uncertainty) and corrected for an estimated average line-of-sight reddening of $E(V - I)_{\text{LMC}} = 0.13$ mag (Bessell 1991).

The period-luminosity relations can be expressed as:

$$M_V = -2.76 (\log P \text{ (d)} - 1.0) - 4.16, \quad (7)$$

$$M_I = -3.06 (\log P \text{ (d)} - 1.0) - 4.87. \quad (8)$$

In fitting the data from NGC 3621, we follow the procedure given in Freedman et al. (1994a). We fix the slope of best fit to that given in the equations above and scale the equations in the magnitude axis until the minimum rms dispersion between the data and the fit is obtained. By using the slopes given above, we minimize any bias that would arise from incompleteness at faint magnitudes in the NGC 3621 data set. We have also experimented with minimum period cutoffs imposed on the data set following the discussion by Sandage et al. (1992). Variation in the distance modulus with period cutoffs up to 18 days is of the order of 0.04 mag.

The magnitude shifts resultant from this method yield V - and I -band apparent distance moduli relative to the LMC. A reddening correction due to the presence of interstellar dust must be applied in order to obtain the true distance modulus (see Madore & Freedman 1991 for a complete description of this correction). The mean color excess $\langle E(V - I) \rangle$ is effectively calculated by returning each of the individual Cepheids to the ridge line of the intrinsic period-color relation. The total scatter in the individual estimates about the average reddening is then effectively used to determine the quoted uncertainty on the mean. In reality however, that scatter contains also the full intrinsic width of the period-color relation. In determining the reddening-corrected true modulus, the derived mean reddening is therefore not used explicitly; rather the V and $(V - I)$ data

are combined in such a way that a reddening-free magnitude $^\dagger W = V - 2.45(V - I)$ is calculated for each Cepheid and differenced against the absolutely calibrated version of the $W - \log P$ relation. The resulting true moduli are then averaged and a mean true modulus is calculated. It is the scatter about this quantity that defines the quoted error in the true modulus. This uncertainty can be significantly smaller than the scaled error in the color excess because of the fact that lines of constant period in the color-magnitude diagram are closely degenerate with reddening trajectories. That is, some fraction of the scatter in the period-color relation (used to calculate reddenings and their errors) is correlated with scatter in the period-luminosity relations and by removing correlated errors due to reddening some (large) fraction of the intrinsic-color-induced scatter is also removed. The final scatter measured in the individually derived true moduli primarily reflects errors in the photometry plus the small degree to which the adopted reddening trajectory departs from the intrinsic color-magnitude correlation.

5.2. Results

A subset of Cepheids with no bright stars within five pixels (i.e., class C and f in Table 2) were selected for P-L fitting; there are 36 such stars with ALLFRAME photometry, and one less in the DoPHOT set. Period-Luminosity relations in the V and I bands are plotted in Figures 10 and 11 for ALLFRAME and DoPHOT data, respectively. Filled circles

† The factor of 2.45 can be simply derived from the extinction law of Cardelli et al. (1989). Using their notation we have $A_I/A_V = 0.7712 - 0.5897/R_V$, where $R_V = 3.3$ for stars with colors similar to those of Cepheids. A reddening free magnitude is thus defined by $W \equiv V - A_V \equiv I - A_I$. Solving these two equations for W yields the equation above.

are used to plot the Cepheids in the selected subset, while the other ones are represented by open circles.

The procedure described in §5.1 yielded V - and I -band apparent distance moduli relative to the LMC of 11.02 ± 0.08 mag and 10.86 ± 0.07 mag for the ALLFRAME data, and 11.05 ± 0.08 mag and 10.85 ± 0.08 mag for the DoPHOT data. The quoted uncertainties reflect *only* the rms dispersion of the NGC 3621 period-luminosity relations. The difference between ALLFRAME and DoPHOT I -band distance moduli is larger than the difference in the V -band distance moduli, due to the larger discrepancy of I -band mean magnitudes discussed in §4.3.

Assuming a distance modulus of 18.50 ± 0.10 mag and a reddening of $E(V - I) = 0.13$ mag for the LMC, we obtained true distance moduli of 29.13 ± 0.18 mag and 29.06 ± 0.18 mag for the ALLFRAME and DoPHOT data, respectively, corresponding to distances of 6.3 ± 0.7 Mpc and 6.1 ± 0.7 Mpc. These results are equivalent to V - and I -band apparent distance moduli of 29.84 ± 0.18 mag and 29.55 ± 0.18 mag for the ALLFRAME data and 29.87 ± 0.18 mag and 29.54 ± 0.18 mag for the DoPHOT data, as well as mean reddening values of $E(V - I) = 0.29 \pm 0.03$ mag and 0.33 ± 0.04 mag for the ALLFRAME and DoPHOT data, respectively.

The preceding results change slightly if the complete set of 69 (ALLFRAME) and 66 (DoPHOT) Cepheids is used: the ALLFRAME distance modulus increases by 0.07 mag, whereas the DoPHOT distance modulus remains the same. The resulting distances are 6.5 ± 0.7 Mpc and 6.1 ± 0.7 Mpc, respectively.

A full description of the different contributions to the uncertainties is presented in Table 4. An important contribution to the error budget is the uncertainty of the effect due to the different metallicities of the LMC and NGC 3621 ($[O/H] = -3.60$ and -3.05 , respectively). Assuming that the coefficient $-\frac{\partial V}{\partial(\log Z)}|_P$ is less than 0.16 mag/dex (based on

unpublished simulations by Wood, Mould and Madore), we have estimated this uncertainty to be ± 0.10 mag.

For comparison with Equations (7) and (8), the NGC 3621 period-luminosity relations based on ALLFRAME results are:

$$m_V = -2.76 (\log P (\text{d}) - 1.0) + 25.68 \pm 0.09 \quad (9)$$

$$m_I = -3.06 (\log P (\text{d}) - 1.0) + 24.68 \pm 0.09. \quad (10)$$

6. Conclusions

We have discovered a total of 69 Cepheid stars in the Sc field spiral galaxy NGC 3621. We have fitted standard V - and I -band period-luminosity relations to a subset of the variables and obtained true distance moduli of 29.13 ± 0.18 and 29.06 ± 0.18 magnitudes for the ALLFRAME and DoPHOT data, respectively. These correspond to distances of 6.3 ± 0.7 and 6.1 ± 0.7 Mpc. Mean reddenings were deduced from the apparent V - and I -band moduli using a standard reddening curve, and they amount to $E(V-I) = 0.29 \pm 0.03$ and 0.33 ± 0.04 magnitudes. There is agreement, within the uncertainties, between the ALLFRAME and DoPHOT results.

7. Acknowledgements

We would like to thank Doug Van Orsow, the program coordinator for this Key Project, as well as the rest of the STScI and NASA support staff that have made this project possible. The HST Key Project on the Extragalactic Distance Scale is supported by NASA

through grant GO-2227-87A from STScI. This work has made use of the NASA/IPAC Extragalactic Database (NED), which is operated by the Jet Propulsion Laboratory, Caltech, under contract with the National Aeronautics and Space Administration.

REFERENCES

- Bessell, M.S. 1991, *A&A*, 242, L17
- Burrows, C.J. et al., 1994, *The Wide Field and Planetary Camera 2 Instrument Handbook* (Baltimore: STScI)
- Cardelli, A. J., et al. 1989, *ApJ*, 354, 245
- Casertano, S. & Baggett, S., 1997, *The Wide Field and Planetary Camera 2 Cycle 5 Calibration Closure Report* (Baltimore: STScI) (see the STScI WFPC2 web-page http://www.stsci.edu/ftp/instrument_news/WFPC2/wfpc2_top.html)
- deVaucouleurs, G., deVaucouleurs, A., Corwin Jr., H., Buta, R., Paturel, G. and Fouqué, P., 1991, *Third Reference Catalogue of Bright Galaxies* (Berlin: Springer-Verlag)
- Ferrarese, L. et al. 1996, *ApJ*, 464, 568
- Freedman, W.L. 1988, *ApJ*, 326, 691
- Freedman, W.L. 1990, *ApJ*, 355, L35
- Freedman, W.L. et al. 1994a, *ApJ*, 427, 628
- Freedman, W.L. et al. 1994b, *ApJ*, 435, L31
- Freedman, W.L. et al. 1994c, *Nature*, 371, 757
- Gardiner, L.T. & Whiteoak, J.B. 1977, *Aust. J. Phys.*, 30, 187
- Hill, R.J. et al. 1997, submitted for publication in *ApJ*
- Hoaglin, D.C., Mosteller, F. & Tukey, J.W. 1983, *Understanding Robust and Exploratory Data Analysis* (New York: Wiley)

- Holtzman, J.A. et al. 1995a, PASP, 107, 156
- Holtzman, J.A. et al. 1995b, PASP, 107, 1065
- Hughes, S.M.G. 1989, AJ, 97, 1634
- Jacoby, G. et al. 1992, PASP, 104, 599
- Kelson, D.D. et al. 1996, ApJ, 463, 26
- Kennicutt, R.C., Freedman, W.L., & Mould, J.R. 1995, AJ, 110, 1476
- Lafier, J. & Kinman, T.D. 1965, ApJS, 11, 216
- Madore, B.F., & Freedman, W.L. 1991, PASP, 103, 933
- Mateo, M. et al. 1997, in preparation
- Mould, J.R. et al. 1995, ApJ, 449, 413
- Saha, A. & Hoessel, J.G. 1990, AJ, 99, 97
- Saha, A. et al. 1996, ApJ, 466, 55
- Sandage, A. and Tammann, G. 1981, *Revised Shapley-Ames Catalog of Bright Galaxies*
(Washington: Carnegie)
- Sandage, A. and Bedke, J. 1985, AJ, 90, 1992
- Sandage, A. et al. 1992, ApJ, 401, L7
- Schechter, P.L., Mateo, M., and Saha, A. 1993, PASP, 105, 1342
- Silbermann, N.A. et al. 1996, ApJ, 470, 1
- Stellingwerf, R.F. 1978, ApJ, 224, 953

Stetson, P.B. 1987, PASP, 99, 191

Stetson, P.B. 1990, PASP, 102, 932

Stetson, P.B. 1994, PASP, 106, 250

Stetson, P.B. et al. 1997, in preparation

Figure Captions

Figure 1: – A wide-field image of NGC 3621 (courtesy Sandage & Bedke 1985), with the footprint of the WFPC2 field of view (see Figure 2)

Figure 2.– A mosaic of the WFPC2 images of NGC 3621, showing the detailed structure of the region outlined in figure 1. Single-chip images, marking the location of the variables, can be found in Figures 7a-d.

Figure 3.– Sampling variance for the V -band observations. The lower variance points indicate periods at which the phase coverage is less uniform, and a corresponding decrease in the probability of detection. Due to the quadratic distribution in time of the observations, an enhanced performance in the detection of variables is obtained. The variance turns over due to the 65 day observing window.

Figure 4.– A comparison of the ALLFRAME and DoPHOT V and I magnitudes for bright and fairly isolated stars present in each chip. Filled and open circles represent V and I . The mean offsets between the two photometric packages for the four chips are as follows: PC1, $\Delta V = -0.026 \pm 0.011$ mag and $\Delta I = -0.039 \pm 0.014$ mag; WF2, $\Delta V = +0.020 \pm 0.010$ mag and $\Delta I = +0.071 \pm 0.010$ mag; WF3, $\Delta V = -0.066 \pm 0.011$ mag and $\Delta I = +0.077 \pm 0.011$ mag; WF4, $\Delta V = -0.057 \pm 0.010$ mag and $\Delta I = -0.018 \pm 0.010$ mag. These differences are consistent with the results for other galaxies examined in the Key Project.

Figure 5.– A comparison of the ALLFRAME and DoPHOT V and I mean phase-weighted magnitudes for Cepheids in each chip. Filled and open circles represent V and I magnitudes. The mean offsets and rms deviations are as follows: PC1, $\Delta V = +0.07 \pm 0.02$ mag and $\Delta I = 0.00 \pm 0.03$ mag; WF2, $\Delta V = +0.01 \pm 0.03$ mag and $\Delta I = +0.09 \pm 0.03$ mag; WF3, $\Delta V = -0.03 \pm 0.03$ mag and $\Delta I = 0.14 \pm 0.05$ mag; WF4, $\Delta V = -0.06 \pm 0.03$ mag and $\Delta I = 0.07 \pm 0.03$ mag. The V - and I -band differences are comparable with the results shown in Figure 4.

Figures 6a-d.– V -band images of the four WFPC2 chips. The circles indicate the position of each of the Cepheids, labelled as in Table 2. Each of the images is oriented such that the bottom left corner has the pixel coordinates 0,0 in each image.

Figures 7a-l.– Finding charts for all the Cepheids. The position of each Cepheid is shown by the arrows. The coordinates are measured relative to the bottom-left corner of the images in Figures 6a-d.

Figures 8a-l.– V - and I -band phased light curves for all the Cepheids, using ALLFRAME data. Filled and open circles represent V and I magnitudes, respectively. Two complete cycles are plotted to facilitate ease of interpretation.

Figure 9.– Color-magnitude diagram of stars in NGC 3621. Filled circles are used to plot the subset of isolated Cepheids used to fit the period-luminosity relation, while open circles represent the remaining Cepheids in the sample.

Figure 10.– Period-luminosity relations in the V (top) and I (bottom) bands based on ALLFRAME photometry. Filled circles are used to plot the subset of isolated Cepheids with no companion star lying within a 5-pixel radius, while open circles represent the crowded Cepheids. The solid lines are the best fits and the dotted lines correspond to the rms dispersion of the LMC period-luminosity relation of Madore & Freedman (1991). Apparent distance moduli obtained from the lines of best fit are 29.84 ± 0.18 and 29.55 ± 0.18 in the V - and I -bands respectively. Including a correction due to reddening this corresponds to a distance of 6.3 ± 0.7 Mpc.

Figure 11.– Period-luminosity relations in the V (top) and I (bottom) bands based on DoPHOT photometry. Filled circles are used to plot the subset of isolated Cepheids with no companion star lying within a 5-pixel radius, while open circles represent the crowded Cepheids. The solid lines are the best fits and the dotted lines correspond to the rms dispersion of the LMC period-luminosity relation of Madore & Freedman (1991). Apparent distance moduli obtained from the lines of best fit are 29.87 ± 0.18 and 29.54 ± 0.18 in the V - and I -bands respectively. Including a correction due to reddening this corresponds to a distance of 6.1 ± 0.7 Mpc.

Table Captions

Table 1: – Log of HST WFPC2 observations of NGC 3621. All observations comprise two cosmic-ray split pairs except for the epoch on January 4th. The Julian Date quoted is the heliocentric Julian Date at mid-exposure.

Table 2: – The Cepheid candidates found in NGC 3621. The columns provide the following information: (1) the identification; (2) the chip in which each variable is located; (3) and (4) the right ascension and declination in (J2000.0) and (5) the description of each of the Cepheids using the key given in the notes to the Table.

Table 3: – The Cepheid candidates found in NGC 3621. The columns provide the following information: (1) the identification; (2) the ALLFRAME period in days; (3) and (4) the ALLFRAME *V*- and *I*-band phase-weighted magnitudes and their uncertainties (5) the; (DoPHOT period in days; (6) and (7) the DoPHOT *V*- and *I*-band phase-weighted magnitudes and their uncertainties.

Table 4: – The contributions to the error budget of the distance modulus of NGC 3621. The uncertainties in the *V*-band and *I*-band P-L relation, are partially correlated (§5.1) and this is taken into account in calculating the uncertainty of the un-reddened P-L relation (R2). This is in turn combined with the *rms* error attributed to the photometric algorithms to arrive at the uncertainty in the absolute distance modulus relative to the LMC. This uncertainty is combined with the uncertainty in the LMC distance modulus and the metallicity effect to arrive at the final uncertainty in the distance modulus.

Appendix Table Captions

Table A1: – The aperture correction and WFPC2 zero-point coefficients used for ALLFRAME photometry.

Tables A2-A5: – Secondary standard photometry for Chips 1-4

Table A6: – *V*-band ALLFRAME data for each of the Cepheids over the twelve epochs.

Table A7: – *I*-band ALLFRAME data for each of the Cepheids over the four epochs.

Table A8: – *V*-band DoPHOT data for each of the Cepheids over the twelve epochs.

Table A9: – *I*-band DoPHOT data for each of the Cepheids over the four epochs.

TABLE 1
HST OBSERVATIONS OF NGC 3621

Obs. Date	JD	Exp. Time (s)	Filter
27/12/94	2449714.37	900 + 900	F555W
27/12/94	2449714.43	900 + 900	F814W
04/01/95	2449722.28	900	F555W
04/01/95	2449722.34	900 + 900	F814W
04/01/95	2449722.41	900 + 900	F439W
15/01/95	2449733.40	900 + 900	F555W
17/01/95	2449735.48	900 + 900	F555W
20/01/95	2449738.43	900 + 900	F555W
24/01/95	2449742.18	900 + 900	F555W
24/01/95	2449742.25	900 + 900	F814W
24/01/95	2449742.32	900 + 900	F439W
28/01/95	2449746.01	900 + 900	F555W
28/01/95	2449746.06	180	F555W
28/01/95	2449746.07	180	F814W
01/02/95	2449750.09	800 + 800	F555W
06/02/95	2449755.25	800 + 800	F555W
12/02/95	2449761.16	800 + 800	F555W
12/02/95	2449761.22	900 + 900	F814W
18/02/95	2449767.39	800 + 800	F555W
25/02/95	2449773.69	900 + 900	F555W

NOTE.—The following reference files were used in the calibration of these exposures. File names follow the conventions adopted by the Space Telescope Science Institute. The file was used for all filters unless indicated otherwise. MASKFILE = e2112084u.r0h; ATODFILE = dbu1405iu.r1h; BIASFILE = e6l10347u.r2h (27/12/94 - 20/1/95) and flj1615tu.r2h (24/1/95 - 25/02/95); DARKFILE = ebh1547qu.r3h (27/12/95), f151225pu.3h (04/01/95 - 17/01/95), fli1004iu.r3h (20/01/95), flk1459hu.r3h (24/01/95 - 01/02/95), f220923mu.r3h (06/02/95 - 12/02/95), and f2h11352u.r3h (18/02/95 - 25/02/95); FLATFILE = e380935cu.r4h (F555W), e380934lu.r4h (F439W) and e391434fu.r4h (F814W); SHADFILE = e371355eu.r5h (shutter A), e371355iu.r5h (shutter B), depending on the shutter used at the start of the exposure; GRAPHTAB = e8210190m.tmg; COMPTAB = eai1341pm.tmc

TABLE 2
CEPHEID CANDIDATES – COORDINATES AND CLASSIFICATION

ID	Chip	R.A. (J2000.0)	Dec.	Comments	ID	Chip	R.A. (J2000.0)	Dec.	Comments
C01	WF2	11:18:21.6	-32:50:19.2	ABfd *	C02	WF4	11:18:14.0	-32:50:58.8	ABC *
C03	PC1	11:18:16.6	-32:50:09.3	ABCd *	C04	WF3	11:18:22.4	-32:51:05.8	aBfd *
C05	WF2	11:18:19.5	-32:49:51.2	aBFs	C06	WF4	11:18:16.3	-32:50:47.7	ABfsd *
C07	WF3	11:18:22.5	-32:50:49.4	ABFFs	C08	PC1	11:18:18.3	-32:50:24.5	DEC *
C09	WF2	11:18:19.7	-32:50:02.4	aBFFs	C10	PC1	11:18:16.8	-32:50:31.4	aBC *
C11	WF4	11:18:16.0	-32:50:50.5	aEFs	C12	PC1	11:18:18.8	-32:50:16.5	ABFFI
C13	PC1	11:18:17.1	-32:50:12.7	ABCd *	C14	WF2	11:18:21.4	-32:49:32.7	ABFFs
C15	WF2	11:18:20.5	-32:50:07.1	ABFFd	C16	PC1	11:18:18.2	-32:50:36.0	ABC *
C17	PC1	11:18:19.0	-32:50:36.3	ABC *	C18	WF2	11:18:19.8	-32:50:20.8	aBFsd
C19	WF4	11:18:16.1	-32:51:34.8	ABFF	C20	WF2	11:18:22.3	-32:50:30.9	ABfd *
C21	PC1	11:18:18.3	-32:50:40.2	aBdF	C22	WF2	11:18:20.1	-32:49:55.0	aBFFs
C23	WF2	11:18:19.6	-32:49:38.8	ABfsd	C24	WF3	11:18:23.5	-32:51:44.2	aBCd *
C25	WF2	11:18:24.4	-32:49:53.9	aBf *	C26	WF3	11:18:19.0	-32:51:38.0	DBF
C27	WF4	11:18:17.3	-32:50:43.5	aBFF	C28	WF4	11:18:17.3	-32:51:12.8	aBfd *
C29	PC1	11:18:18.2	-32:50:39.9	ABCd *	C30	WF4	11:18:15.5	-32:51:44.8	DBF
C31	WF2	11:18:21.3	-32:49:53.9	aBF	C32	WF2	11:18:19.4	-32:50:35.2	aBFF
C33	WF2	11:18:20.3	-32:49:40.0	ABFs	C34	WF4	11:18:16.1	-32:51:26.2	aEFF
C35	PC1	11:18:18.3	-32:50:26.0	aBC *	C36	WF4	11:18:14.7	-32:51:03.8	Def *
C37	WF2	11:18:21.4	-32:50:18.3	aBfd *	C38	WF2	11:18:19.7	-32:50:10.8	aBFFsd
C39	WF2	11:18:20.0	-32:50:16.1	ABFF	C40	WF3	11:18:18.7	-32:51:25.2	DBfsd *
C41	WF4	11:18:14.5	-32:51:10.7	ABC *	C42	WF2	11:18:21.6	-32:49:46.7	aBFFd
C43	WF2	11:18:20.6	-32:50:01.2	DEFFs	C44	WF3	11:18:18.9	-32:51:08.3	ABFd
C45	WF2	11:18:20.0	-32:49:48.5	aEfs *	C46	WF3	11:18:23.7	-32:50:52.7	ABf *
C47	WF4	11:18:18.0	-32:50:51.0	DBf *	C48	WF4	11:18:18.1	-32:51:11.5	aECd *
C49	WF2	11:18:19.8	-32:50:15.6	aBCs *	C50	WF2	11:18:20.3	-32:50:15.4	ABFs
C51	PC1	11:18:17.6	-32:50:14.3	ABFF	C52	WF3	11:18:23.6	-32:51:47.3	aBf *
C53	WF4	11:18:16.3	-32:51:26.4	ABf *	C54	WF2	11:18:20.7	-32:49:59.7	ABfd *
C55	WF4	11:18:16.6	-32:51:00.9	aBf *	C56	WF2	11:18:23.2	-32:50:34.7	aBCd *
C57	PC1	11:18:18.2	-32:50:12.5	aEfsd	C58	WF2	11:18:19.5	-32:49:56.6	aBfsd
C59	WF2	11:18:20.2	-32:50:19.9	aEFs	C60	PC1	11:18:16.1	-32:50:20.2	ABC *
C61	WF4	11:18:18.2	-32:51:05.7	aBf *	C62	PC1	11:18:18.0	-32:50:35.5	aECd *
C63	WF3	11:18:20.5	-32:51:43.2	DBfd *	C64	WF2	11:18:19.3	-32:50:42.8	aBF
C65	WF4	11:18:17.2	-32:51:09.6	DEF	C66	PC1	11:18:18.4	-32:50:37.5	ABfd *
C67	PC1	11:18:17.4	-32:50:32.6	AECd *	C68	WF2	11:18:19.5	-32:50:29.3	aEFsd
C69	WF3	11:18:21.3	-32:51:46.7	DBFd					

NOTE.—The key to the code used to describe each Cepheid is: (A) well-sampled rise and decline in the lightcurve, (a) well-sampled decline only, (B) *V*-band peak-to-peak lightcurve amplitude of 0.75 mag or greater, (C) isolated star, (D) poorly sampled lightcurve, (E) low-amplitude lightcurve, (F) companion within 4 pixel radius, (FF) two or more companion stars within 4 pixel radius, (I) bad image defect, (d) affected by cosmic rays, (f) companion within 8 pixel radius, but not overlapping (ff) bad confusion in the wings, (i) minor image defect, (s) large sky gradient. (*) indicates that the Cepheid was incorporated into the final sample.

TABLE 3
CEPHEID CANDIDATES – PROPERTIES

ID	ALLFRAME			DoPHOT		
	Period (d)	<i>V</i>	<i>I</i>	Period (d)	<i>V</i>	<i>I</i>
C01	60.0±5.0	23.52±0.04	22.61±0.05	59.1±3.8	23.58±0.03	22.56±0.03
C02	45.5±4.5	23.88±0.02	22.79±0.03	49.2±2.0	23.89±0.04	22.67±0.04
C03	44.7±5.4	24.38±0.03	22.97±0.04	46.6±4.0	24.32±0.05	23.10±0.05
C04	40.9±3.1	23.81±0.02	22.90±0.04	39.8±1.2	23.97±0.03	22.83±0.03
C05	40.7±3.2	24.78±0.05	23.40±0.08	39.4±4.0	24.73±0.07	23.44±0.06
C06	39.0±3.0	24.82±0.04	23.53±0.05	40.4±1.2	25.00±0.09	23.47±0.08
C07	38.3±2.5	23.57±0.04	22.76±0.04
C08	37.7±2.3	24.96±0.04	22.95±0.04	39.3±1.5	25.00±0.05	22.84±0.05
C09	34.5±0.5	24.09±0.07	23.11±0.08	30.6±0.6	24.56±0.09	23.29±0.08
C10	34.0±4.0	24.09±0.04	22.99±0.04	37.2±3.8	24.05±0.04	22.98±0.04
C11	32.7±0.1	25.94±0.07	24.70±0.11	30.7±1.3	26.05±0.14	24.73±0.13
C12	32.0±2.5	25.23±0.07	23.74±0.12	34.1±4.0	25.28±0.09	23.79±0.08
C13	31.7±3.4	24.39±0.03	23.28±0.04	32.4±5.0	24.21±0.06	23.19±0.06
C14	31.5±2.5	23.28±0.03	22.76±0.05	28.8±1.4	23.56±0.06	22.74±0.05
C15	31.5±2.4	25.20±0.07	23.52±0.06	30.7±3.0	25.12±0.07	23.37±0.07
C16	31.2±2.4	24.50±0.03	23.28±0.04	34.9±2.5	24.39±0.05	23.24±0.05
C17	28.3±2.5	23.89±0.03	22.84±0.04	30.2±2.0	23.84±0.03	22.79±0.03
C18	27.8±2.2	25.30±0.06	24.11±0.08	27.8±2.0	25.19±0.11	23.98±0.10
C19	27.7±2.1	23.99±0.03	22.95±0.04	31.7±3.4	23.95±0.05	23.02±0.05
C20	26.4±2.4	24.78±0.05	23.71±0.05	26.8±0.9	24.73±0.07	23.67±0.07
C21	26.3±2.0	24.81±0.03	23.64±0.05	24.8±0.9	24.68±0.10	23.65±0.09
C22	26.2±3.2	24.14±0.04	23.18±0.06	25.7±3.9	24.13±0.06	23.10±0.06
C23	25.6±1.2	25.23±0.08	23.89±0.08	25.9±1.6	25.14±0.09	23.73±0.08
C24	25.4±1.3	24.28±0.04	23.23±0.05	22.7±0.8	24.29±0.08	23.27±0.07
C25	25.3±0.5	25.30±0.06	24.14±0.06	25.5±0.8	25.23±0.08	23.96±0.07
C26	24.7±0.8	24.77±0.03	23.76±0.05	21.5±0.4	24.72±0.07	23.62±0.06
C27	24.5±1.9	24.60±0.06	23.59±0.08	26.1±0.5	24.86±0.08	23.64±0.07
C28	24.4±2.1	24.26±0.05	23.11±0.06	23.1±1.2	24.24±0.05	23.21±0.05
C29	24.4±1.5	25.21±0.03	23.89±0.05	23.2±3.0	25.11±0.08	23.95±0.07
C30	23.8±1.9	25.54±0.05	24.14±0.07	24.0±1.9	25.57±0.11	24.11±0.10
C31	23.8±1.8	24.63±0.05	23.31±0.05	22.3±1.5	24.57±0.06	23.21±0.05
C32	23.5±2.3	24.11±0.04	23.26±0.08	22.3±2.0	24.13±0.05	23.10±0.05
C33	23.3±1.8	25.96±0.09	24.07±0.09	23.7±2.4	25.70±0.16	24.44±0.14
C34	23.1±1.8	24.80±0.05	23.84±0.06

TABLE 3—*Continued*

ID	ALLFRAME			DoPHOT		
	Period (d)	V	I	Period (d)	V	I
C35	22.8±3.1	24.77±0.03	23.60±0.05	26.1±0.5	24.82±0.07	23.66±0.06
C36	22.7±1.8	24.79±0.03	23.74±0.06	21.2±1.5	24.87±0.07	23.74±0.07
C37	22.2±1.6	24.92±0.05	23.65±0.04	22.0±1.7	25.02±0.09	23.62±0.08
C38	21.5±1.7	24.08±0.05	23.30±0.06	21.3±1.2	24.20±0.06	23.21±0.06
C39	21.2±0.8	24.70±0.04	23.75±0.06	24.5±1.4	24.46±0.09	23.51±0.08
C40	21.0±0.7	24.97±0.04	23.71±0.04	20.7±1.0	24.96±0.07	23.55±0.06
C41	20.7±2.3	24.37±0.03	23.48±0.04	22.0±1.7	24.32±0.03	23.36±0.03
C42	19.9±1.9	25.16±0.06	23.87±0.08	18.5±0.7	24.92±0.07	23.66±0.07
C43	19.9±0.6	23.86±0.05	23.05±0.06	22.1±1.5	23.97±0.05	23.08±0.05
C44	19.2±0.6	24.78±0.04	23.89±0.07	17.7±1.9	24.96±0.08	23.71±0.07
C45	18.8±0.8	24.43±0.05	23.04±0.07	18.8±1.0	24.58±0.06	22.95±0.06
C46	18.7±0.8	24.42±0.04	23.13±0.12
C47	18.5±1.4	24.37±0.04	23.58±0.06	19.1±0.6	24.53±0.06	23.52±0.06
C48	18.4±1.1	25.18±0.05	24.02±0.07	18.8±0.3	25.13±0.09	23.87±0.08
C49	18.2±1.2	25.23±0.06	24.11±0.10	20.5±0.6	25.13±0.08	23.88±0.07
C50	18.0±1.4	25.22±0.07	24.09±0.09	17.7±1.7	25.24±0.10	23.96±0.09
C51	17.8±1.3	25.01±0.04	23.82±0.07	17.7±1.9	25.09±0.10	23.77±0.09
C52	17.8±0.9	24.49±0.04	23.75±0.05	17.0±2.0	24.53±0.07	23.56±0.06
C53	17.5±1.4	24.79±0.04	24.07±0.07	17.0±2.0	24.93±0.07	23.85±0.07
C54	17.4±1.2	24.63±0.04	23.98±0.08	18.8±1.2	24.68±0.08	23.83±0.07
C55	17.0±1.3	25.28±0.06	24.39±0.09	15.7±0.8	25.45±0.09	24.27±0.08
C56	16.5±1.3	25.06±0.04	24.14±0.06	16.6±0.4	24.96±0.09	23.97±0.08
C57	16.3±0.8	25.17±0.05	24.18±0.07	16.8±0.8	25.04±0.11	23.98±0.10
C58	16.2±1.3	25.24±0.09	24.12±0.09	16.3±1.2	25.24±0.13	23.93±0.12
C59	16.2±0.9	25.30±0.06	24.43±0.08	15.5±1.7	25.26±0.12	24.35±0.11
C60	14.8±1.1	24.81±0.04	23.63±0.05	15.3±1.4	24.72±0.08	23.95±0.07
C61	13.9±0.3	25.04±0.04	24.18±0.07	13.9±1.0	24.98±0.09	24.05±0.08
C62	13.8±0.5	25.61±0.05	24.44±0.08	13.5±0.6	25.53±0.08	24.49±0.08
C63	13.0±0.2	25.12±0.06	24.29±0.08	13.2±0.8	25.12±0.08	24.28±0.08
C64	12.2±1.0	25.11±0.05	24.38±0.09	12.3±1.7	24.90±0.12	24.15±0.11
C65	12.1±0.1	25.19±0.05	24.10±0.06	12.4±0.5	25.10±0.09	23.83±0.08
C66	11.9±0.9	25.57±0.06	24.23±0.08	12.5±1.2	25.38±0.09	24.07±0.09
C67	11.5±0.6	25.28±0.05	24.15±0.07	11.7±0.9	25.15±0.10	24.18±0.09
C68	10.0±0.3	25.21±0.06	24.41±0.10	10.0±0.5	25.18±0.12	24.36±0.11
C69	9.4±0.2	25.49±0.06	24.78±0.11	9.5±0.5	25.43±0.13	24.35±0.12

TABLE 4
ERROR BUDGET FOR NGC 3621

Source of Uncertainty	Error	Comment
CEPHEID PL CALIBRATION		
(a) LMC True Modulus	± 0.10	
(b) V PL Zero Point	± 0.05	
(c) I PL Zero Point	± 0.03	
(S1) Systematic Uncertainty	± 0.12	(a),(b),(c) combined in quadrature
NGC 3621 MODULUS		
(d) HST V-Band Zero Point	± 0.05	
(e) HST I-Band Zero Point	± 0.05	
(R1) Cepheid True Modulus	± 0.15	(d),(e) coupled by reddening law
(f) PL Fit (V)	± 0.08	
(g) PL Fit (I)	± 0.08	
(R2) Cepheid True Modulus	± 0.10	(f),(g) partially correlated
(S2) Metallicity Uncertainty	± 0.10	from M31 metallicity gradient test
TOTAL UNCERTAINTY		
(R) Random Errors	± 0.18	(R1) and (R2) combined in quadrature
(S) Systematic Errors	± 0.16	(S1) and (S2) combined in quadrature

TABLE A1
COEFFICIENTS USED FOR ALLFRAME PHOTOMETRY

Chip	Filter	Aperture Correction	WFPC2 Zeropoint	C Coeff.
PC1	V	-0.067 ± 0.02	22.510	-1.036
PC1	I	-0.077 ± 0.03	21.616	-1.940
WF2	V	-0.014 ± 0.02	22.522	-0.971
WF2	I	$+0.026 \pm 0.02$	21.657	-1.796
WF3	V	-0.007 ± 0.02	22.530	-0.956
WF3	I	$+0.032 \pm 0.03$	21.638	-1.809
WF4	V	-0.011 ± 0.02	22.506	-0.984
WF4	I	$+0.045 \pm 0.03$	21.609	-1.895

NOTE.—The ALLFRAME instrumental magnitudes ($F555W$ and $F814W$ of Eqns. 1-2) are obtained from the fitted magnitudes after applying the correction $m_{\text{inst}} = m_{\text{fit}} + 2.5 * \log t + C$. The coefficient C equals $-25.00 + 0.016 + 2.5 * \log 4 + AC + ZP$, where t is the exposure time, -25.00 is the ALLFRAME zeropoint, $+0.016$ accounts for a pixel area normalization, $2.5 \log 4$ accounts for the image conversion to integer data described in §2.1, AC is the aperture correction and ZP is the WFPC2 zeropoint.

TABLE A2
SECONDARY PHOTOMETRY STARS FOR PC1

R.A.	Dec.	ALLFRAME		DoPHOT	
		V	I	V	I
11:18:16.21	-32:50:22.4	23.67±0.02	23.19±0.03	23.80±0.05	23.36±0.05
11:18:16.42	-32:50:12.2	24.32±0.02	24.26±0.05	24.46±0.11	24.43±0.10
11:18:16.45	-32:50:24.8	23.79±0.02	23.33±0.03	23.91±0.04	23.45±0.04
11:18:16.52	-32:50:22.7	24.24±0.02	21.75±0.02	24.25±0.04	21.85±0.04
11:18:16.53	-32:50:27.8	24.07±0.02	23.80±0.04	24.15±0.06	23.86±0.06
11:18:16.55	-32:50:08.3	24.10±0.02	24.06±0.05	24.18±0.08	24.17±0.07
11:18:16.58	-32:50:30.0	24.31±0.02	24.13±0.04	24.32±0.06	24.16±0.05
11:18:16.65	-32:50:30.3	23.50±0.02	22.90±0.03	23.51±0.06	22.90±0.05
11:18:16.74	-32:50:30.3	24.52±0.02	22.25±0.02	24.58±0.04	22.30±0.04
11:18:16.74	-32:50:36.7	22.87±0.02	22.36±0.02	22.96±0.03	22.44±0.03
11:18:16.98	-32:50:37.1	23.64±0.02	23.62±0.04	23.64±0.05	23.61±0.05
11:18:17.01	-32:50:39.0	24.81±0.03	24.83±0.06	24.80±0.09	24.95±0.08
11:18:17.04	-32:50:36.7	23.54±0.02	23.36±0.03	23.56±0.05	23.42±0.05
11:18:17.07	-32:50:37.0	23.91±0.02	23.03±0.03	23.95±0.05	23.06±0.05
11:18:17.13	-32:50:17.1	24.24±0.02	24.01±0.04	24.20±0.07	24.04±0.07
11:18:17.18	-32:50:34.8	24.89±0.04	24.45±0.07	25.02±0.12	24.46±0.11
11:18:17.19	-32:50:16.6	24.48±0.02	24.59±0.08	24.53±0.11	24.73±0.10
11:18:17.21	-32:50:39.1	22.94±0.02	22.54±0.02	22.89±0.05	22.57±0.05
11:18:17.27	-32:50:37.6	23.79±0.02	23.71±0.03	23.81±0.05	23.76±0.05
11:18:17.28	-32:50:18.8	24.74±0.02	22.65±0.02	24.84±0.05	22.68±0.04
11:18:17.29	-32:50:22.8	23.15±0.04	23.52±0.03	23.04±0.04	23.16±0.04
11:18:17.30	-32:50:37.5	23.68±0.02	23.43±0.03	23.69±0.04	23.53±0.04
11:18:17.32	-32:50:36.0	23.12±0.02	21.54±0.02	23.01±0.03	21.59±0.03
11:18:17.37	-32:50:19.8	23.75±0.02	23.56±0.03	23.81±0.05	23.59±0.05
11:18:17.38	-32:50:37.3	24.57±0.02	23.22±0.03	24.52±0.05	23.21±0.05
11:18:17.54	-32:50:31.9	24.06±0.02	23.79±0.04	24.05±0.06	23.77±0.05
11:18:17.55	-32:50:24.9	24.83±0.02	24.43±0.07	24.83±0.08	24.32±0.08
11:18:17.77	-32:50:35.6	24.07±0.02	23.78±0.04	24.06±0.06	23.87±0.06
11:18:17.79	-32:50:22.4	24.20±0.02	24.04±0.04	24.19±0.06	24.08±0.05
11:18:17.95	-32:50:22.7	24.92±0.02	22.60±0.02	25.04±0.06	22.67±0.06
11:18:18.11	-32:50:25.0	23.59±0.02	22.67±0.02	23.63±0.04	22.70±0.04
11:18:18.33	-32:50:34.8	23.65±0.02	23.20±0.03	23.72±0.05	23.20±0.05
11:18:18.38	-32:50:26.0	25.22±0.02	23.48±0.03	25.05±0.05	23.61±0.05
11:18:18.38	-32:50:38.6	24.63±0.02	24.64±0.06	24.67±0.09	24.63±0.09
11:18:18.40	-32:50:37.2	24.64±0.02	24.29±0.05	24.67±0.08	24.36±0.08
11:18:18.47	-32:50:34.1	24.78±0.02	24.67±0.07	24.86±0.10	24.75±0.10
11:18:18.51	-32:50:23.0	24.32±0.02	24.36±0.06	24.37±0.07	24.35±0.07
11:18:18.62	-32:50:10.5	25.05±0.03	22.19±0.02	25.14±0.06	22.24±0.05
11:18:18.69	-32:50:16.1	25.01±0.03	24.77±0.07	24.96±0.10	24.72±0.10

TABLE A3
SECONDARY PHOTOMETRY STARS FOR WF2

R.A.	Dec.	ALLFRAME		DoPHOT	
		V	I	V	I
11:18:18.84	-32:50:37.5	23.48±0.02	22.53±0.03	23.34±0.05	22.50±0.05
11:18:19.06	-32:50:36.3	23.84±0.02	22.93±0.03	23.88±0.06	22.87±0.05
11:18:19.34	-32:50:31.4	23.18±0.02	22.96±0.03	23.24±0.04	22.91±0.04
11:18:19.68	-32:50:35.9	23.29±0.02	23.08±0.04	23.24±0.05	23.01±0.04
11:18:20.10	-32:50:42.2	23.38±0.02	23.43±0.04	23.51±0.06	23.33±0.06
11:18:20.33	-32:50:22.5	24.07±0.03	23.55±0.05	23.94±0.06	23.31±0.06
11:18:20.61	-32:50:28.9	23.14±0.02	22.83±0.04	23.11±0.04	22.73±0.04
11:18:20.62	-32:50:05.8	23.89±0.02	23.27±0.04	23.88±0.06	23.14±0.06
11:18:20.65	-32:50:18.6	23.69±0.02	23.87±0.04	23.68±0.06	23.73±0.07
11:18:20.80	-32:50:43.1	23.25±0.02	22.24±0.02	23.18±0.04	22.19±0.04
11:18:20.95	-32:50:38.6	24.10±0.03	23.60±0.03	23.92±0.04	23.54±0.06
11:18:21.52	-32:49:59.8	23.16±0.02	22.88±0.04	23.23±0.03	22.78±0.03
11:18:21.56	-32:50:19.1	23.52±0.03	22.58±0.03	23.62±0.03	22.57±0.03
11:18:21.74	-32:50:45.8	23.99±0.02	22.10±0.02	23.98±0.06	22.04±0.05
11:18:22.06	-32:49:35.0	24.15±0.03	24.37±0.07	23.99±0.08	24.17±0.07
11:18:22.08	-32:50:14.8	22.93±0.02	22.52±0.03	22.98±0.04	22.35±0.04
11:18:22.15	-32:49:42.6	23.99±0.02	23.53±0.04	23.92±0.06	23.38±0.06
11:18:22.17	-32:50:46.3	24.01±0.02	23.78±0.03	23.97±0.05	23.63±0.06
11:18:22.38	-32:50:22.7	23.21±0.02	22.98±0.03	23.22±0.09	22.92±0.08
11:18:22.40	-32:50:15.0	23.78±0.02	23.29±0.03	23.74±0.03	23.23±0.03
11:18:22.45	-32:49:59.1	23.86±0.02	23.80±0.04	23.76±0.07	23.55±0.06
11:18:22.52	-32:50:01.3	24.03±0.03	23.72±0.04	23.90±0.05	23.58±0.06
11:18:22.52	-32:50:33.0	23.99±0.02	23.48±0.03	24.00±0.06	23.42±0.06
11:18:22.59	-32:49:46.9	23.91±0.02	23.61±0.06	23.88±0.08	23.70±0.11
11:18:22.63	-32:50:24.1	23.21±0.02	21.97±0.02	23.27±0.03	21.94±0.03
11:18:22.72	-32:50:32.0	23.82±0.02	23.70±0.04	23.77±0.06	23.55±0.05
11:18:23.02	-32:50:03.4	23.14±0.02	22.94±0.03	23.12±0.03	22.87±0.03
11:18:23.13	-32:50:27.2	23.19±0.02	23.04±0.03	23.12±0.04	22.91±0.04
11:18:23.14	-32:49:36.7	23.95±0.02	24.01±0.05	23.96±0.08	23.92±0.07
11:18:23.27	-32:49:47.4	23.92±0.02	23.61±0.03	23.90±0.04	23.53±0.04
11:18:23.34	-32:49:41.8	24.01±0.02	23.52±0.03	23.98±0.04	23.44±0.04
11:18:23.39	-32:49:56.5	23.57±0.02	23.01±0.03	23.51±0.03	22.99±0.03
11:18:23.42	-32:50:07.4	23.21±0.02	23.06±0.03	23.24±0.04	23.04±0.04
11:18:23.45	-32:49:41.9	23.14±0.02	22.68±0.02	23.14±0.03	22.66±0.03
11:18:23.55	-32:49:41.5	23.21±0.02	22.39±0.03	23.23±0.03	22.38±0.03
11:18:23.55	-32:49:54.4	23.73±0.02	23.33±0.03	23.61±0.04	23.24±0.04
11:18:23.66	-32:50:11.0	23.61±0.02	21.41±0.02	23.57±0.03	21.41±0.02
11:18:23.81	-32:49:36.0	23.96±0.02	23.52±0.03	23.97±0.03	23.50±0.03
11:18:24.02	-32:49:52.4	23.41±0.02	23.48±0.03	23.34±0.04	23.39±0.04
11:18:24.48	-32:50:03.1	23.10±0.02	21.82±0.02	23.15±0.04	21.81±0.04
11:18:24.49	-32:50:03.8	22.17±0.01	21.13±0.02	22.14±0.02	21.13±0.01
11:18:24.64	-32:50:12.1	23.81±0.02	23.75±0.03	23.86±0.04	23.76±0.03
11:18:24.67	-32:50:43.7	23.67±0.02	23.52±0.03	23.67±0.05	23.47±0.05
11:18:24.81	-32:50:04.6	23.60±0.02	23.66±0.03	23.70±0.06	23.70±0.06
11:18:24.86	-32:50:02.8	23.16±0.02	23.18±0.03	23.15±0.04	23.16±0.04

TABLE A4
SECONDARY PHOTOMETRY STARS FOR WF3

R.A. (J2000.0)	Dec.	ALLFRAME		DoPHOT	
		V	I	V	I
11:18:18.38	-32:51:52.7	24.43±0.03	22.70±0.03	24.49±0.05	22.71±0.05
11:18:18.49	-32:51:42.0	23.94±0.02	23.23±0.03	23.98±0.05	23.16±0.05
11:18:18.61	-32:51:11.5	24.20±0.03	24.49±0.06	24.43±0.10	24.35±0.09
11:18:18.71	-32:50:48.7	24.23±0.03	23.68±0.04	24.35±0.05	23.57±0.05
11:18:19.21	-32:51:16.3	23.18±0.02	22.88±0.03	23.18±0.05	22.81±0.05
11:18:19.51	-32:51:04.6	24.31±0.02	21.97±0.02	24.39±0.04	21.92±0.04
11:18:19.52	-32:50:49.2	23.59±0.03	22.68±0.03	23.55±0.06	22.50±0.05
11:18:19.55	-32:51:12.8	24.56±0.03	24.31±0.05	24.58±0.08	24.23±0.07
11:18:19.85	-32:51:02.9	24.18±0.03	23.91±0.04	24.19±0.07	23.76±0.07
11:18:19.86	-32:51:19.0	24.28±0.03	22.68±0.03	24.32±0.06	22.62±0.05
11:18:19.98	-32:51:49.3	24.20±0.02	24.10±0.04	24.26±0.07	24.00±0.07
11:18:20.04	-32:50:58.8	24.08±0.03	23.87±0.04	24.15±0.07	23.75±0.07
11:18:20.22	-32:51:32.6	24.17±0.03	23.79±0.04	24.03±0.05	23.69±0.05
11:18:20.87	-32:50:53.7	23.41±0.02	20.80±0.02	23.55±0.04	20.80±0.04
11:18:21.13	-32:51:45.6	24.28±0.03	21.94±0.02	24.37±0.04	21.93±0.04
11:18:21.21	-32:51:59.3	24.14±0.02	23.46±0.04	24.26±0.05	23.33±0.05
11:18:21.27	-32:51:43.0	24.52±0.03	24.35±0.05	24.54±0.07	24.29±0.07
11:18:21.47	-32:51:36.2	24.22±0.03	24.21±0.05	24.20±0.07	24.04±0.07
11:18:21.50	-32:51:10.7	24.34±0.03	23.73±0.04	24.40±0.07	23.70±0.06
11:18:21.55	-32:51:20.2	24.20±0.02	24.32±0.05	24.29±0.07	24.22±0.07
11:18:22.03	-32:51:12.0	23.49±0.02	23.32±0.03	23.55±0.04	23.22±0.04
11:18:22.14	-32:51:21.9	24.26±0.03	24.62±0.06	24.38±0.10	24.45±0.09
11:18:22.27	-32:51:26.0	24.05±0.03	23.98±0.04	24.08±0.05	23.84±0.05
11:18:22.28	-32:51:10.1	23.03±0.02	22.90±0.03	23.10±0.03	22.85±0.02
11:18:22.29	-32:51:49.0	23.90±0.03	22.10±0.03	24.07±0.04	22.17±0.04
11:18:22.41	-32:51:35.6	24.39±0.03	24.28±0.05	24.36±0.07	24.11±0.06
11:18:22.42	-32:51:00.1	24.44±0.03	24.32±0.05	24.56±0.08	24.21±0.07
11:18:22.61	-32:51:48.7	24.11±0.02	23.96±0.04	24.16±0.06	23.78±0.06
11:18:23.26	-32:51:58.5	23.98±0.03	23.80±0.05	24.06±0.06	23.69±0.06
11:18:23.45	-32:51:44.1	24.22±0.03	22.21±0.02	24.29±0.04	22.17±0.04
11:18:23.57	-32:51:08.0	23.24±0.02	21.35±0.02	23.40±0.04	21.32±0.04
11:18:23.77	-32:51:05.9	23.79±0.02	23.91±0.03	23.89±0.06	23.85±0.06
11:18:23.93	-32:51:53.5	24.40±0.02	23.90±0.04	24.50±0.06	23.84±0.06
11:18:24.07	-32:51:00.8	24.32±0.03	24.01±0.04	24.37±0.07	23.92±0.07
11:18:24.25	-32:50:57.6	24.27±0.03	24.30±0.06	24.39±0.07	24.37±0.06
11:18:24.36	-32:50:56.3	23.97±0.03	21.22±0.02	24.10±0.04	21.27±0.04

TABLE A5
SECONDARY STANDARD PHOTOMETRY FOR WF4

R.A.	Dec.	ALLFRAME		DoPHOT	
		V	I	V	I
11:18:12.84	-32:51:17.8	24.59±0.02	22.76±0.02	24.80±0.10	22.81±0.09
11:18:13.02	-32:51:03.2	23.28±0.02	23.24±0.03	23.37±0.06	23.29±0.06
11:18:13.37	-32:51:13.2	24.25±0.02	24.03±0.04	24.33±0.06	23.98±0.06
11:18:13.45	-32:51:23.1	24.14±0.02	22.53±0.02	24.13±0.03	22.58±0.03
11:18:13.47	-32:50:49.1	24.62±0.02	24.58±0.05	24.72±0.07	24.61±0.09
11:18:13.69	-32:50:41.6	24.26±0.02	24.12±0.04	24.38±0.06	24.16±0.07
11:18:13.90	-32:51:08.1	24.45±0.02	24.21±0.04	24.57±0.06	24.24±0.06
11:18:13.95	-32:50:57.8	24.63±0.02	24.19±0.05	24.73±0.07	24.20±0.07
11:18:14.06	-32:50:58.8	24.10±0.02	22.63±0.02	24.08±0.04	22.65±0.04
11:18:14.44	-32:50:58.6	24.65±0.03	23.93±0.04	24.77±0.09	24.03±0.08
11:18:14.58	-32:51:06.2	24.08±0.02	23.83±0.04	24.20±0.06	23.87±0.06
11:18:14.59	-32:51:10.7	24.44±0.02	23.32±0.03	24.21±0.04	23.37±0.04
11:18:14.67	-32:51:20.6	23.72±0.02	23.21±0.03	23.81±0.04	23.26±0.04
11:18:15.30	-32:51:25.4	24.23±0.02	22.67±0.02	24.25±0.03	22.70±0.03
11:18:15.32	-32:51:17.6	24.57±0.03	24.06±0.04	24.55±0.07	24.10±0.07
11:18:15.36	-32:51:34.0	24.42±0.02	24.43±0.06	24.54±0.09	24.49±0.09
11:18:15.82	-32:51:07.8	24.57±0.02	24.36±0.05	24.63±0.07	24.32±0.07
11:18:16.07	-32:51:38.8	24.46±0.02	22.29±0.02	24.50±0.04	22.30±0.04
11:18:16.12	-32:51:02.8	24.79±0.03	24.66±0.06	24.80±0.10	24.65±0.10
11:18:16.33	-32:51:04.0	24.51±0.02	22.44±0.03	24.58±0.04	22.46±0.04
11:18:16.49	-32:51:35.4	24.62±0.02	22.35±0.02	24.68±0.06	22.45±0.05
11:18:16.50	-32:51:52.4	24.45±0.02	23.86±0.04	24.54±0.05	23.85±0.05
11:18:16.58	-32:51:08.9	24.29±0.02	23.80±0.03	24.30±0.06	23.80±0.05
11:18:16.68	-32:51:05.7	24.59±0.03	24.20±0.07	24.67±0.10	24.32±0.08
11:18:16.93	-32:51:34.5	24.45±0.02	23.41±0.03	24.51±0.05	23.45±0.05
11:18:16.96	-32:50:50.8	23.95±0.02	23.65±0.04	23.92±0.06	23.57±0.06
11:18:17.14	-32:50:52.9	24.40±0.02	23.75±0.08	24.46±0.12	23.69±0.11
11:18:17.23	-32:51:22.2	23.66±0.02	21.81±0.02	23.72±0.03	21.87±0.03
11:18:17.28	-32:51:16.1	24.68±0.03	24.46±0.05	24.77±0.08	24.54±0.08
11:18:17.33	-32:51:44.2	24.67±0.02	22.34±0.02	24.79±0.04	22.38±0.04
11:18:17.42	-32:51:26.6	23.70±0.02	21.44±0.01	23.76±0.03	21.52±0.02
11:18:17.57	-32:51:50.0	24.55±0.02	24.68±0.06	24.61±0.07	24.68±0.07
11:18:17.60	-32:51:08.0	24.63±0.02	24.38±0.06	24.71±0.10	24.45±0.09
11:18:17.64	-32:51:56.8	24.65±0.02	22.80±0.03	24.65±0.06	22.88±0.05
11:18:17.79	-32:51:02.7	24.28±0.02	24.31±0.05	24.30±0.07	24.15±0.07
11:18:17.80	-32:50:59.3	24.04±0.02	23.86±0.04	24.16±0.08	23.97±0.08
11:18:17.82	-32:51:10.6	24.50±0.02	24.16±0.05	24.51±0.07	24.06±0.07
11:18:17.84	-32:51:38.0	24.65±0.02	24.54±0.06	24.74±0.09	24.49±0.09
11:18:17.96	-32:51:37.3	24.43±0.02	24.44±0.05	24.54±0.11	24.35±0.10
11:18:17.97	-32:51:39.3	23.85±0.02	21.97±0.02	23.95±0.04	22.08±0.04
11:18:18.00	-32:51:07.0	24.12±0.02	23.32±0.03	24.16±0.05	23.34±0.05
11:18:18.36	-32:50:49.1	24.18±0.02	24.35±0.06	24.17±0.10	24.17±0.09

TABLE A6
ALLFRAME F555W PHOTOMETRY

JD	m±Δm	m±Δm	m±Δm	m±Δm	m±Δm
	C01	C02	C03	C04	C05
2449714.37	...	23.66 ± 0.07	24.42 ± 0.09	24.31 ± 0.10	25.47 ± 0.24
2449722.28	23.67 ± 0.14	23.97 ± 0.08	24.65 ± 0.12	24.39 ± 0.10	25.56 ± 0.20
2449733.40	23.87 ± 0.16	24.12 ± 0.08	24.78 ± 0.09	23.54 ± 0.05	24.35 ± 0.14
2449735.48	23.78 ± 0.21	24.15 ± 0.08	24.54 ± 0.08	23.49 ± 0.07	24.44 ± 0.12
2449738.43	23.60 ± 0.13	24.22 ± 0.10	24.13 ± 0.10	23.71 ± 0.07	24.53 ± 0.13
2449742.18	23.26 ± 0.11	24.23 ± 0.11	23.97 ± 0.07	23.76 ± 0.07	24.82 ± 0.14
2449746.01	23.24 ± 0.09	24.14 ± 0.11	23.94 ± 0.06	23.74 ± 0.10	24.80 ± 0.19
2449750.09	23.32 ± 0.08	23.65 ± 0.09	24.20 ± 0.09	23.86 ± 0.09	25.07 ± 0.19
2449755.25	23.45 ± 0.08	23.39 ± 0.08	24.37 ± 0.08	24.15 ± 0.09	25.51 ± 0.31
2449761.16	23.48 ± 0.10	23.63 ± 0.07	24.58 ± 0.10	24.15 ± 0.08	25.55 ± 0.26
2449767.39	23.60 ± 0.09	23.99 ± 0.06	24.83 ± 0.10	23.68 ± 0.07	24.24 ± 0.12
2449773.69	...	24.21 ± 0.08	24.85 ± 0.09	23.59 ± 0.07	24.46 ± 0.12
	C06	C07	C08	C09	C10
2449714.37	25.36 ± 0.13	23.57 ± 0.11	24.81 ± 0.12	23.84 ± 0.21	23.64 ± 0.08
2449722.28	24.73 ± 0.08	23.96 ± 0.11	24.44 ± 0.23	24.20 ± 0.23	24.08 ± 0.08
2449733.40	24.63 ± 0.13	24.14 ± 0.14	24.67 ± 0.14	24.53 ± 0.23	24.50 ± 0.27
2449735.48	24.50 ± 0.11	23.54 ± 0.28	24.84 ± 0.09	24.41 ± 0.34	24.52 ± 0.09
2449738.43	24.74 ± 0.10	23.19 ± 0.12	24.87 ± 0.11	24.41 ± 0.26	24.54 ± 0.11
2449742.18	24.89 ± 0.13	23.28 ± 0.11	24.95 ± 0.09	23.93 ± 0.22	24.67 ± 0.09
2449746.01	25.02 ± 0.13	23.30 ± 0.16	24.93 ± 0.14	23.79 ± 0.21	23.67 ± 0.06
2449750.09	25.19 ± 0.13	23.43 ± 0.16	25.14 ± 0.12	23.87 ± 0.23	23.64 ± 0.09
2449755.25	25.38 ± 0.17	23.62 ± 0.18	25.20 ± 0.16	24.24 ± 0.19	23.91 ± 0.09
2449761.16	24.80 ± 0.13	23.86 ± 0.17	25.33 ± 0.15	24.24 ± 0.24	24.22 ± 0.09
2449767.39	24.45 ± 0.10	24.06 ± 0.19	25.28 ± 0.24	24.41 ± 0.26	24.49 ± 0.09
2449773.69	24.83 ± 0.11	23.55 ± 0.12	24.71 ± 0.08	23.94 ± 0.19	24.58 ± 0.09
	C11	C12	C13	C14	C15
2449714.37	26.02 ± 0.22	24.92 ± 0.22	24.53 ± 0.09	23.72 ± 0.14	24.57 ± 0.23
2449722.28	25.92 ± 0.22	25.16 ± 0.33	24.88 ± 0.13	22.97 ± 0.10	25.43 ± 0.18
2449733.40	25.56 ± 0.19	25.76 ± 0.31	23.79 ± 0.07	23.46 ± 0.09	25.66 ± 0.25
2449735.48	25.60 ± 0.14	25.50 ± 0.24	23.92 ± 0.06	23.46 ± 0.13	25.57 ± 0.21
2449738.43	25.85 ± 0.18	25.42 ± 0.23	24.15 ± 0.07	23.53 ± 0.10	25.62 ± 0.28
2449742.18	25.76 ± 0.15	24.75 ± 0.15	24.35 ± 0.09	23.58 ± 0.10	24.98 ± 0.18
2449746.01	26.07 ± 0.23	24.82 ± 0.15	24.57 ± 0.08	23.66 ± 0.12	24.74 ± 0.19
2449750.09	26.04 ± 0.19	25.04 ± 0.18	24.66 ± 0.09	23.25 ± 0.12	24.98 ± 0.19
2449755.25	26.23 ± 0.32	25.30 ± 0.15	24.94 ± 0.13	22.87 ± 0.12	25.32 ± 0.21
2449761.16	26.49 ± 0.30	25.72 ± 0.23	24.69 ± 0.10	23.14 ± 0.10	25.39 ± 0.24
2449767.39	25.58 ± 0.19	25.81 ± 0.20	24.01 ± 0.10	23.39 ± 0.12	25.71 ± 0.23
2449773.69	25.83 ± 0.20	24.92 ± 0.25	24.27 ± 0.08	23.67 ± 0.13	24.90 ± 0.17

TABLE A6—*Continued*

JD	$m \pm \Delta m$	$m \pm \Delta m$	$m \pm \Delta m$	$m \pm \Delta m$	$m \pm \Delta m$
	C16	C17	C18	C19	C20
2449714.37	24.16 ± 0.06	23.60 ± 0.11	25.08 ± 0.16	23.46 ± 0.08	24.49 ± 0.08
2449722.28	24.51 ± 0.08	24.01 ± 0.13	25.46 ± 0.21	23.96 ± 0.08	24.62 ± 0.24
2449733.40	25.08 ± 0.12	24.39 ± 0.11	25.59 ± 0.21	24.58 ± 0.12	25.15 ± 0.15
2449735.48	25.10 ± 0.11	24.40 ± 0.13	25.60 ± 0.24	24.40 ± 0.09	24.75 ± 0.12
2449738.43	24.82 ± 0.17	23.65 ± 0.07	25.00 ± 0.28	24.55 ± 0.09	24.33 ± 0.11
2449742.18	23.96 ± 0.08	23.45 ± 0.07	25.02 ± 0.18	23.39 ± 0.09	24.54 ± 0.15
2449746.01	24.12 ± 0.09	23.61 ± 0.08	25.18 ± 0.20	23.66 ± 0.08	24.75 ± 0.16
2449750.09	24.38 ± 0.13	23.88 ± 0.10	25.37 ± 0.21	23.99 ± 0.12	24.98 ± 0.13
2449755.25	24.51 ± 0.09	24.08 ± 0.12	25.49 ± 0.19	24.11 ± 0.15	25.23 ± 0.19
2449761.16	24.79 ± 0.10	24.23 ± 0.10	25.85 ± 0.22	24.49 ± 0.10	24.92 ± 0.12
2449767.39	25.01 ± 0.11	23.74 ± 0.11	24.95 ± 0.13	24.01 ± 0.09	24.41 ± 0.12
2449773.69	24.28 ± 0.09	23.72 ± 0.12	25.21 ± 0.15	23.79 ± 0.10	24.94 ± 0.12
	C21	C22	C23	C24	C25
2449714.37	25.40 ± 0.14	24.71 ± 0.15	25.36 ± 0.17	24.82 ± 0.13	25.71 ± 0.17
2449722.28	24.42 ± 0.07	23.95 ± 0.11	26.40 ± 0.40	24.21 ± 0.09	26.09 ± 0.27
2449733.40	24.95 ± 0.12	24.39 ± 0.13	24.89 ± 0.14	24.83 ± 0.11	25.22 ± 0.12
2449735.48	25.09 ± 0.10	24.45 ± 0.17	25.14 ± 0.14	24.78 ± 0.18	25.37 ± 0.23
2449738.43	25.19 ± 0.10	24.50 ± 0.18	25.05 ± 0.17	24.82 ± 0.19	25.49 ± 0.18
2449742.18	25.23 ± 0.12	24.52 ± 0.18	25.47 ± 0.24	23.89 ± 0.11	25.95 ± 0.21
2449746.01	25.15 ± 0.13	23.52 ± 0.10	25.75 ± 0.24	23.90 ± 0.10	26.00 ± 0.31
2449750.09	24.31 ± 0.14	23.87 ± 0.10	25.57 ± 0.23	24.09 ± 0.10	24.86 ± 0.13
2449755.25	24.70 ± 0.11	24.28 ± 0.12	24.80 ± 0.14	24.44 ± 0.11	25.01 ± 0.15
2449761.16	25.14 ± 0.14	24.43 ± 0.18	25.06 ± 0.20	24.69 ± 0.13	25.21 ± 0.19
2449767.39	25.23 ± 0.12	24.62 ± 0.19	25.74 ± 0.24	23.69 ± 0.10	25.72 ± 0.22
2449773.69	24.31 ± 0.08	23.84 ± 0.13	26.06 ± 0.31	24.25 ± 0.10	24.97 ± 0.14
	C26	C27	C28	C29	C30
2449714.37	24.27 ± 0.08	24.97 ± 0.24	24.92 ± 0.13	25.70 ± 0.19	25.47 ± 0.16
2449722.28	25.22 ± 0.09	24.59 ± 0.22	24.10 ± 0.12	25.26 ± 0.17	25.98 ± 0.21
2449733.40	25.53 ± 0.15	24.92 ± 0.19	24.79 ± 0.12	25.22 ± 0.12	25.88 ± 0.18
2449735.48	24.80 ± 0.08	25.05 ± 0.20	24.57 ± 0.11	25.53 ± 0.19	25.05 ± 0.18
2449738.43	24.26 ± 0.12	25.00 ± 0.19	24.83 ± 0.12	25.59 ± 0.17	25.11 ± 0.14
2449742.18	24.56 ± 0.09	24.34 ± 0.17	23.64 ± 0.09	25.79 ± 0.14	25.36 ± 0.13
2449746.01	24.63 ± 0.12	24.34 ± 0.16	23.95 ± 0.10	25.41 ± 0.19	25.45 ± 0.15
2449750.09	24.95 ± 0.12	24.43 ± 0.15	24.21 ± 0.12	24.72 ± 0.15	26.10 ± 0.30
2449755.25	25.24 ± 0.13	24.64 ± 0.25	24.50 ± 0.08	25.08 ± 0.14	25.74 ± 0.18
2449761.16	24.13 ± 0.10	24.98 ± 0.19	24.81 ± 0.11	25.71 ± 0.15	25.20 ± 0.17
2449767.39	24.61 ± 0.11	24.25 ± 0.18	23.79 ± 0.07	25.85 ± 0.21	25.51 ± 0.17
2449773.69	25.44 ± 0.15	24.63 ± 0.19	24.27 ± 0.08	24.53 ± 0.08	25.98 ± 0.16

TABLE A6—*Continued*

JD	$m \pm \Delta m$	$m \pm \Delta m$	$m \pm \Delta m$	$m \pm \Delta m$	$m \pm \Delta m$
	C31	C32	C33	C34	C35
2449714.37	25.35 ± 0.20	24.34 ± 0.12	25.39 ± 0.22	25.28 ± 0.23	25.28 ± 0.11
2449722.28	...	24.59 ± 0.21	26.20 ± 0.33	24.56 ± 0.09	24.54 ± 0.10
2449733.40	25.02 ± 0.19	24.08 ± 0.13	26.51 ± 0.38	24.96 ± 0.17	25.25 ± 0.13
2449735.48	25.17 ± 0.18	24.16 ± 0.13	26.09 ± 0.29	25.15 ± 0.10	25.23 ± 0.12
2449738.43	25.25 ± 0.15	24.37 ± 0.16	25.44 ± 0.18	24.96 ± 0.16	25.33 ± 0.12
2449742.18	24.18 ± 0.09	24.60 ± 0.13	25.52 ± 0.19	24.85 ± 0.16	24.23 ± 0.09
2449746.01	24.36 ± 0.10	24.49 ± 0.15	25.94 ± 0.29	24.37 ± 0.13	24.52 ± 0.11
2449750.09	24.58 ± 0.17	23.55 ± 0.12	26.02 ± 0.27	24.74 ± 0.12	24.76 ± 0.11
2449755.25	24.83 ± 0.12	24.00 ± 0.14	26.71 ± 0.47	24.91 ± 0.14	25.22 ± 0.13
2449761.16	25.05 ± 0.15	24.28 ± 0.12	25.49 ± 0.25	25.15 ± 0.19	25.42 ± 0.11
2449767.39	24.09 ± 0.10	24.55 ± 0.23	25.90 ± 0.29	24.55 ± 0.10	24.39 ± 0.07
2449773.69	24.75 ± 0.17	23.68 ± 0.13	26.38 ± 0.41	24.84 ± 0.18	24.83 ± 0.09
	C36	C37	C38	C39	C40
2449714.37	25.02 ± 0.10	24.58 ± 0.13	24.56 ± 0.20	24.17 ± 0.11	25.24 ± 0.12
2449722.28	24.68 ± 0.12	25.56 ± 0.19	23.58 ± 0.12	25.00 ± 0.16	25.05 ± 0.12
2449733.40	25.12 ± 0.14	24.48 ± 0.08	24.33 ± 0.23	24.77 ± 0.17	25.19 ± 0.11
2449735.48	24.91 ± 0.13	24.39 ± 0.11	24.51 ± 0.14	24.09 ± 0.10	24.85 ± 0.08
2449738.43	24.95 ± 0.11	24.71 ± 0.10	24.51 ± 0.15	24.36 ± 0.13	24.48 ± 0.08
2449742.18	24.41 ± 0.08	24.97 ± 0.16	23.81 ± 0.09	24.65 ± 0.10	24.70 ± 0.10
2449746.01	24.56 ± 0.13	25.35 ± 0.19	23.72 ± 0.11	25.10 ± 0.15	24.96 ± 0.15
2449750.09	24.86 ± 0.12	25.43 ± 0.17	24.06 ± 0.13	25.13 ± 0.15	...
2449755.25	25.08 ± 0.14	24.39 ± 0.12	24.58 ± 0.17	24.12 ± 0.13	24.98 ± 0.12
2449761.16	24.96 ± 0.12	24.89 ± 0.15	24.41 ± 0.15	24.57 ± 0.13	24.52 ± 0.10
2449767.39	24.61 ± 0.10	...	23.69 ± 0.20	25.05 ± 0.14	25.25 ± 0.17
2449773.69	25.08 ± 0.14	25.50 ± 0.22	24.44 ± 0.17	25.44 ± 0.18	25.67 ± 0.26
	C41	C42	C43	C44	C45
2449714.37	24.02 ± 0.08	24.65 ± 0.12	23.71 ± 0.16	25.31 ± 0.18	24.53 ± 0.17
2449722.28	24.85 ± 0.08	25.71 ± 0.29	24.04 ± 0.21	24.75 ± 0.10	24.76 ± 0.22
2449733.40	23.83 ± 0.07	24.59 ± 0.12	23.60 ± 0.15	25.41 ± 0.14	24.64 ± 0.16
2449735.48	23.97 ± 0.10	24.69 ± 0.16	23.75 ± 0.12	24.98 ± 0.16	24.53 ± 0.19
2449738.43	24.30 ± 0.11	25.12 ± 0.18	23.87 ± 0.16	24.36 ± 0.09	24.58 ± 0.19
2449742.18	24.45 ± 0.12	25.42 ± 0.19	24.11 ± 0.17	24.75 ± 0.11	24.30 ± 0.16
2449746.01	24.80 ± 0.16	25.73 ± 0.29	24.10 ± 0.16	24.89 ± 0.17	24.21 ± 0.17
2449750.09	24.71 ± 0.09	25.38 ± 0.19	23.91 ± 0.16	25.19 ± 0.18	24.47 ± 0.15
2449755.25	23.89 ± 0.12	24.83 ± 0.15	23.69 ± 0.13	24.37 ± 0.08	24.67 ± 0.16
2449761.16	24.46 ± 0.14	25.49 ± 0.20	23.93 ± 0.14	24.75 ± 0.13	24.14 ± 0.12
2449767.39	24.84 ± 0.14	25.52 ± 0.25	23.90 ± 0.21	25.08 ± 0.18	24.45 ± 0.16
2449773.69	24.14 ± 0.09	24.98 ± 0.19	23.69 ± 0.17	24.75 ± 0.12	24.63 ± 0.15

TABLE A6—*Continued*

JD	$m \pm \Delta m$	$m \pm \Delta m$	$m \pm \Delta m$	$m \pm \Delta m$	$m \pm \Delta m$
	C46	C47	C48	C49	C50
2449714.37	25.26 ± 0.21	24.00 ± 0.13	25.49 ± 0.16	25.75 ± 0.23	24.77 ± 0.14
2449722.28	24.42 ± 0.07	24.81 ± 0.14	25.24 ± 0.21	25.86 ± 0.23	25.77 ± 0.25
2449733.40	24.99 ± 0.20	24.06 ± 0.11	25.40 ± 0.19	25.64 ± 0.18	24.86 ± 0.19
2449735.48	24.91 ± 0.15	24.05 ± 0.08	25.34 ± 0.20	25.64 ± 0.19	25.02 ± 0.17
2449738.43	24.76 ± 0.11	24.35 ± 0.10	25.43 ± 0.14	25.58 ± 0.22	25.39 ± 0.23
2449742.18	24.00 ± 0.09	24.76 ± 0.11	24.78 ± 0.13	24.66 ± 0.12	25.77 ± 0.22
2449746.01	24.21 ± 0.12	24.56 ± 0.17	24.97 ± 0.17	24.90 ± 0.15	25.55 ± 0.21
2449750.09	24.63 ± 0.12	24.03 ± 0.09	25.29 ± 0.13	25.42 ± 0.24	24.63 ± 0.12
2449755.25	24.85 ± 0.19	24.18 ± 0.09	25.41 ± 0.19	25.47 ± 0.27	25.15 ± 0.18
2449761.16	23.83 ± 0.09	24.68 ± 0.13	24.85 ± 0.11	24.64 ± 0.13	26.15 ± 0.37
2449767.39	24.26 ± 0.15	24.63 ± 0.16	25.33 ± 0.21	25.50 ± 0.19	24.62 ± 0.14
2449773.69	24.93 ± 0.15	24.40 ± 0.14	25.68 ± 0.21	25.98 ± 0.26	25.58 ± 0.27
	C51	C52	C53	C54	C55
2449714.37	25.63 ± 0.18	24.42 ± 0.10	24.73 ± 0.14	24.04 ± 0.11	25.17 ± 0.11
2449722.28	24.75 ± 0.10	25.22 ± 0.14	25.22 ± 0.15	25.14 ± 0.19	26.08 ± 0.22
2449733.40	25.37 ± 0.16	24.63 ± 0.08	24.96 ± 0.13	24.35 ± 0.13	25.57 ± 0.11
2449735.48	24.71 ± 0.10	24.66 ± 0.10	24.92 ± 0.17	24.48 ± 0.12	25.60 ± 0.20
2449738.43	24.60 ± 0.13	24.92 ± 0.18	25.18 ± 0.17	24.82 ± 0.15	25.83 ± 0.26
2449742.18	25.07 ± 0.12	24.81 ± 0.10	25.04 ± 0.12	25.18 ± 0.15	25.15 ± 0.16
2449746.01	25.35 ± 0.15	24.07 ± 0.08	24.43 ± 0.10	24.90 ± 0.16	24.99 ± 0.18
2449750.09	25.47 ± 0.21	24.35 ± 0.13	24.78 ± 0.13	24.19 ± 0.08	25.47 ± 0.14
2449755.25	24.58 ± 0.12	24.83 ± 0.09	25.31 ± 0.16	24.67 ± 0.15	25.54 ± 0.23
2449761.16	25.22 ± 0.16	24.06 ± 0.11	24.31 ± 0.10	25.05 ± 0.16	24.90 ± 0.17
2449767.39	25.46 ± 0.22	24.55 ± 0.13	24.87 ± 0.11	24.22 ± 0.12	25.74 ± 0.20
2449773.69	24.55 ± 0.09	25.28 ± 0.17	25.54 ± 0.18	24.95 ± 0.16	25.60 ± 0.14
	C56	C57	C58	C59	C60
2449714.37	25.08 ± 0.13	25.10 ± 0.13	24.81 ± 0.19	25.47 ± 0.20	24.57 ± 0.09
2449722.28	25.30 ± 0.14	25.74 ± 0.20	25.12 ± 0.12
2449733.40	24.61 ± 0.08	25.38 ± 0.17	...	25.82 ± 0.16	24.95 ± 0.12
2449735.48	24.72 ± 0.13	25.83 ± 0.16	...	25.60 ± 0.19	25.33 ± 0.12
2449738.43	25.11 ± 0.17	25.42 ± 0.15	25.77 ± 0.38	25.32 ± 0.32	25.13 ± 0.11
2449742.18	25.50 ± 0.17	24.85 ± 0.14	25.51 ± 0.23	24.82 ± 0.15	24.27 ± 0.07
2449746.01	25.31 ± 0.16	25.01 ± 0.09	24.75 ± 0.17	25.12 ± 0.12	24.73 ± 0.16
2449750.09	24.63 ± 0.17	25.57 ± 0.19	25.28 ± 0.21	25.60 ± 0.22	25.24 ± 0.14
2449755.25	25.14 ± 0.14	25.07 ± 0.12	25.87 ± 0.30	25.39 ± 0.20	24.81 ± 0.08
2449761.16	25.37 ± 0.17	25.24 ± 0.13	24.76 ± 0.15	25.16 ± 0.20	24.86 ± 0.15
2449767.39	24.69 ± 0.10	25.52 ± 0.16	25.33 ± 0.23	26.00 ± 0.38	25.20 ± 0.16
2449773.69	25.60 ± 0.17	24.80 ± 0.12	26.02 ± 0.35	24.87 ± 0.13	24.61 ± 0.12

TABLE A6—*Continued*

JD	$m \pm \Delta m$	$m \pm \Delta m$	$m \pm \Delta m$	$m \pm \Delta m$	$m \pm \Delta m$
	C61	C62	C63	C64	C65
2449714.37	25.24 ± 0.12	25.63 ± 0.16	24.86 ± 0.14	25.66 ± 0.18	25.33 ± 0.18
2449722.28	25.27 ± 0.13	25.06 ± 0.13	25.97 ± 0.24	25.35 ± 0.19	25.37 ± 0.16
2449733.40	24.96 ± 0.10	25.66 ± 0.19	25.38 ± 0.19	25.02 ± 0.10	25.34 ± 0.12
2449735.48	24.94 ± 0.17	25.30 ± 0.11	25.63 ± 0.22	25.39 ± 0.17	24.73 ± 0.13
2449738.43	25.16 ± 0.16	25.37 ± 0.13	25.48 ± 0.21	25.59 ± 0.24	25.08 ± 0.16
2449742.18	25.06 ± 0.13	25.92 ± 0.16	24.89 ± 0.10	24.64 ± 0.11	25.45 ± 0.22
2449746.01	24.74 ± 0.12	25.94 ± 0.17	25.09 ± 0.15	25.10 ± 0.16	25.19 ± 0.27
2449750.09	25.05 ± 0.08	25.29 ± 0.14	25.53 ± 0.13	25.32 ± 0.18	24.92 ± 0.13
2449755.25	25.32 ± 0.18	25.92 ± 0.21	24.72 ± 0.12	24.89 ± 0.14	25.33 ± 0.20
2449761.16	24.85 ± 0.13	25.66 ± 0.18	25.59 ± 0.22	25.40 ± 0.14	24.86 ± 0.17
2449767.39	25.38 ± 0.18	25.82 ± 0.20	24.77 ± 0.11	25.07 ± 0.17	25.60 ± 0.18
2449773.69	24.90 ± 0.12	25.72 ± 0.21	25.68 ± 0.19	25.56 ± 0.22	25.09 ± 0.13
	C66	C67	C68	C69	
2449714.37	25.88 ± 0.23	24.98 ± 0.12	25.05 ± 0.20	25.32 ± 0.17	
2449722.28	25.13 ± 0.17	25.51 ± 0.18	25.46 ± 0.19	25.98 ± 0.18	
2449733.40	25.20 ± 0.16	25.46 ± 0.13	25.07 ± 0.20	25.14 ± 0.11	
2449735.48	25.52 ± 0.17	25.30 ± 0.11	25.00 ± 0.18	25.25 ± 0.14	
2449738.43	26.13 ± 0.28	25.04 ± 0.14	25.42 ± 0.22	25.87 ± 0.26	
2449742.18	25.74 ± 0.19	25.47 ± 0.19	25.12 ± 0.15	25.26 ± 0.16	
2449746.01	25.15 ± 0.13	25.37 ± 0.16	24.95 ± 0.18	25.40 ± 0.18	
2449750.09	25.93 ± 0.22	25.10 ± 0.14	25.74 ± 0.34	25.72 ± 0.24	
2449755.25	25.46 ± 0.19	25.87 ± 0.20	24.93 ± 0.18	25.44 ± 0.15	
2449761.16	25.68 ± 0.13	24.95 ± 0.14	25.42 ± 0.25	25.10 ± 0.20	
2449767.39	25.47 ± 0.15	25.62 ± 0.16	25.19 ± 0.15	26.00 ± 0.27	
2449773.69	25.84 ± 0.24	25.06 ± 0.12	25.16 ± 0.20	25.51 ± 0.11	

TABLE A7
ALLFRAME F814W PHOTOMETRY

JD	m±Δm	m±Δm	m±Δm	m±Δm	m±Δm
	C01	C02	C03	C04	C05
2449714.43	22.62 ± 0.09	22.60 ± 0.06	22.99 ± 0.07	23.33 ± 0.07	23.85 ± 0.18
2449722.34	22.81 ± 0.10	22.77 ± 0.06	23.18 ± 0.08	23.35 ± 0.09	23.95 ± 0.17
2449742.25	22.52 ± 0.08	23.04 ± 0.07	22.77 ± 0.05	22.79 ± 0.06	23.37 ± 0.12
2449761.22	22.55 ± 0.09	22.60 ± 0.06	23.17 ± 0.10	23.19 ± 0.08	23.80 ± 0.19
	C06	C07	C08	C09	C10
2449714.43	24.16 ± 0.11	22.75 ± 0.09	22.95 ± 0.06	23.07 ± 0.11	22.81 ± 0.06
2449722.34	23.55 ± 0.09	22.95 ± 0.08	22.84 ± 0.07	23.17 ± 0.18	22.96 ± 0.07
2449742.25	23.47 ± 0.07	22.63 ± 0.06	22.87 ± 0.10	23.11 ± 0.14	23.37 ± 0.09
2449761.22	23.48 ± 0.12	22.95 ± 0.09	23.24 ± 0.07	23.11 ± 0.19	23.02 ± 0.06
	C11	C12	C13	C14	C15
2449714.43	24.69 ± 0.13	23.62 ± 0.21	23.28 ± 0.07	23.14 ± 0.10	23.29 ± 0.13
2449722.34	24.99 ± 0.21	23.90 ± 0.22	23.71 ± 0.08	22.52 ± 0.08	23.50 ± 0.11
2449742.25	24.71 ± 0.17	23.49 ± 0.19	23.17 ± 0.07	22.99 ± 0.10	23.47 ± 0.10
2449761.22	24.75 ± 0.18	23.91 ± 0.12	23.57 ± 0.10	22.67 ± 0.10	23.70 ± 0.12
	C16	C17	C18	C19	C20
2449714.43	23.00 ± 0.06	22.71 ± 0.09	23.98 ± 0.11	22.91 ± 0.05	23.46 ± 0.10
2449722.34	23.30 ± 0.08	22.98 ± 0.08	24.30 ± 0.15	23.18 ± 0.09	23.79 ± 0.07
2449742.25	23.01 ± 0.07	22.66 ± 0.09	23.95 ± 0.13	22.79 ± 0.07	23.51 ± 0.08
2449761.22	23.58 ± 0.09	22.97 ± 0.09	24.37 ± 0.23	23.38 ± 0.07	23.79 ± 0.12
	C21	C22	C23	C24	C25
2449714.43	23.86 ± 0.08	23.62 ± 0.13	23.91 ± 0.12	23.83 ± 0.12	24.21 ± 0.11
2449722.34	23.49 ± 0.10	23.13 ± 0.09	24.38 ± 0.21	23.33 ± 0.08	24.72 ± 0.16
2449742.25	23.97 ± 0.11	23.65 ± 0.13	24.01 ± 0.12	23.19 ± 0.09	24.34 ± 0.11
2449761.22	23.79 ± 0.08	23.19 ± 0.11	23.89 ± 0.15	23.67 ± 0.13	24.10 ± 0.13
	C26	C27	C28	C29	C30
2449714.43	23.53 ± 0.11	24.16 ± 0.18	23.70 ± 0.10	24.15 ± 0.12	24.10 ± 0.11
2449722.34	23.94 ± 0.11	23.67 ± 0.17	23.19 ± 0.08	24.06 ± 0.12	24.45 ± 0.14
2449742.25	23.63 ± 0.10	23.61 ± 0.11	23.00 ± 0.08	24.21 ± 0.13	24.02 ± 0.11
2449761.22	23.50 ± 0.06	24.18 ± 0.18	23.62 ± 0.10	24.03 ± 0.13	23.94 ± 0.14
	C31	C32	C33	C34	C35
2449714.43	23.69 ± 0.13	23.31 ± 0.15	23.95 ± 0.14	24.13 ± 0.14	23.98 ± 0.11
2449722.34	23.22 ± 0.08	23.56 ± 0.17	23.98 ± 0.11	23.72 ± 0.11	23.45 ± 0.08
2449742.25	23.05 ± 0.07	23.48 ± 0.14	24.05 ± 0.18	23.96 ± 0.10	23.26 ± 0.06
2449761.22	23.50 ± 0.13	23.41 ± 0.17	23.85 ± 0.25	23.94 ± 0.09	24.06 ± 0.11

TABLE A7—*Continued*

JD	m±Δm	m±Δm	m±Δm	m±Δm	m±Δm
	C36	C37	C38	C39	C40
2449714.43	24.16 ± 0.10	23.47 ± 0.07	23.59 ± 0.11	23.51 ± 0.11	23.92 ± 0.08
2449722.34	23.70 ± 0.07	23.99 ± 0.10	23.03 ± 0.12	23.87 ± 0.14	23.68 ± 0.08
2449742.25	23.56 ± 0.07	23.82 ± 0.09	23.14 ± 0.09	23.83 ± 0.11	23.70 ± 0.07
2449761.22	24.02 ± 0.11	23.69 ± 0.08	23.45 ± 0.13	23.71 ± 0.15	23.59 ± 0.08
	C41	C42	C43	C44	C45
2449714.43	23.32 ± 0.06	23.69 ± 0.09	22.94 ± 0.15	24.11 ± 0.10	23.07 ± 0.10
2449722.34	23.76 ± 0.08	24.10 ± 0.16	23.26 ± 0.12	24.00 ± 0.14	23.23 ± 0.12
2449742.25	23.51 ± 0.09	23.88 ± 0.12	23.21 ± 0.12	23.91 ± 0.12	23.06 ± 0.08
2449761.22	23.41 ± 0.08	24.12 ± 0.15	23.29 ± 0.10	23.80 ± 0.13	23.01 ± 0.10
	C46	C47	C48	C49	C50
2449714.43	23.52 ± 0.31	23.45 ± 0.11	24.12 ± 0.12	24.39 ± 0.16	23.89 ± 0.12
2449722.34	23.07 ± 0.23	23.66 ± 0.17	24.21 ± 0.10	24.39 ± 0.12	24.33 ± 0.16
2449742.25	23.00 ± 0.21	23.77 ± 0.13	23.89 ± 0.13	23.62 ± 0.15	24.36 ± 0.15
2449761.22	22.88 ± 0.18	23.79 ± 0.09	23.75 ± 0.14	23.88 ± 0.19	24.52 ± 0.24
	C51	C52	C53	C54	C55
2449714.43	24.20 ± 0.16	23.71 ± 0.06	23.90 ± 0.14	23.59 ± 0.10	24.20 ± 0.13
2449722.34	23.73 ± 0.10	24.18 ± 0.10	24.44 ± 0.18	24.21 ± 0.17	24.88 ± 0.27
2449742.25	23.82 ± 0.13	23.85 ± 0.11	24.12 ± 0.16	24.41 ± 0.15	24.28 ± 0.16
2449761.22	23.89 ± 0.12	23.53 ± 0.09	23.61 ± 0.10	24.44 ± 0.21	23.98 ± 0.12
	C56	C57	C58	C59	C60
2449714.43	24.13 ± 0.09	24.09 ± 0.14	23.85 ± 0.12	24.37 ± 0.15	23.89 ± 0.10
2449722.34	24.26 ± 0.10	24.35 ± 0.17	...	24.97 ± 0.16	24.17 ± 0.13
2449742.25	24.45 ± 0.14	23.89 ± 0.12	24.42 ± 0.19	24.19 ± 0.12	23.63 ± 0.10
2449761.22	24.48 ± 0.11	24.07 ± 0.12	23.78 ± 0.13	24.22 ± 0.14	23.88 ± 0.11
	C61	C62	C63	C64	C65
2449714.43	24.21 ± 0.14	24.43 ± 0.14	24.23 ± 0.15	24.60 ± 0.18	24.11 ± 0.10
2449722.34	24.30 ± 0.15	24.19 ± 0.11	24.91 ± 0.22	24.59 ± 0.15	24.14 ± 0.10
2449742.25	24.32 ± 0.13	24.58 ± 0.17	24.10 ± 0.12	24.02 ± 0.13	24.29 ± 0.14
2449761.22	24.02 ± 0.11	24.52 ± 0.20	24.49 ± 0.18	24.84 ± 0.24	23.94 ± 0.14
	C66	C67	C68	C69	
2449714.43	24.35 ± 0.17	24.02 ± 0.13	24.24 ± 0.17	24.70 ± 0.17	
2449722.34	24.05 ± 0.11	24.32 ± 0.14	24.76 ± 0.16	25.08 ± 0.22	
2449742.25	24.31 ± 0.14	24.26 ± 0.15	24.47 ± 0.19	24.69 ± 0.19	
2449761.22	24.42 ± 0.18	24.03 ± 0.11	24.65 ± 0.26	24.42 ± 0.16	

TABLE A8
DoPHOT F555W PHOTOMETRY

JD	$m \pm \Delta m$	$m \pm \Delta m$	$m \pm \Delta m$	$m \pm \Delta m$	$m \pm \Delta m$
	C01	C02	C03	C04	C05
2449714.37	23.65±0.07	23.74±0.07	24.44±0.11	24.31±0.10	25.11±0.20
2449722.28	23.87±0.06	24.04±0.08	24.70±0.09	24.20±0.07	25.15±0.11
2449733.40	23.96±0.07	24.26±0.10	24.74±0.13	23.57±0.06	24.23±0.10
2449735.48	23.84±0.09	24.33±0.07	24.59±0.12	23.68±0.06	24.43±0.11
2449738.43	23.62±0.06	24.40±0.08	24.08±0.11	23.96±0.07	24.49±0.12
2449742.18	23.32±0.06	24.36±0.08	23.89±0.08	23.87±0.07	24.73±0.13
2449746.01	23.30±0.06	24.28±0.08	23.97±0.05	24.17±0.06	24.80±0.14
2449750.09	23.33±0.06	23.72±0.06	24.11±0.09	24.18±0.09	25.08±0.17
2449755.25	23.41±0.08	23.49±0.06	24.28±0.11	24.30±0.09	25.22±0.21
2449761.16	23.55±0.06	23.70±0.06	24.39±0.11	24.49±0.08	25.33±0.18
2449767.39
2449773.69	23.81±0.08	24.23±0.10	24.78±0.13	23.53±0.08	24.22±0.11
	C06	C07	C08	C09	C10
2449714.37	25.33±0.16	24.10±0.11	23.68±0.08
2449722.28	24.57±0.14	24.20±0.06
2449733.40	24.62±0.13	...	24.58±0.12	24.91±0.18	24.50±0.11
2449735.48	24.64±0.11	...	24.89±0.12	24.94±0.17	24.54±0.10
2449738.43	24.91±0.11	...	24.87±0.12	24.91±0.16	24.56±0.16
2449742.18	25.00±0.13	...	24.91±0.12	24.42±0.13	24.59±0.12
2449746.01	25.12±0.17	...	24.90±0.11	24.28±0.12	23.72±0.08
2449750.09	25.16±0.16	...	25.03±0.15	24.47±0.13	23.64±0.06
2449755.25	25.51±0.18	...	25.14±0.16	24.62±0.16	23.90±0.08
2449761.16	25.31±0.14	24.97±0.20	24.11±0.10
2449767.39	25.26±0.14
2449773.69	24.75±0.14	...	24.54±0.13	24.07±0.11	24.59±0.11
	C11	C12	C13	C14	C15
2449714.37	26.09±0.29	25.23±0.17	24.43±0.13	24.10±0.11	24.65±0.18
2449722.28	...	25.60±0.20	24.87±0.17	23.12±0.05	25.25±0.13
2449733.40	25.74±0.18	25.99±0.34	23.70±0.08	23.69±0.08	25.56±0.25
2449735.48	25.75±0.18	25.57±0.26	23.87±0.09	23.74±0.09	25.45±0.21
2449738.43	26.05±0.23	25.32±0.18	24.08±0.08	23.91±0.09	25.47±0.26
2449742.18	25.92±0.18	24.69±0.11	24.17±0.11	23.91±0.11	24.88±0.15
2449746.01	26.29±0.28	25.03±0.12	24.43±0.13	24.02±0.11	24.69±0.11
2449750.09	26.25±0.30	25.00±0.18	24.44±0.15	23.63±0.08	25.01±0.11
2449755.25	26.19±0.37	25.21±0.21	24.74±0.16	23.28±0.08	25.29±0.16
2449761.16	26.35±0.36	26.00±0.32	24.43±0.13	23.45±0.08	25.32±0.22
2449767.39
2449773.69	25.68±0.24	25.16±0.23	...	23.90±0.11	24.72±0.16

TABLE A8—*Continued*

JD	$m \pm \Delta m$	$m \pm \Delta m$	$m \pm \Delta m$	$m \pm \Delta m$	$m \pm \Delta m$
	C16	C17	C18	C19	C20
2449714.37	24.10±0.08	23.52±0.08	24.90±0.12	23.43±0.06	24.38±0.24
2449722.28	24.53±0.08	23.96±0.08	25.25±0.14	23.91±0.06	24.84±0.13
2449733.40	25.05±0.14	24.39±0.11	25.50±0.20	24.54±0.11	25.18±0.16
2449735.48	25.06±0.17	24.34±0.11	25.37±0.21	24.48±0.11	24.75±0.11
2449738.43	24.75±0.16	23.63±0.07	24.96±0.14	24.57±0.10	24.29±0.09
2449742.18	23.87±0.08	23.48±0.07	24.96±0.13	23.37±0.06	24.49±0.10
2449746.01	24.13±0.10	23.63±0.07	25.16±0.16	23.68±0.07	24.66±0.11
2449750.09	24.28±0.14	23.91±0.08	25.25±0.17	23.88±0.09	25.00±0.12
2449755.25	24.45±0.11	24.10±0.08	25.29±0.23	24.25±0.10	25.24±0.20
2449761.16	24.64±0.13	24.25±0.09	25.57±0.24	24.49±0.11	24.89±0.12
2449767.39	24.95±0.15	23.76±0.08
2449773.69	24.19±0.08	23.58±0.09	25.00±0.14	23.78±0.07	24.77±0.11
	C21	C22	C23	C24	C25
2449714.37	25.27±0.18	24.68±0.16	25.28±0.20	24.84±0.09	25.41±0.22
2449722.28	24.42±0.07	23.85±0.06	26.15±0.41	24.01±0.05	25.72±0.16
2449733.40	24.89±0.14	24.41±0.12	24.80±0.14	24.84±0.12	25.02±0.13
2449735.48	25.04±0.17	24.55±0.12	25.11±0.18	24.85±0.10	25.32±0.17
2449738.43	25.06±0.14	24.58±0.12	25.05±0.15	...	25.41±0.17
2449742.18	25.16±0.14	24.62±0.13	25.37±0.18	23.99±0.08	25.89±0.26
2449746.01	25.14±0.15	23.66±0.07	25.72±0.37	24.08±0.10	25.82±0.24
2449750.09	24.25±0.13	24.00±0.10	25.49±0.27	24.33±0.11	24.88±0.12
2449755.25	24.59±0.13	24.32±0.10	24.81±0.10	24.52±0.11	25.14±0.16
2449761.16	24.97±0.16	24.53±0.12	24.95±0.17	24.82±0.12	25.21±0.11
2449767.39	25.15±0.18	25.68±0.19
2449773.69	24.20±0.10	23.81±0.12	25.97±0.43	24.21±0.16	24.82±0.14
	C26	C27	C28	C29	C30
2449714.37	24.25±0.08	25.01±0.14	24.94±0.12	25.56±0.21	25.39±0.16
2449722.28	24.94±0.09	24.59±0.10	24.08±0.06	25.18±0.14	...
2449733.40	25.60±0.26	24.88±0.15	...	25.08±0.13	25.92±0.22
2449735.48	24.93±0.12	25.13±0.18	24.64±0.06	25.43±0.22	25.23±0.17
2449738.43	24.42±0.09	25.04±0.17	24.65±0.13	25.51±0.18	25.26±0.15
2449742.18	24.70±0.10	24.59±0.14	23.73±0.07	25.72±0.21	25.47±0.16
2449746.01	24.89±0.11	24.71±0.14	24.06±0.07	25.46±0.19	25.56±0.17
2449750.09	25.24±0.22	24.89±0.18	24.23±0.05	24.64±0.16	26.04±0.30
2449755.25	25.37±0.19	25.13±0.18	24.66±0.11	24.99±0.14	25.79±0.26
2449761.16	24.29±0.09	25.38±0.23	24.91±0.13	25.30±0.13	25.19±0.14
2449767.39	...	24.64±0.18	...	25.57±0.17	...
2449773.69	25.31±0.14	24.80±0.14	24.25±0.09	24.43±0.09	25.70±0.23

TABLE A8—*Continued*

JD	$m \pm \Delta m$	$m \pm \Delta m$	$m \pm \Delta m$	$m \pm \Delta m$	$m \pm \Delta m$
	C31	C32	C33	C34	C35
2449714.37	25.20±0.19	24.28±0.11	25.24±0.22	...	25.25±0.16
2449722.28	24.46±0.27	24.68±0.13	25.65±0.20	...	24.57±0.09
2449733.40	24.87±0.13	24.14±0.10	26.16±0.20	...	25.28±0.16
2449735.48	25.02±0.09	24.27±0.11	25.84±0.22	...	25.26±0.16
2449738.43	25.18±0.11	24.52±0.13	25.38±0.18	...	25.31±0.16
2449742.18	24.19±0.07	24.66±0.13	25.34±0.17	...	24.19±0.09
2449746.01	24.39±0.07	24.63±0.13	25.70±0.24	...	24.60±0.12
2449750.09	24.54±0.11	23.67±0.07	25.85±0.26	...	24.67±0.13
2449755.25	24.82±0.11	24.09±0.08	26.30±0.43	...	25.18±0.17
2449761.16	24.96±0.16	24.47±0.12	25.44±0.16	...	25.25±0.18
2449767.39	...	24.63±0.14	24.40±0.11
2449773.69	24.55±0.10	23.63±0.11	26.04±0.33	...	24.80±0.12
	C36	C37	C38	C39	C40
2449714.37	25.07±0.12	24.59±0.14	24.68±0.13	24.10±0.08	25.16±0.13
2449722.28	24.72±0.09	25.66±0.18	23.66±0.05	24.88±0.10	24.74±0.09
2449733.40	25.21±0.14	24.58±0.13	...	24.59±0.18	25.15±0.12
2449735.48	25.18±0.12	24.60±0.19	24.74±0.13	24.00±0.08	24.93±0.11
2449738.43	25.13±0.11	24.81±0.19	24.61±0.14	24.26±0.10	24.57±0.10
2449742.18	24.57±0.08	25.12±0.19	23.97±0.09	24.58±0.10	24.73±0.09
2449746.01	24.75±0.11	25.55±0.25	23.97±0.10	25.14±0.17	25.14±0.13
2449750.09	25.06±0.12	25.65±0.26	24.24±0.11	25.04±0.20	25.47±0.19
2449755.25	25.35±0.16	24.63±0.20	24.69±0.16	24.13±0.10	25.14±0.15
2449761.16	25.03±0.11	25.08±0.21	24.74±0.12	24.54±0.10	24.61±0.10
2449767.39	25.26±0.14	...
2449773.69	25.02±0.15	25.41±0.21	24.41±0.14	25.16±0.18	25.59±0.23
	C41	C42	C43	C44	C45
2449714.37	24.08±0.07	24.55±0.12	24.02±0.09	25.33±0.18	24.71±0.14
2449722.28	24.83±0.06	25.30±0.16	24.26±0.10	24.54±0.13	24.89±0.18
2449733.40	23.81±0.06	24.50±0.12	23.87±0.08	25.47±0.19	24.84±0.13
2449735.48	24.09±0.06	24.60±0.13	23.92±0.08	25.15±0.16	24.74±0.14
2449738.43	24.38±0.08	24.93±0.14	24.05±0.09	24.65±0.12	24.79±0.16
2449742.18	24.55±0.08	25.16±0.17	24.22±0.10	24.92±0.13	24.56±0.11
2449746.01	24.90±0.11	25.39±0.21	24.27±0.11	25.16±0.17	24.46±0.13
2449750.09	24.75±0.09	24.81±0.18	24.06±0.09	25.53±0.20	24.67±0.15
2449755.25	23.95±0.06	24.92±0.19	23.83±0.09	24.51±0.08	24.88±0.14
2449761.16	24.60±0.07	25.21±0.21	24.08±0.10	24.92±0.15	24.36±0.12
2449767.39
2449773.69	24.16±0.07	24.81±0.18	23.79±0.08	24.61±0.17	24.76±0.13

TABLE A8—*Continued*

JD	$m \pm \Delta m$	$m \pm \Delta m$	$m \pm \Delta m$	$m \pm \Delta m$	$m \pm \Delta m$
	C46	C47	C48	C49	C50
2449714.37	...	24.11±0.06	25.39±0.18	25.43±0.21	24.71±0.13
2449722.28	...	24.78±0.09	...	25.40±0.14	25.54±0.19
2449733.40	...	24.23±0.09	25.43±0.18	25.39±0.18	24.79±0.15
2449735.48	...	24.35±0.08	25.38±0.17	25.42±0.13	25.14±0.16
2449738.43	...	24.57±0.11	25.43±0.17	25.46±0.16	25.51±0.20
2449742.18	...	24.99±0.12	24.80±0.12	24.56±0.09	25.73±0.24
2449746.01	...	25.01±0.08	24.99±0.15	24.98±0.13	25.65±0.22
2449750.09	25.24±0.16	25.24±0.18	24.76±0.12
2449755.25	...	24.40±0.10	25.53±0.24	25.39±0.21	25.29±0.16
2449761.16	...	24.96±0.12	24.82±0.11	24.64±0.11	25.78±0.18
2449767.39	...	24.85±0.13
2449773.69	...	24.30±0.10	25.30±0.19	25.56±0.25	25.49±0.21
	C51	C52	C53	C54	C55
2449714.37	25.61±0.21	24.45±0.08	24.80±0.12	24.12±0.08	25.09±0.12
2449722.28	24.96±0.11	25.10±0.11	25.25±0.09	25.10±0.12	25.97±0.21
2449733.40	25.40±0.23	24.60±0.10	25.01±0.13	24.37±0.08	25.57±0.10
2449735.48	24.78±0.16	24.78±0.11	25.22±0.13	24.48±0.09	25.67±0.18
2449738.43	24.63±0.15	25.06±0.14	25.43±0.18	24.93±0.13	26.00±0.21
2449742.18	25.10±0.20	24.90±0.11	25.26±0.12	25.25±0.14	25.26±0.11
2449746.01	25.51±0.24	24.23±0.16	24.63±0.09	25.01±0.14	25.35±0.09
2449750.09	25.31±0.18	24.54±0.11	24.98±0.13	24.25±0.08	25.67±0.15
2449755.25	24.82±0.15	24.91±0.14	25.53±0.13	24.75±0.11	25.56±0.22
2449761.16	25.21±0.20	24.20±0.10	24.46±0.08	25.10±0.13	24.98±0.13
2449767.39
2449773.69	24.57±0.15	25.05±0.17	25.59±0.19	24.85±0.14	25.48±0.18
	C56	C57	C58	C59	C60
2449714.37	...	25.07±0.17	24.80±0.23	25.34±0.21	24.57±0.11
2449722.28	25.16±0.11	25.08±0.21	25.76±0.20	25.55±0.23	25.08±0.12
2449733.40	24.54±0.10	25.48±0.21	25.13±0.24	25.72±0.22	24.86±0.14
2449735.48	24.75±0.10	...	25.68±0.21	25.64±0.22	25.20±0.11
2449738.43	24.99±0.17	25.47±0.22	25.41±0.34	25.60±0.17	25.11±0.14
2449742.18	25.42±0.17	24.76±0.15	25.45±0.30	24.84±0.11	24.29±0.08
2449746.01	25.35±0.15	24.92±0.15	24.92±0.21	25.12±0.16	24.76±0.13
2449750.09	24.65±0.12	25.35±0.24	25.36±0.30	25.58±0.26	25.18±0.16
2449755.25	25.15±0.14	...	26.09±0.32	25.40±0.18	24.65±0.07
2449761.16	25.33±0.16	25.06±0.17	25.13±0.21	25.24±0.19	24.77±0.16
2449767.39
2449773.69	25.36±0.16	24.75±0.16	25.63±0.39	24.65±0.13	24.61±0.13

TABLE A8—*Continued*

JD	$m \pm \Delta m$	$m \pm \Delta m$	$m \pm \Delta m$	$m \pm \Delta m$	$m \pm \Delta m$
	C61	C62	C63	C64	C65
2449714.37	25.12±0.15	25.69±0.21	24.78±0.13	25.50±0.19	25.23±0.14
2449722.28	25.12±0.13	25.04±0.12	25.73±0.13	25.12±0.13	25.29±0.17
2449733.40	24.89±0.13	25.71±0.23	25.38±0.19	24.92±0.13	25.38±0.14
2449735.48	25.00±0.13	25.32±0.16	25.74±0.17	25.38±0.19	24.91±0.13
2449738.43	...	25.38±0.16	25.49±0.16	25.34±0.18	25.18±0.13
2449742.18	25.11±0.16	25.72±0.13	24.90±0.12	24.59±0.10	...
2449746.01	24.71±0.12	25.88±0.15	25.25±0.11	25.08±0.18	25.28±0.16
2449750.09	25.11±0.14	25.23±0.12	...	25.29±0.19	25.03±0.13
2449755.25	25.26±0.16	25.87±0.26	24.80±0.12	24.79±0.13	25.55±0.21
2449761.16	24.83±0.13	25.57±0.23	25.59±0.19	25.29±0.16	24.95±0.15
2449767.39	...	25.70±0.14	...	25.12±0.18	...
2449773.69	24.70±0.11	25.76±0.25	...	25.40±0.23	25.03±0.14
	C66	C67	C68	C69	
2449714.37	25.71±0.17	24.95±0.13	25.03±0.16	25.22±0.16	
2449722.28	25.14±0.13	25.61±0.20	25.30±0.14	25.57±0.16	
2449733.40	25.18±0.16	25.44±0.18	25.02±0.15	25.02±0.13	
2449735.48	25.56±0.19	25.23±0.15	24.99±0.14	25.24±0.14	
2449738.43	25.74±0.21	24.96±0.12	25.46±0.21	25.82±0.18	
2449742.18	25.76±0.25	25.39±0.19	25.11±0.16	25.27±0.13	
2449746.01	...	25.40±0.21	25.07±0.14	25.36±0.26	
2449750.09	26.13±0.37	24.95±0.14	...	25.81±0.22	
2449755.25	25.36±0.17	25.70±0.25	25.06±0.19	25.50±0.19	
2449761.16	25.86±0.24	24.76±0.17	25.50±0.24	25.12±0.13	
2449767.39	25.45±0.14	25.61±0.21	25.35±0.11	...	
2449773.69	25.82±0.29	24.95±0.17	25.05±0.19	25.30±0.21	

TABLE A9
DoPHOT F814W PHOTOMETRY

JD	m±Δm	m±Δm	m±Δm	m±Δm	m±Δm
	C01	C02	C03	C04	C05
2449714.43	22.58±0.06	22.61±0.06	23.08±0.08	23.05±0.07	23.80±0.19
2449722.34	22.79±0.06	22.72±0.06	23.33±0.10	23.13±0.08	23.86±0.15
2449742.25	22.53±0.05	23.05±0.06	22.88±0.08	22.78±0.06	23.35±0.13
2449761.22	22.54±0.05	22.64±0.05	23.35±0.10	23.25±0.07	24.03±0.20
	C06	C07	C08	C09	C10
2449714.43	24.02±0.09	...	22.97±0.07	23.16±0.10	22.83±0.06
2449722.34	23.43±0.09	...	22.87±0.07	23.34±0.12	22.98±0.07
2449742.25	23.50±0.08	...	22.86±0.11	23.30±0.11	23.44±0.10
2449761.22	23.50±0.08	...	23.27±0.08	23.56±0.15	23.06±0.08
	C11	C12	C13	C14	C15
2449714.43	24.73±0.12	23.86±0.15	23.20±0.10	23.18±0.10	23.23±0.10
2449722.34	24.94±0.25	24.10±0.17	23.65±0.11	22.54±0.07	23.35±0.11
2449742.25	24.85±0.20	23.54±0.08	23.18±0.08	23.18±0.11	23.39±0.10
2449761.22	24.98±0.26	24.04±0.14	23.51±0.13	22.71±0.08	23.63±0.13
	C16	C17	C18	C19	C20
2449714.43	23.02±0.06	22.69±0.08	23.89±0.13	22.85±0.07	23.65±0.07
2449722.34	23.37±0.10	22.89±0.07	24.07±0.19	23.09±0.12	23.71±0.09
2449742.25	23.03±0.08	22.71±0.06	23.84±0.13	22.74±0.06	23.54±0.08
2449761.22	23.56±0.11	23.06±0.08	24.18±0.16	23.37±0.08	23.81±0.08
	C21	C22	C23	C24	C25
2449714.43	23.93±0.12	23.41±0.12	23.75±0.15	23.68±0.11	24.06±0.13
2449722.34	23.56±0.12	22.92±0.09	24.20±0.16	23.08±0.08	24.55±0.12
2449742.25	24.05±0.15	23.58±0.13	23.95±0.10	23.13±0.08	24.40±0.13
2449761.22	23.80±0.11	23.38±0.11	23.72±0.13	23.64±0.09	23.99±0.11
	C26	C27	C28	C29	C30
2449714.43	23.48±0.09	23.91±0.18	23.68±0.09	24.16±0.17	23.99±0.11
2449722.34	23.69±0.10	23.58±0.13	23.11±0.07	24.04±0.15	24.29±0.14
2449742.25	23.66±0.09	23.50±0.12	22.94±0.06	24.26±0.18	24.06±0.13
2449761.22	23.61±0.08	23.97±0.20	23.57±0.09	24.12±0.16	24.00±0.12
	C31	C32	C33	C34	C35
2449714.43	23.51±0.11	23.23±0.11	24.43±0.15	...	24.04±0.13
2449722.34	23.15±0.09	23.43±0.11	24.18±0.12	...	23.52±0.09
2449742.25	23.17±0.08	23.42±0.13	24.45±0.19	...	23.30±0.08
2449761.22	23.62±0.09	23.31±0.12	24.48±0.24	...	24.00±0.15

TABLE A9—*Continued*

JD	$m \pm \Delta m$	$m \pm \Delta m$	$m \pm \Delta m$	$m \pm \Delta m$	$m \pm \Delta m$
	C36	C37	C38	C39	C40
2449714.43	24.08±0.11	23.46±0.07	23.55±0.12	23.46±0.10	23.78±0.11
2449722.34	23.60±0.09	23.91±0.10	23.04±0.09	23.70±0.14	23.44±0.06
2449742.25	23.55±0.07	23.90±0.07	23.17±0.09	23.87±0.11	23.57±0.09
2449761.22	24.13±0.13	23.60±0.08	23.75±0.13	23.57±0.14	23.49±0.08
	C41	C42	C43	C44	C45
2449714.43	23.27±0.07	23.66±0.08	23.07±0.08	23.90±0.10	23.12±0.08
2449722.34	23.66±0.07	23.78±0.08	23.37±0.09	23.76±0.10	23.21±0.06
2449742.25	23.50±0.08	23.85±0.12	23.26±0.08	23.79±0.13	23.09±0.08
2449761.22	23.39±0.07	24.00±0.14	23.23±0.08	23.94±0.13	23.07±0.08
	C46	C47	C48	C49	C50
2449714.43	...	23.35±0.10	24.13±0.12	24.09±0.17	23.81±0.11
2449722.34	...	23.80±0.09	24.08±0.13	24.05±0.10	24.02±0.16
2449742.25	...	23.89±0.12	23.90±0.12	23.71±0.08	24.42±0.16
2449761.22	...	23.96±0.13	23.71±0.11	23.78±0.13	24.51±0.22
	C51	C52	C53	C54	C55
2449714.43	24.36±0.18	23.60±0.09	23.77±0.10	23.54±0.10	24.20±0.10
2449722.34	23.68±0.13	23.92±0.13	24.37±0.16	24.03±0.16	24.85±0.16
2449742.25	23.89±0.09	23.92±0.10	24.16±0.13	24.39±0.15	24.28±0.13
2449761.22	23.94±0.14	23.53±0.08	23.70±0.08	24.41±0.17	24.03±0.11
	C56	C57	C58	C59	C60
2449714.43	24.09±0.13	24.11±0.18	23.72±0.12	24.43±0.16	23.95±0.14
2449722.34	24.05±0.13	24.41±0.18	...	24.83±0.23	24.25±0.16
2449742.25	24.39±0.16	23.87±0.13	24.10±0.19	24.14±0.15	23.70±0.11
2449761.22	24.26±0.14	24.09±0.14	23.84±0.16	24.08±0.18	23.91±0.13
	C61	C62	C63	C64	C65
2449714.43	24.00±0.14	24.56±0.18	24.14±0.09	24.53±0.17	24.05±0.11
2449722.34	24.08±0.14	24.24±0.12	24.73±0.13	24.29±0.21	23.89±0.11
2449742.25	24.36±0.10	24.73±0.21	24.19±0.10	23.95±0.13	24.17±0.13
2449761.22	24.07±0.14	24.61±0.20	24.54±0.17	24.85±0.24	23.85±0.14
	C66	C67	C68	C69	
2449714.43	24.27±0.18	24.00±0.13	24.26±0.19	24.43±0.19	
2449722.34	24.12±0.14	24.30±0.16	24.83±0.16	24.61±0.21	
2449742.25	24.26±0.16	24.25±0.13	24.61±0.22	24.54±0.19	
2449761.22	24.37±0.17	24.03±0.13	24.91±0.33	24.41±0.17	